THE CHEMISORPTION OF HYDROGEN ATOMS ON METAL SURFACES

A Thesis

submitted in part-fulfilment of the requirements of the Ph.D. Degree of University of London

by

Patrick James Herley, M.Sc., Ph.D.(Rhodes).

Department of Physical and Inorganic Chemistry,
Imperial College of Science and Technology,

December 1963.

ACKNOWLEDGEMENTS

The author is indebted to Professor R. M. Barrer, Sc.D.(Camb.) D.Sc.(N.Z.), F.R.S., F.R.I.C., for the provision of research facilities.

Thanks are especially due to Professor F. C. Tompkins, D.Sc., F.R.S., F.R.I.C., for his valuable guidance, for the innumerable discussions and for his keen interest in all aspects of this work.

The author is also indebted to the Royal Commission for the Exhibition of 1851 for the award of an Overseas Research Scholarship held throughout the tenure of this research.

Thanks are also due to Mr. A. Madell and Mr. D. Alger for their assistance with the technical aspects of the work.

ABSTRACT

Varying volumes of hydrogen atoms were chemisorbed on metallic films of copper, silver, gold, nickel (presaturated with molecular hydrogen), zinc and cadmium at 78°K. The rates of desorption of hydrogen from these metals have been measured in the temperature range 78°K. - 273°K. as well as the total volume of gas desorbed at each temperature as a function of the total dosage on the surface.

The results are reproducible and it has been shown that the overall desorption rate is complex and involves both a first and second order process occurring simultaneously and independently on the metallic surface. The apparent (Arrhenius) activation energies for the desorption process have been determined for various dosages on all the metal films. Mobility energies for the adatoms on the surface have been calculated and the variation of the distribution of sites of varying mobility energies has been evaluated over the temperature range studied.

CONTENTS

1. INTRODUCTION

The characteristics of the metal-hydrogen bond arise from the interaction between the unsaturated cohesive forces normally operative on the surface of the metal and the molecules of the reacting gas. Such interactions can result in ionic or covalent bond formation. The heats involved in most chemisorption studies are large ($\gtrsim$ 10 kcal.mole.$^{-1}$), but if dissociation of the adsorbed molecule takes place on adsorption, the heat of dissociation may be lost and a lower heat of adsorption result.

Plots of the heat of adsorption against coverage invariably show a decrease in the heat at high coverages[1-6], although the shape of the curve differs considerably; quite often the relation is linear[1, 7] or nearly so[8] over a considerable range of θ. The cause of this decrease has been ascribed to surface heterogeneity[9, 10, 11] and to repulsive interactions[12, 13].

That the surfaces of evaporated metal films are extremely heterogeneous is undoubtedly true. Heterogeneity may arise in several ways; through lattice defects, dislocations, the occurrence of different crystal planes, edges, corners and impurity centres, but if it were wholly responsible one would expect large differences between films and filaments of different crystal habit, yet there is little variation[1,14,15]. Thus, although structural heterogeneity is important, some other explanation must be forthcoming. The theory of repulsive interactions was developed by Roberts[16] and Miller[13]. These interactions may be of short range in which case only nearest neighbours are considered or long

range/...

range when due to dipole interactions. On the basis of unspecified short range fixed interaction forces they showed that considerable differences in the differential heat against coverage relations could be expected depending on the mobility of the adatoms. For immobile adsorption of atoms the relation is linear. For immobile adsorption with dissociation into two adatoms it is nearly linear but slightly convex outwards, while for mobile adsorption the relation is sigmoid varying from linear to a sharp step about half coverage depending on the interaction potential. If the interaction forces themselves are functions of coverage the situation is much less simple, and the distinction between mobile and immobile curves is less marked. Perhaps a better criteria for mobility was that developed by Beeck[14]. He suggested that in the case of immobile adsorption the first fraction of gas admitted will be adsorbed and remain on the first metal surface encountered, on or near to the outer surface. Thus the measured calorimetric heat will be an integral heat corresponding to large fractional coverage of a small section of the total surface. On further additions of gas the process is repeated on the outer surface adjacent to the first section and so on until the film is completely covered. Thus the differential heat against coverage plot would be expected to be a straight line of zero slope. For mobile films, however, a steady fall in differential heat should occur. Such behaviour is found with hydrogen on iron[3]; at 90°K. it appears to be immobile while at 296°K. it is mobile. The mobility of hydrogen on tungsten above 200°K. has been confirmed by field emission microscopy[17,18]. This technique is being increasingly employed in the study of surface mobility, e.g.

oxygen on/...

oxygen on tungsten[19], hydrogen on nickel[20], and the adsorption of metal atoms[21,22,23,24].

In recent studies of surface reactions the main stress has been upon correlating the thermodynamics and kinetics of the processes at the solid-gas interface with the electronic structure of the solid[25]. The electronic structure or, more precisely, the occupancy of the d-band has been particularly stressed as a deciding factor in elucidating the nature of the bond formed on adsorption of molecular or atomic hydrogen[26,27,28]. For example, the influence of the d-band character of the metal on its catalytic properties has been studied in detail; the ortho-para hydrogen conversion on a series of palladium-gold[26] alloys showed there was a sharp rise in the activation energy as the d-band occupancy of palladium was filled with gold. Magnetic susceptibility data for nickel by Selwood[29] and Eley[30] further emphasize the importance of the d-band in chemisorption.

The general trend of the initial heats of adsorption has been correlated[8,31,32,33] with the percentage d-character of the metallic bonds[34]. This interpretation required that the bond between the metal and the adatom was essentially covalent[26,27,28], which seems more in accord with experiment than ionic bonding; for instance, the measurement of work function changes due to adsorption[35,36,37] showed that the apparent electric moment of a surface adatom complex is much smaller than would be expected for ionic adsorption. Only with some alkali metal films on tungsten[38,39,40] are the effects comparable. For hydrogen, calculations[26] showed that ionic adsorption would be endothermic

while crude/...

while crude estimates of the covalent bond energies[41,42] are in reasonable agreement with the observed heats. Trapnell[43] studied the chemisorption of several gases on a large number of evaporated metals and concluded that metals with vacancies in the d-band are very much more active adsorbents than other metals. For example, while all the transition metals rapidly chemisorb molecular hydrogen at ordinary temperatures, copper, silver and gold do not. It is difficult, however, to assess the correlation between the d-band and the heat of chemisorption simply in a single parameter; such a parameter will merely provide a limiting condition for bond formation.

Instead of stressing the electronic structure, Ehrlich[44] has discussed the detailed mechanisms of surface reactions by application of the standard techniques of chemical kinetics to the molecular dissociation and reconstitution phenomena occurring at a solid interface. Since the advent of ultra high vacuum techniques, it seems a well established criteria that the dissociative adsorption of hydrogen on clean surfaces of the transition metals proceeds at an immeasurably fast rate with negligible or zero activation energy at liquid nitrogen temperatures[14,45]. Observations in the field emission microscope on nickel show hydrogen chemisorption occurring as low as even 20°K.[46]

At 0°K., where the entropy change on adsorption is zero, adsorption will take place exothermically provided $2X-D \nless 0$ (FIGURE 1), where X is the desorption energy of the hydrogen atom from the surface (the M-H bond energy) and D is the desorption energy of the hydrogen molecule. Since the adsorption process involves dissociation and, for nickel, the

interatomic/...

interatomic spacing at the interface is considerably larger than that of the diatom (Ni: 2.49 A^{o}, H_2: 0.75 A^{o}), a hydrogen molecule on the nickel surface cannot form bonds as strong as those of an isolated hydrogen atom.

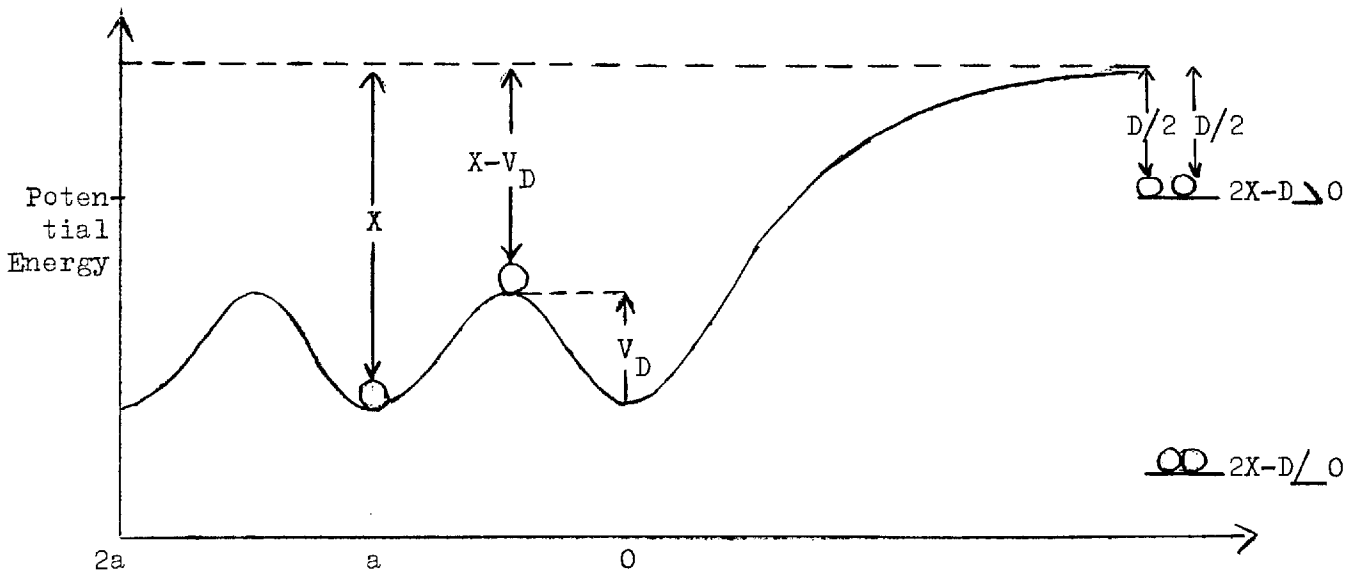

FIGURE 1 (after Ehrlich[44])

The maximum interaction between the diatom and the solid surface results when one atom is located at the minimum of the potential energy well and the other in a non-equilibrium position, e.g. in nickel, the second atom is at the top of the sinusoidal energy barrier, the height of which is the mobility energy for surface diffusion, V_D. If, as Ehrlich[44] suggests, the activation energy for dissociative adsorption arises from the difference in interaction of the two atoms with the surface when their separation is that of the unperturbed hydrogen molecule on the surface and the interaction with the surface when the two adatoms are bound in their equilibrium positions, then the potential energy change,

E, from the/...

$\triangle E$, from the gas to the activated state is:-

$$\triangle E = D - (2X - V_D) \quad \ldots\ldots\ldots\ldots\ldots\ldots \quad (1.1)$$

and $-\triangle H$, the heat of adsorption $\approx 2X - D$ whence,

$$\triangle E = \triangle H + V_D \quad \ldots\ldots\ldots\ldots\ldots\ldots \quad (1.2)$$

Hence, e.g. for the nickel-hydrogen system as $\theta \rightarrow 0$, $X \rightarrow 67$, $D = 103$ and $V_D = 7$[20], all in kcal.mole.$^{-1}$ Hence $\triangle E = -24$ kcal.mole.$^{-1}$, i.e. no activation energy is required for dissociative adsorption at $\theta \approx 0$. However, the heats of adsorption fall with increasing θ[47], so that if V_D is constant, when $-\triangle H \approx 7$ kcal.mole.$^{-1}$, $\triangle E \approx 0$. For sufficiently high θ, therefore, $\triangle E$ will become measurable. (It may be noted that Gundry's estimate of θ[48,49] based on the Beeck criterion (296°K., 1 mm.Hg.) is undoubtedly too high and that when $\triangle E = 0$, $\theta = 0.8$).

However, an alternative approach to that of Ehrlich's can be found in the activated surface migration theory, initially proposed by Porter and Tompkins[51] and later critically modified by Gundry and Tompkins[52]. Porter and Tompkins originally envisaged the slow activated process to be diffusion over a non uniform surface from sites of lower to those of higher adsorption potential. An essential feature of this theory was that the higher potential sites were not filled directly from the gas phase; direct deposition being prevented by the higher activation energy barrier for the transition from the Van der Waals layer to the chemisorbed layer.

The limitation of this theory was that the slow uptake would involve those sites with high activation energies for mobility and consequently those of high potential. Once covered, they would then be the last to

be removed/...

be removed by pumping and a much faster readsorption rate would be expected. In actual fact an identical rate was found[48] so adsorption must be occurring on sites where the potential is fairly small.

The modified theory regards the slow activated process as essentially attributable to the transition of a chemisorbed adatom at its original site to a different state of lower potential energy. The mechanism of the slow process was formulated as follows:- Van der Waals adsorption occurs on exposure of the metal film to hydrogen molecules. At the low pressures under consideration and since the Van der Waals heat of adsorption for hydrogen molecules is small, the isotherm over this pressure range is confined to the Henry's Law region i.e.

$$[H_2] \propto a_1 p \qquad \ldots\ldots\ldots\ldots\ldots\ldots \quad (1.3)$$

where a_1 is a constant and $[H_2]$ is the number of hydrogen molecules per unit area of the film. It was assumed that the final chemisorbed state, C_f, (FIGURE 2) was attained only by passing through an initial chemisorbed state, C_i, of higher potential energy. (VIDE Dowden[28])

Dowden envisaged particular surface metal atoms possessing a certain life time as multiply charged positive ions resulting in the abstraction of electrons from the sorbate into one of the ionized levels now formed. Such charged states of the atom are thus kinetically important, although from an equilibrium consideration the process corresponds to the entry of the electron at the Fermi level. He has further suggested[52] that the C_i state could involve solely d-orbitals and that the bonding might go to the stronger hybridised bonds of the dsp-type in the C_f state - this involved readjustment of the surface hybridised metal to sorbate bonding

plus differently/...

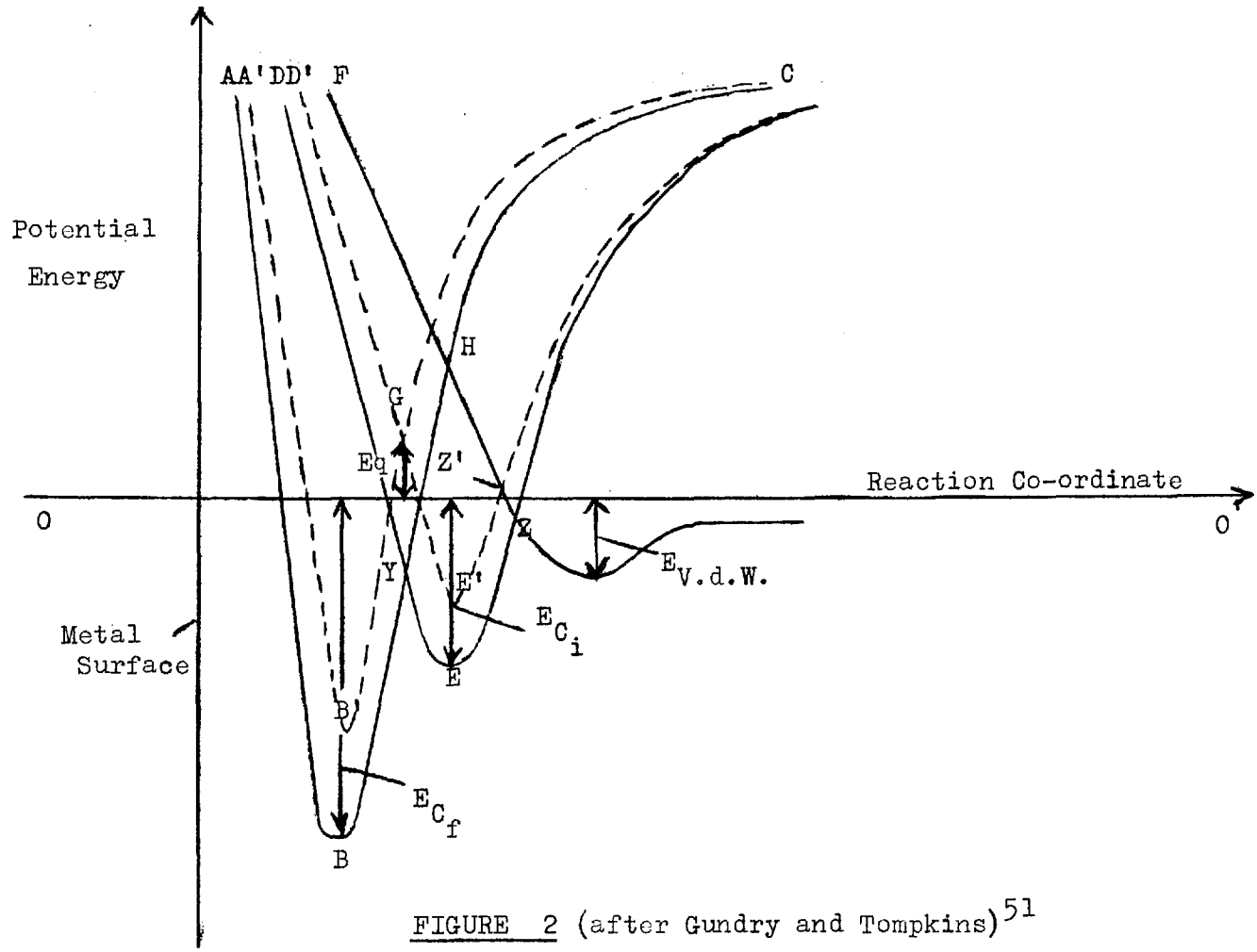

FIGURE 2 (after Gundry and Tompkins)[51]

plus differently hybridised metal to metal bonding to obtain the minimum free energy of the surface complex.

The familiar Lennard-Jones potential plot is shown in FIGURE 2 and it includes the additional curve DEC for the C_i state ($E_{C_f} > E_{C_i} > E_{VdW}$). E is an enthalpy of adsorption and the slopes decrease such that AB > DE > FZ. For hydrogen state C_i is dissociative and we can define an equilibrium constant, K_i, such that:-

$$K_i = [H_{C_i}]^2 / [H_2] \qquad \ldots\ldots\ldots\ldots\ldots\ldots (1.4)$$

where/...

where $\left[H_{C_i}\right]$ = the number of hydrogen atoms per unit area of the film in the chemisorbed state C_i. Substituting in equation (1.3) we get:-

$$K = a_1 K_i = \left[H_{C_i}\right]^2 / p = \text{constant} \exp(-\triangle F^1/RT) \quad \ldots(1.5)$$

where $\triangle F^1$ is the free energy difference per mole for hydrogen adsorption in the C_i state and in the Van der Waals layer. Hence, for hydrogen:-

$$\left[H_{C_i}\right] = \text{constant } p^{\frac{1}{2}} \exp(-\triangle F^1/2RT) \quad \ldots\ldots\ldots\ldots\ldots (1.6)$$

It was then postulated that the process:-

$$\left[H_{C_i}\right] \longrightarrow \left[H_{C_f}\right] \quad \ldots\ldots\ldots\ldots\ldots\ldots\ldots\ldots (1.7)$$

was a unimolecular one involving transformation (rehybridisation) of the hydrogen atoms to a state of lower potential energy. Provided, therefore, that the transmission coefficients at points Y and Z approach unity, it is evident that no activation energy is required to proceed from the Van der Waal's state through C_i to C_f.

However, the measured heat of chemisorption decreases with the amount sorbed, (q), thus, after an amount q^1 has been sorbed, the potential energy curve changes from ABC, DEC to A^1B^1C and D^1E^1C. When the point of intersection, G, is raised above OO^1 the transformation C_i to C_f required an enthalpy of activation, E(q), which increases with the increase of q. For increasing values ($\triangle$ 500 cal.) of the free energy of activation, $E^1(q)$, the transference from C_i to C_f becomes slow compared with the rate of adsorption from and desorption to, the Van der Waal's layer so that the equilibrium (equation 1.3) is rapidly set up at the beginning of the slow process and remains substantially so throughout. Simultaneously E^1 remains a constant distance below OO^1. The rate r_s

is therefore/...

is therefore given by

$$r_s = \text{constant } p^{\frac{1}{2}} \exp(-\Delta F^1/2RT) \exp(-E^1(q)/RT \quad \ldots\ldots (1.8)$$

where $E^1(q)$ was required to be an explicit function of q.

As the rate measurements usually extended over a 5-10% variation in coverage and since the heat of adsorption was found to decrease linearly with q over this range[48], if the relevant slopes of the curves BG and DG are reasonably straight, E(q), the enthalpy of activation, will increase linearly with q. It seems also feasible that $E^1(q)$ will vary likewise. However, it is of importance to note that if ΔF^1 does not remain constant with dosage and there is every likelihood that some variation will result, this would be reflected in the constantcy of the $E^1(q)$ vs q plot.

Writing $E^1(q) = C(q - q_o)$ ..... (1.9)

where q_o is the value of q when G reaches OO^1 we have

$$r_s = \text{constant } p^{\frac{1}{2}} \exp(-cq/RT) \quad \ldots\ldots (1.10)$$

for hydrogen, which with $b = c/RT$ and $a = \text{constant } p^{\frac{1}{2}}$, is the Elovich equation[53].

The kinetics of hydrogen atom recombination on the metal surface have been dealt with by Leypunsky[54-57] and later, in more detail, again by Ehrlich[44], both deriving essentially the same recombination expression (equation 1.12). At low temperatures of deposition the only interactions occurring are those between the adatom and the lattice. However, as the temperature is increased the vibrational amplitude of the atoms around their equilibrium positions increases until at a sufficiently high temperature the M-H bond is ruptured and evaporation will result. If, however, each binding site is not completely isolated and the potential

wells overlap/...

wells overlap sufficiently, movement over the surface, involving a smaller potential barrier than evaporation will result at lower temperatures. Motion over the surface is thus dictated by V_D (see FIGURE 1). If the adatoms spend a time τ_v at their sites before migrating and spend an average time, τ_m, before losing their migration energy and become relocalised, the rate, r_c, at which two atoms collide will be given by

$$r_c = \sqrt{2}\, n^2 \sigma_o \left[\tau_m / (\tau_m + \tau_c) \right] \Omega \qquad \ldots\ldots\ldots\ldots \quad (1.11)$$

using a hard sphere approximation[58], where n is the concentration of adatoms per unit area, σ_o, the hard sphere collision diameter and Ω the average velocity of the migrating atoms parallel to the surface. The ratio of the average time spent migrating between binding sites to the time spent in a potential well, τ_m/τ_v, is equal to the ratio of the partition functions for the two respective states and is thus given by the product of an appropriate entropy term and a Boltzmann factor, $\exp (- V_D/kT)$. At low temperatures $\tau_v \gg \tau_m$. $\Omega\ \tau_m$ is the mean free path of the migrating atom and at low temperatures can be approximated by the mean separation of the binding sites, a. Since the collision diameter will be of the same order of magnitude as a, equation (1.11) becomes

$$r_c \sim \sqrt{2}\ (n^2/N)\ \nu_D \exp \left[-V_D/kT \right] \qquad \ldots\ldots\ldots\ldots\ldots\ldots \quad (1.12)$$

where $N = 1/a^2$ and $1/\tau_v = \nu_D \exp \left[- V_D/kT \right]$ = the frequency of jumping out of the binding sites. (At higher temperatures where $kT \sim V_D$, $\tau_m \gg \tau_v$ and we obtain

$$r_c = \sqrt{2}\ n^2\ \sigma_o \Omega, \quad \Omega = (\pi kT/2m)^{\frac{1}{2}} \qquad \ldots\ldots\ldots\ldots\ldots \quad (1.13)$$

which is/...

which is precisely the expression for the rate of collision in an ideal two dimensional hard sphere gas).

Ehrlich has also introduced a steric factor, K_m ($\pm$ 1/10) to account for the configuration of the adatom complex, the efficiency of energy transfer and the shape of the potential energy curve. The final equation is thus:-

$$r_c = \sqrt{2}\, K_m\, (n^2/N)\ \nu_D \exp\left[- V_D/kT\right] \quad \ldots\ldots\ldots\ldots\ldots (1.14)$$

The process of heterogeneous recombination is essentially comprised of two rate processes; surface recombination, as discussed above, and direct recombination. The latter involves direct interaction between a gas phase atom and an adatom resulting in molecule production. In the steady state, the rate at which atoms become chemisorbed can be equated to the sum of the rates of those processes leading to the depletion of the adsorbed layer. The various rates of surface atom depletion are listed below together with the corresponding rate of chemisorption of the atoms.

Rates of surface depletion:-

(a) Through surface recombination:

$$r_c = \sqrt{2}\ K_m\, (n^2/N)\ \nu_D \exp\left[-V_D/kT\right] \quad \ldots\ldots\ldots\ldots\ldots (1.14)$$

(b) Through direct collision from the gas:

$$(n/N)\left\{ p/(2\pi m_1 kT)^{\frac{1}{2}}\ (2K_D \exp\left[- E_D/kT\right])\right\} \quad \ldots\ldots\ldots\ldots\ldots (1.15)$$

where $K_D \exp\left[- E_D/kT\right]$ expresses the minimum probability of success of a collision between a gas phase atom and an adatom producing a molecule.

(c) Through return of a reflected atom:

$$(1 - K_D \exp\left[- E_D/kT\right])\ \quad \ldots\ldots\ldots\ldots\ldots\ldots\ldots\ldots (1.16)$$

(d) Through the/...

(d) Through the rate of evaporation from the surface:

$$N \nu_E \exp \left[- X/kT \right] \quad \ldots\ldots\ldots\ldots\ldots\ldots\ldots\ldots \quad (1.17)$$

Rate of bombardment with surface

$$p / (2\pi mkT)^{\frac{1}{2}} \quad \ldots\ldots\ldots\ldots\ldots\ldots\ldots\ldots \quad (1.18)$$

The recombination coefficient, γ :-

$$\frac{\sum \text{rates of surface depletion through (a) and (b)}}{\text{Rate of bombardment with the surface.}}$$

There have been several measurements of the relative efficiencies of metals for hydrogen atom recombination and their recombination coefficients[59-65]. Early work in this field was carried out by Langmuir[66] and later detailed rate measurements include those of the Leningrad school[67-72], Bryce[73] and Brennan and Fletcher[74,75] on filaments and the less extensive Japanese studies[64,65]. Roginsky and Schechter[67] found only small differences in γ for hydrogen atoms on Pt, Pd, W, Ag and Fe. Wood and Wise[61,62] have carefully compared the efficiency of a series of metals in hydrogen atom recombination. For copper they found the activation energy for heterogeneous recombination to be 600 cal.mole.$^{-1}$ (333°K. to 693°K.) and for gold 900 cal.mole.$^{-1}$ (448°K. to 838°K.).

Reliable determinations of the rates of surface recombination at low temperatures are not available to date. Quantitative measurements were attempted by Leypunsky[54-57] for atomic hydrogen on evaporated films of copper and nickel. He found rapid uptakes exceeding ten times the monolayer capacity for molecular hydrogen on nickel and more than fourteen times the available surface site concentration for copper.

No activated/...

No activated adsorption of hydrogen molecules was found on copper while for hydrogen atoms the amount sorbed during the fast uptakes was practically independent of the amount previously adsorbed. He also found that the desorption of atomic hydrogen as molecules proceeded with an activation energy of 24.0 kcal.mole.$^{-1}$ on nickel films. For copper the enthalpy of activation as calculated from the temperature coefficients was 2-4 kcal.mole.$^{-1}$ while that found from the kinetic formula was 10-17 kcal.mole.$^{-1}$. This discrepancy he attributed to a large steric factor.

Blodgett[76] has extended Langmuir's early work[66] on the uptake of atomic hydrogen on metals. In one experiment she found the amount taken up by a copper film equivalent to fourteen monolayers of atomic hydrogen. There was little recovery of the sorbed gas until the temperature was above 200°K. In their surface potential studies pronounced adsorption of hydrogen atoms on copper, silver, gold and mercury films was noted by Mignolet[77,78] and Tompkins et al[79] at 90°K. despite the absence of any detectable dissociative adsorption from the molecular gas at higher temperatures. Pritchard[80] has proceeded to show that the additional uptakes of hydrogen atoms on copper films at 90°K. beyond the concentration corresponding to the maximum on the surface potential against coverage plot have no effect on the surface potential. He suggested the possibility of "solution" or sorbtion of the atoms into the metal bulk. From his surface potential measurements for hydrogen chemisorbed on copper films he found that the adatoms showed immobility at 90°K. and that the onset of mobile adsorption appears at 195°K. but no gas was evolved at either temperature. For silver and gold films,

however,/...

however, he again found immobility of the adatoms at 90°K. but on warming to 195°K. desorption occurred. These conclusions agree with the results of Nakada, Sugiura and Shida[81] who found that hydrogen atoms recombined more rapidly on silver than on copper.

More recently, Pritchard[82], using an improved technique, repeated his study of the relationships between the surface potentials of hydrogen and coverage on annealed films of copper and gold. He found changes in the surface potential-coverage relations and in the stability of the adsorbed layer near coverages of one quarter and one half, consistent with the formation of double-spaced face centred square and single-spaced simple square arrays on the face-centred (100) faces of the metals. He also measured the rates of desorption of hydrogen from a copper film in the temperature range 26°C. to -30°C. and found an apparent activation energy of 24 kcal.mole.$^{-1}$ decreasing to 8 kcal.mole.$^{-1}$ with increasing coverage.

2. OBJECTS OF THE RESEARCH

The original project was threefold; to obtain (a) sticking probabilities, S, of hydrogen atoms, (b) adsorption isotherms of hydrogen atoms and hence the heats of adsorption and (c) surface mobility activation energies of hydrogen atoms derived from the rates of desorption, all on a clean metal surface which could not adsorb hydrogen molecules in a dissociative manner.

From the hydrogen molecule pressure in the gas phase and the temperature of the hot tungsten filament used to produce the hydrogen atoms, the rate of atomisation could be evaluated from the very accurate work of Brennan[74]. Since for hydrogen molecules at pressures of 10^{-3} mm.Hg. and lower the mean free path of the hydrogen atoms produced at the surface of the filament far exceeds the dimensions of the spherical adsorption vessel the rate of bombardment of the film by hydrogen atoms will be known and from a measurement of the rate of uptake, the sticking probability would be accessible. The pressures required in sticking probability experiments are low, 10^{-8} mm.Hg. at most[102] otherwise adsorption proceeds at an immeasurably fast rate. Here, however, by keeping the temperature of the filament at 1300°K., equilibrium pressures of hydrogen atoms of 10^{-14} - 10^{-17} mm.Hg. were easily and reproducibly obtained. However, if $S \neq 1$ then the concentration of hydrogen atoms must accumulate in the gas phase as the process proceeds and a means of measuring the concentration of hydrogen atoms in the gas phase by an independent method became essential. Unfortunately no gauge[103] sufficiently sensitive for the low concentrations in a static system could be developed.

Similarly/...

Similarly, attempts to obtain isotherms at low hydrogen atom pressures (10^{-14} mm.Hg.) and higher temperatures proved unsuccessful because of having no independent means of measuring the pressure of the atoms and also because while saturation of the surface layer proceeded, hydrogen atoms also penetrated into the metal bulk and the uptake was found to proceed indefinitely.

However, atoms deposited from a beam would become randomly chemisorbed over the surface since the driving force for the adsorption was large and there would be no barrier to the process. For metals such as copper, silver, gold, cadmium and zinc, the M-H bond energy, X, is such that $2X \angle D$, where D is the dissociation energy of the molecule so if the adatoms were rendered mobile by interrupting the deposition and raising the substrate's temperature, the hydrogen adatoms would collide on the surface to form hydrogen molecules which would then be immediately desorbed. The rate determining process would thus be surface diffusion and from the temperature coefficient of the rate of hydrogen molecule evolution, the activation energy for mobility could be obtained.

No direct measurements or detailed investigations have been carried out of the variation of these effects with various concentrations of hydrogen atoms on the surfaces of the metals mentioned above at low temperatures. Thus valuable information regarding the surface energetics could be obtained from measurement of the relative volumes of hydrogen molecules desorbed and their rate of desorption from the surfaces of those metals on which varying concentrations of hydrogen atoms were deposited at $78^{\circ}K$. It was also of interest to study these effects on a metal surface previously saturated with dissociatively adsorbed hydrogen molecules at $78^{\circ}K$. e.g. nickel.

3. APPARATUS/...

3. APPARATUS AND EXPERIMENTAL PROCEDURES

1. Description of the Apparatus

The apparatus used for the subsequent experiments was constructed of Pyrex glass and is shown diagrammatically in FIGURE 3. It can be subdivided into four main sections; the pumping system, the gas storage and purification section, the gas dosing system and, finally, the adsorption or reaction system.

The pumping system

The pumping system consisted of a modified divergent nozzle "Crawford" diffusion pump[83] backed by a two stage mercury diffusion pump which in turn was backed by a "Hyvac" rotary oil pump. Mercury was prevented from passing into the oil pump or the adsorption section by traps cooled in liquid air. To facilitate rapid evacuation, tubing connected directly to the pumps was mainly 25 mm. in diameter while throughout the rest of the apparatus the diameter of the tubing used was 11.8 mm.

The ultimate vacuum attainable in the apparatus was better than 10^{-6} mm.Hg. and reactions were not attempted until the accumulation of gas in the apparatus was less than 2×10^{-6} mm.Hg. in three hours. The apparatus was kept pumping continuously with the exception of the reaction sections which were isolated from the pumps as required.

Taps were greased with Apiezon L grease. A freshly regreased apparatus required several days continuous pumping with all the accessible glass being simultaneously flamed out by means of a hand torch. During this period the reaction section was baked out by means

of an/...

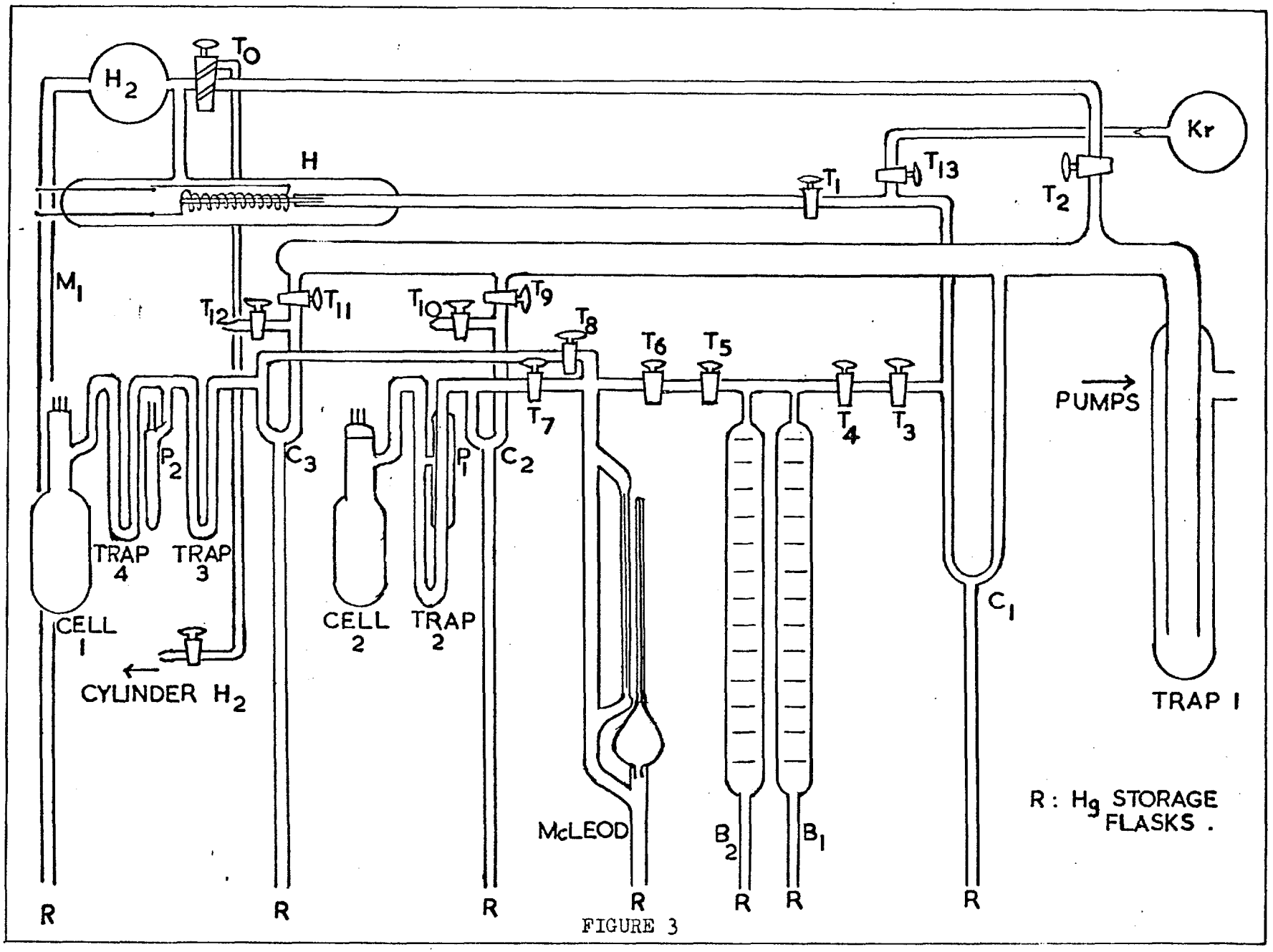
H2
T0
H
T1
T13
T2
Kr
M1
T12
T11
T10
T9
T8
T6
T5
T7
T4
T3
PUMPS
P2
C3
P1
C2
C1
TRAP 4
TRAP 3
CELL 1
CYLINDER H2
CELL 2
TRAP 2
McLEOD
B2
B1
TRAP 1
R
R
R
R
R
R
R
R : Hg STORAGE FLASKS .

FIGURE 3

of an electric furnace and heating tapes at a temperature of about 380°C. and the taps were turned repeatedly until the grease attained a temperature slightly below its softening point.

The gas storage and purification section

This section could be isolated from the dosing system by the mercury cut off C_1, and was evacuated via tap T_2, and the two-way tap T_o. The hydrogen storage bulb was pumped to the hardest vacuum and thoroughly outgassed before being flushed several times with hydrogen from a cylinder. The pressure in the storage bulb is recorded on the mercury manometer, M_1. After flushing repeatedly, a sample of gas was retained and the purification commenced. This process was repeated before each purification and no purified gas was kept for periods of longer than a day.

The hydrogen was purified by diffusion through an indirectly heated palladium thimble H; the purified gas passing by way of tap T_1, into the dosing system. A considerable volume of hydrogen was allowed to diffuse through the thimble to waste before a sample of the gas was permitted to pass into the dosing system.

For surface area measurements "Specpure" krypton gas could be introduced into the system via tap T_{13}.

The gas dosing system

By means of tap T_1 the purified hydrogen was introduced into the dosing system with the cut off C_1 raised, tap T_3 open and tap T_4 closed. The incremental pressure was read on a cathetometer. Tap T_3 was then closed and with tap T_5 closed, tap T_4 was opened to introduce the gas

into the/...

into the gas burettes B_1 and B_2. Finally, by means of taps T_5 and T_6, a known volume of the expanded gas was dosed into the reaction section.

The following volumes of this section of the apparatus were calibrated by water ($\pm$0.05 cc.):

Volume between tap T_3 and tap T_4:-	4.25 ccs.
Volume between tap T_4, tap T_5, and the final calibration mark on the gas burettes:-	38.20 ccs.
Volume of each gas burette (marked in 1 cc. divisions):-	150.0 ccs.
Volume between tap T_5 and tap T_6:-	4.15 ccs.

The reaction system

In order to facilitate a prolonged and thoroughly rigorous outgassing procedure two similar adsorption sections were introduced into the apparatus after tap T_6. These sections could be isolated from the main pumping line by means of taps T_{11} or T_9, or the cut offs C_2 or C_3, respectively.

Essentially each comprised the McLeod gauge, a cut off, cold traps, a Pirani gauge and the reaction cell. Their corresponding air admission taps were T_{12} and T_{10} respectively. The taps T_8 and T_7 provided selective isolation for each system during the reaction process. The rates of uptake or desorption of the gas from the film in the cell were measured by the pressure change in the static system read on the McLeod gauge of range 1×10^{-5} to 2×10^{-1} mm.Hg. and on the Pirani gauges with accurate and rapid responses from 5×10^{-5} to 5×10^{-3} mm.Hg.

Both the/...

Both the Pirani gauges and the U-traps were designed for Dewar flasks which could be allowed to remain overnight without any appreciable refrigerant evaporation; after a period of two days the flasks still remained three quarters filled.

2. Calibration of the Volumes of the Reaction Systems and the McLeod Gauge

The volumes of the two systems were calibrated as far as possible with water and then calibrated using gas expansion.

McLeod gauge:

Volume of bulb (by water)	343.0 ccs.
Diameter of capillary (by mercury)	0.09776 cms.

System 1

Volume of cell (by water)	380.0 ccs.
Volume of Pirani gauge (by water)	60.0 ccs.
Volume of trap T_3 (by water)	41.0 ccs.
Volume of trap T_4 (by water)	60.0 ccs.
Total volume at room temperature (by gas expansion)	1134.0 ccs.

System 2

Volume of cell (by water)	249.0 ccs.
Volume of trap T_2 and Pirani gauge (by water)	33.0 ccs.
Total volume at room temperature (by gas expansion)	756.0 ccs.

3. The Pirani Gauges

As the Pirani gauges were primarily intended for use in the rate measurements, rapid response and facility of reading were properties

of particular/...

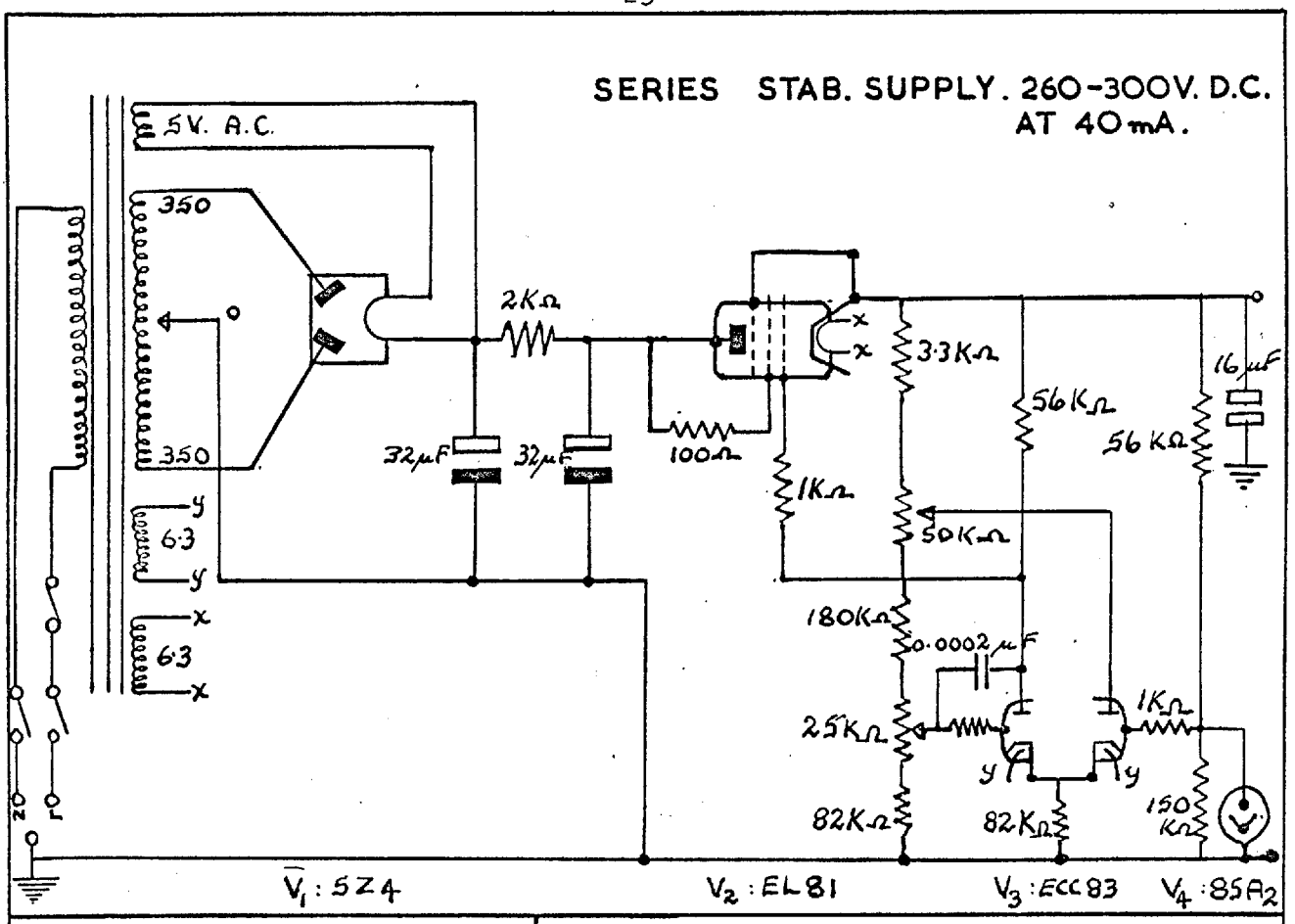
SERIES STAB. SUPPLY. 260-300V. D.C.
AT 40mA.
5V. A.C.
350
350
6·3
6·3
2KΩ
32μF
32μF
100Ω
1KΩ
3·3KΩ
56KΩ
56 KΩ
16μF
50KΩ
180KΩ
0·0002μF
25KΩ
1KΩ
82KΩ
82KΩ
150 KΩ
V1 : 5Z4
V2 : EL81
V3 : ECC83
V4 : 85A2

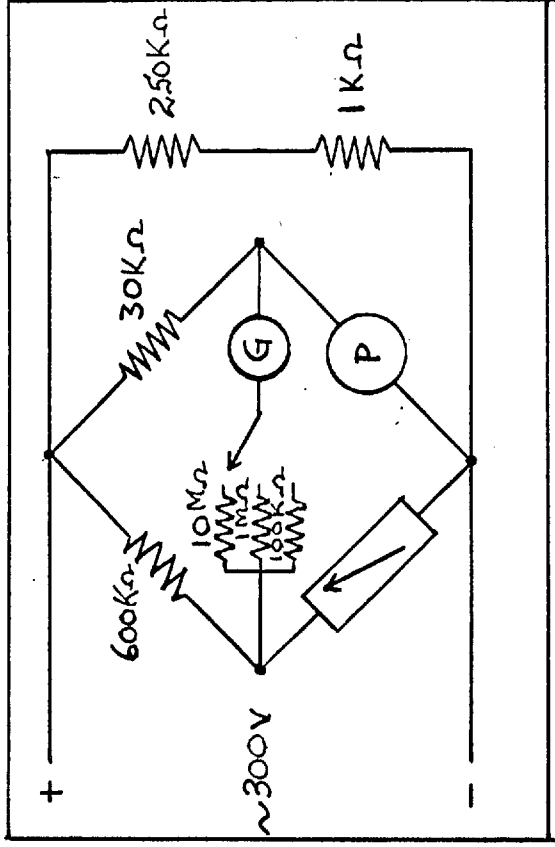
250KΩ
1 KΩ
30KΩ
G
P
10MΩ
1MΩ
100KΩ
600KΩ
~300V
+
-

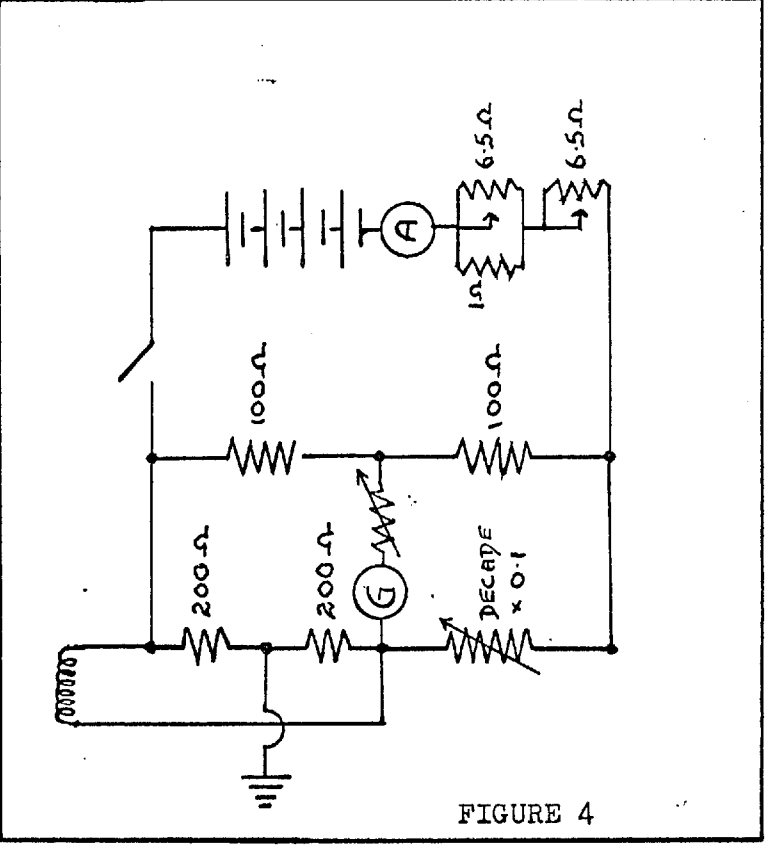
6·5Ω
6·5Ω
A
1Ω
100Ω
100Ω
200Ω
200Ω
G
DECADE
x 0·1

FIGURE 4

of particular importance. The constructional details of the heads were of the simplest possible design[84]. A tungsten filament of about 120 ohms resistance was stretched between and spot welded to nickel clips which in turn were spot welded to tungsten support rods (1.5 mm. diameter), care being taken to avoid twisting of the wire during the stretching of the filament. The tungsten support rods were glass coated as far as possible and were held in pinched or button glass/metal seals. For maximum sensitivity the gauges were operated with their heads immersed in liquid nitrogen. The refrigerant level was always maintained at a constant height, well above the top of the filament. In both systems the heads were protected from mercury vapour by means of cold traps.

The measuring circuit was a simple Wheatstone Bridge (FIGURE 4). A highly stabilised voltage of about 300 volts D.C. at 40 mA was supplied across the bridge. This was stepped down by high resistors in two of the ratio arms, thus producing a constant voltage and, virtually, a constant current supply since the current drawn through the Pirani was almost negligible. The ratio of the fixed arms of the bridge was 20 to 1. A Tinsley galvanometer type SS2.45.5269 A of variable sensitivities (210 mm., 21 mm., 2.1 mm., 0.21 mm. per μ.amp. respectively, periodic time, 2 sec.) was used in the measuring circuit.

The Pirani zero, R_o, was the resistance of the filament at 10^{-6} mm.Hg. pressure and $78^{o}K$. Equilibrium and stability were established after about 45 minutes after switching on the current supply. No fluctuations occurred in the zero value during the experiments. An

overall decrease/...

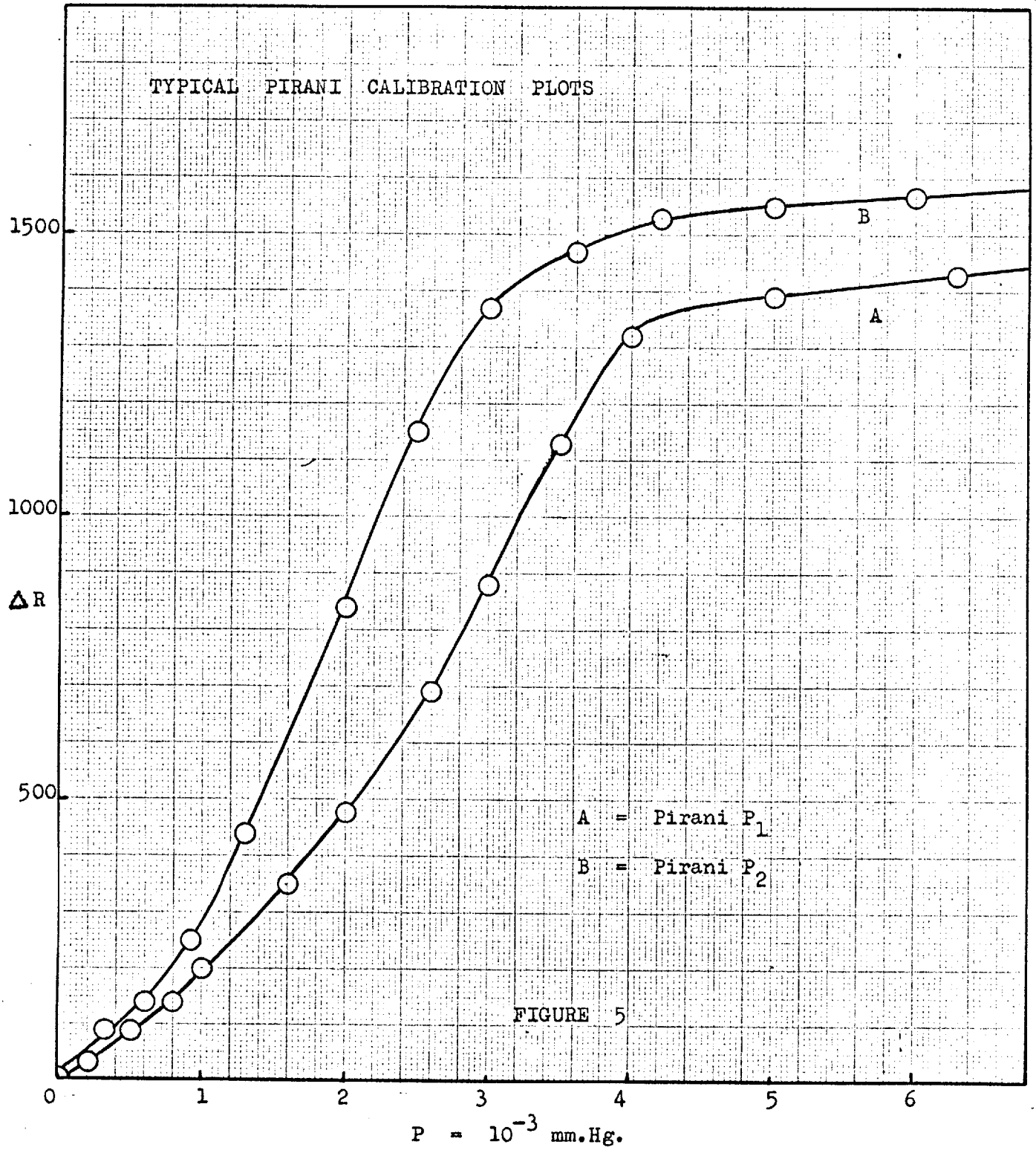
TYPICAL PIRANI CALIBRATION PLOTS
1500
1000
500
ΔR
B
A
A = Pirani P_1
B = Pirani P_2
0
1
2
3
4
5
6
P = 10^{-3} mm.Hg.

FIGURE 5

overall decrease in R_o of about 10-20 ohms was found after some 3-4 months operating time but R_o could be returned to its original value by suitable outgassing of the tungsten filament.

The incremental decrease in the resistance (R_o - R) was used throughout as a measure of the pressure. Typical calibration curves for hydrogen are shown in FIGURE 5. These were not found to be strictly reproducible from run to run, but during each run sufficient McLeod gauge readings were taken to check the calibration. The sensitivity of the gauges fell sharply above 4.0×10^{-3} mm.Hg. so higher pressures were always read on the McLeod gauge.

4. The Reaction Cells

Essentially of the same basic design but differing in volume, the experimental arrangement of the cells consisted of an atomising filament suspended from 1.5 mm. diameter ground tungsten leads, glass coated and pinched sealed into the neck of a cylindrical Pyrex glass reaction vessel. The volume of the cells were 380 and 249 ccs. respectively. The throwing filament was suspended as shown (FIGURE 6). The glass/metal pinched seal was capable of carrying 10 amps. safely and the rods were connected by porcelain connectors to a transformer and variable mains voltage supply for throwing the film. The necks of the vessels were elongated so that the film bulbs could be completely immersed in coolant to a depth of several cms.

The larger cell (bulb dimensions: length 11.0 cms., diameter 6.8 cms.) was mainly used for nickel while the smaller cell (bulb dimensions: length 9.0 cms., diameter 5.6 cms.) was used for the remaining metals.

Initially/...

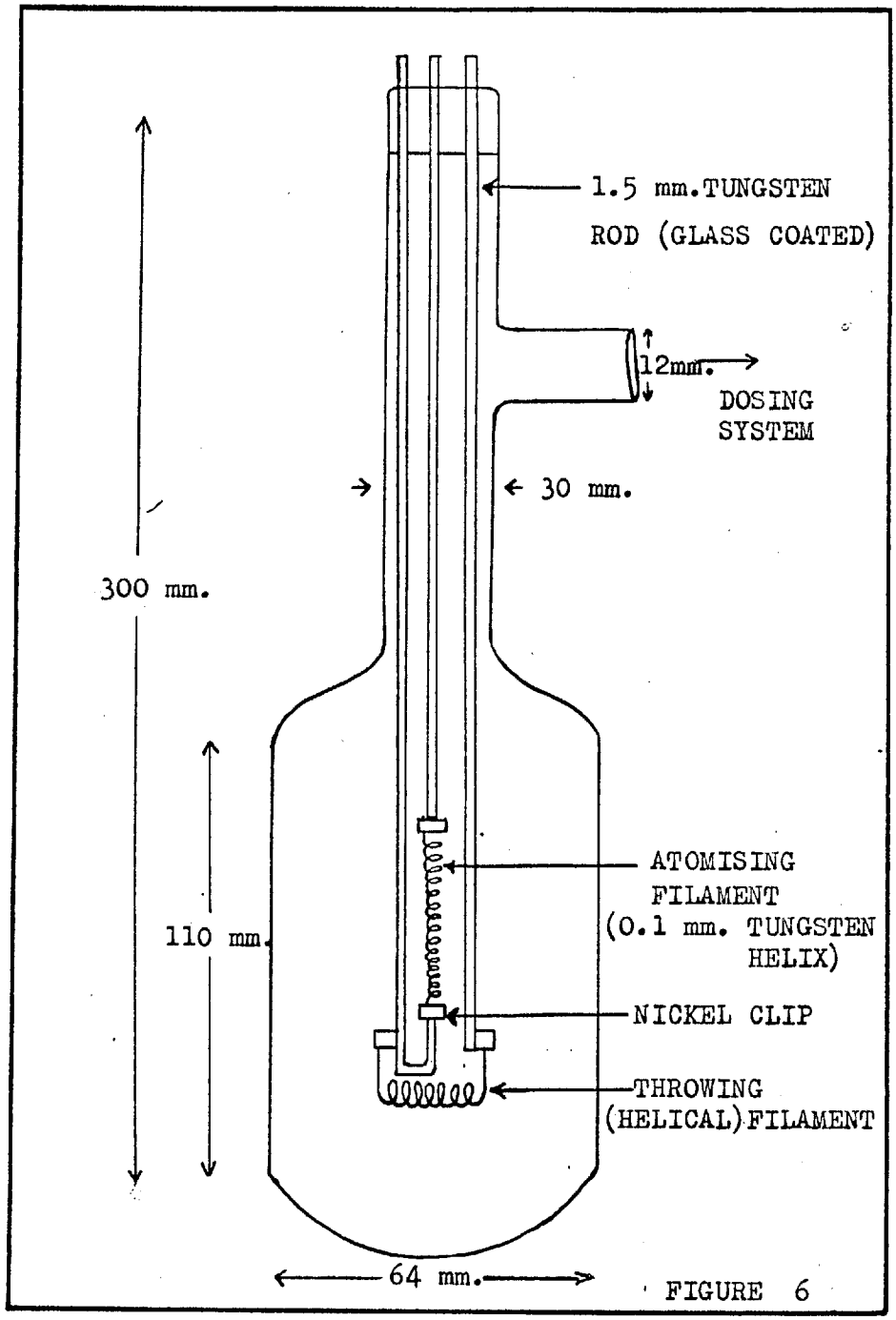
1.5 mm.TUNGSTEN
ROD (GLASS COATED)
12mm.
DOSING
SYSTEM
30 mm.
300 mm.
110 mm.
ATOMISING
FILAMENT
(0.1 mm. TUNGSTEN
HELIX)
NICKEL CLIP
THROWING
(HELICAL) FILAMENT
64 mm.

FIGURE 6

Initially a close fitting glass shield was placed in the neck of the cell to prevent any film being thrown above the open end of the bulb but it was of sufficient clearance to allow passage of the tungsten rods. However, as the film very seldom coated the neck of the cell to any marked degree, this was later discontinued. No difference was noted in adsorption or desorption characteristics of the experiments on removal of the shield.

After completion of the experiment the cells were cut along the neck well away from the pinched seal and the whole assembly (bulb, neck and rods) well cleaned with HCl. The whole assembly was then in turn rinsed with a dilute caustic solution followed by a distilled water and Teepol rinse and, eventually, by several rinses with distilled water. The glass interior was then carefully wiped dry with cotton wool and absorbent paper before being dried in a current of hot air.

5. The Filaments

(i) Film throwing filaments

The various films were thrown in the cell using the filaments tabulated below in TABLE 1. The 0.5 mm. tungsten hairpin used as the heater was thoroughly cleaned by A.C. electrolysis in a dilute caustic solution before use.

The helices were wound on to the heater as tightly as possible by means of a pin chuck and pin vice to prevent "hot spots" developing during the outgassing of the wire.

TABLE 1/...

TABLE 1

Metal	Heater	Shape of metal hairpin	Diameter of wire used (mm.)	Current for throwing (mA)	Approx. time of throwing (hrs.)
Nickel	Nickel	hairpin	0.5	6.0	1-2
Cadmium	Tungsten	helix	1.0	3.0	1
Zinc	Tungsten	helix	±1.5	4.0	1-2
Copper	Tungsten	helix	0.5	6.0	2½-3
Silver	Tungsten	coiled coil	1.0	2.8	1
Gold	Tungsten	helix	0.2	4.5	1-2

The wires were all supplied by Johnson Matthey Ltd., and their purities are tabulated below in TABLE 2.

TABLE 2

Metal	% Purity	Impurities (p.p.m.)
Nickel	SpecPure	Si:7, Fe:5, Mg:2, Al:2, Ca,Cu,Si:1 each
Cadmium	99.95 (Grade 1)	Not quoted
Zinc	99.90 (Grade 1)	Not quoted
Copper	99.99 (Grade 1)	Not quoted
Silver	SpecPure	Bi, Cu, Fe, Pb, Mg, Na, $\angle$ 1
Gold	SpecPure	Ag:3, Cu,Si:1 each, Na, $\angle$ 1
Tungsten	Thorium Free (Grade 1)	Fe:30,000, P and S:10,000

(ii) The atomising filaments

The atomising filaments of the cells consisted of 25 cm. lengths of 0.1 mm. black drawn, high purity, thorium free, tungsten wire ex Mullards Ltd. (Blackburn). The wire was carefully coiled into a helix of 2.5 mm. diameter, about 3.0 cms. in length, and A.C. electrolysed in a dilute caustic solution to remove any surface impurities.

It was/...

It was then carefully rinsed in distilled water, dried on absorbent paper and spot welded between a pair of nickel clips on the tungsten supports as shown (FIGURE 6). The filament was situated in the cell so that at the pressures under consideration (10^{-3} mm.Hg. and lower) the atoms would impinge on the surface of the cell before colliding with each other.

During the outgassing procedure of a new filament it was found necessary to keep a low pressure of hydrogen in the cell to prevent any oxide film from being thrown on to the cell walls. The final outgassing was carried out above 2,500°C. and this served to age the filament.

The resistance of the filament was measured using the circuit described in FIGURE 4. The atomising filament formed one arm of a Wheatstone bridge circuit. The arm in series with it was a decade resistance box capable of reading to 1/10th ohm. The other bridge arms were 100 ohms each. The bridge current was supplied by accumulators. The current necessary to produce the required temperature of the filament was obtained by adjustment of the decade resistance. Very little fluctuation, if any, occurred during an experiment. In parallel with the filament was a 400 ohm resistor (2 x 200 ohm wire wound resistors), centre tapped to earth.

The filament temperature was determined using a Cambridge disappearing filament optical pyrometer with an accuracy of $\pm 10^{\circ}$K. Accurate temperature calibration of the filament proved exceedingly difficult as the temperature along the axis of the coil varied by about 50°K. However, at a fixed resistance, the highest temperature on the coil was

reproducible/...

reproducible. The calibrations were carried out on the filament in vacuo. Except where as otherwise stated the atomising filament was maintained at 1100°C.

6. Experimental Procedure

(i) Outgassing

After the initial outgassing of the tungsten atomising filament no further outgassing of this filament was carried out apart from flashing above 2,500°C. just before the commencement of a run. After fitting a tared, throwing filament on to the nickel sleeves and sealing the cell, the system was evacuated to 10^{-6} mm.Hg. and the outgassing heaters were switched on. The film bulb was baked in a glass-walled furnace at 360°C., the Pirani head and cold traps and associated tubing with heating tapes at 220°C. while any other naked glass ware was flamed out with the hand torch, the taps being turned intermittently. This heating procedure was continued for about 24 hours after which time the throwing filament and glassware were alternately heated for periods of 12 hours or more, up to a total outgassing period of three to four days. Surface oxide was removed from the throwing filament and the nickel clips by heating the former to above red heat in a few mm.Hg. of hydrogen. The hydrogen was pumped away after a few minutes and the treatment repeated until no trace of surface oxide was visible. The filament was then heated just below its evaporation temperature until no measurable quantity of gas was evolved in a vacuum of 10^{-6} mm.Hg. over a period of several hours.

(ii) Film throwing

Prior to/...

Prior to throwing the film the cold traps were cooled in liquid nitrogen and the reaction system was baked out for a further 12 hours so that the mercury vapour was condensed from this section. The remaining heaters were then subsequently removed and, after cooling, the cell and Pirani gauge were immersed in liquid nitrogen. The filament temperature was then slowly raised to the temperature of throwing with the pumps on for all but the last 30 minutes of throwing, as spurious bursts of gas were found to be evolved from the filaments while throwing the film. No build up of pressure was observed during the isolation period. The current was switched off when the film was adjudged sufficiently thick and the liquid nitrogen bath removed.

The film was then thermally cycled several times between liquid nitrogen temperature and about 10°C. above room temperature remaining at the higher temperature for about 10 minutes per cycle. Unless otherwise specified this procedure was carried out for all the films used. Colour changes were observed for the films of copper, silver and gold on warming; for copper, from deep green to red-brown, for silver, from deep purple to grey-white and for gold, from deep red to yellow. These colour changes are presumably related to the aggregation of the metallic particles on sintering. After four thermal cycles, the films were found to be sufficiently reproducible for the subsequent experiments.

The films covered all the available glass and exposed metal in the bulb of the cell. Slight shadowing occurred in the neck and on the inner surface of the pinched seal but for the purpose of surface area

calculations/...

calculations this comparatively small area was neglected. After completion of the experiment the cell was carefully cut down from the apparatus, opened and the filament removed and reweighed.

(iii) Temperature baths

To effect the rapid changes in temperature necessary between 78°K. and 305°K., a number of constant temperature baths of high thermal capacity were used. The temperatures were checked, where possible, using a copper-constantin thermocouple and a potentiometer. Details of the baths are given below in TABLE 3.

TABLE 3

Temp. °K.	Bath	Temp. Fluctuation °K
78	Boiling nitrogen	-
90	Boiling oxygen	-
113	Melting isopentane	±1.0
142	Melting n-pentane	±1.5
148	Melting methyl cyclohexane	±1.0
160	Melting ether	±1.0
178	Melting toluene	±1.0
195	Carbon dioxide in alcohol mixture	±1.0
210	Melting chloroform	±1.0
223	Melting diethyl malonate	±0.5
250	Melting carbon tetrachloride	±0.5
261	Melting methyl benzoate	±0.5
273	Melting ice	±0.1

The freezing baths were prepared by carefully adding liquid nitrogen with vigorous stirring.

7. Sorption and Desorption Measurements

It was possible to calculate the number of molecules adsorbed on the film/...

the film at any stage simply by subtracting from the number of molecules added, N_A, the number which are present in the gas phase at that pressure and the given temperature. The number of molecules added was calculated from the volume of the dosing section, the temperature and the gas pressure. The number of molecules remaining in the gas phase is, however, a function of the pressure. Differences in pressure in the cold regions from those at room temperature arise due to thermomolecular flow. The necessity of such corrections has been adequately demonstrated by Tompkins and Wheeler[85], Porter[86] and other workers[87,88]. Various theoretical approaches have been made, of these that due to Liang[89-92] is the most simple and easy to compute as compared with the derivation of Webers and Keesom[93] and its later development[94].

More recently Bennett and Tompkins[95] suggested a modification of Liang's empirical equation by the introduction of a factor:-

$(\phi gX)/(\phi g \text{ calc.}) = f$, to give

$$R = \frac{P_1}{P_2} = \frac{\alpha_{He}(f.\phi gX)^2 + \beta_{He}(f.\phi g.X) + R_M}{\alpha_{He}(f\phi gX)^2 + \beta_{He}(f.\phi g.X) + 1} \quad \ldots\ldots\ldots \quad (3.1)$$

where

f = 1 for tubing internal diameter $\lesssim$ 1 cm.

= 1.22 for tubing internal diameter $\gtrsim$ 1 cm.

P_1 = pressure (mm.Hg.) at lower temperature, T_1.

P_2 = pressure (mm.Hg.) at room temperature, T_2.

$X = P_2 d$

d = internal diameter of tubing under investigation.

$R_M = (T_1/T_2)^{\frac{1}{2}} \lesssim 1$, T_1, T_2; ^{o}K.

α_{He} = /...

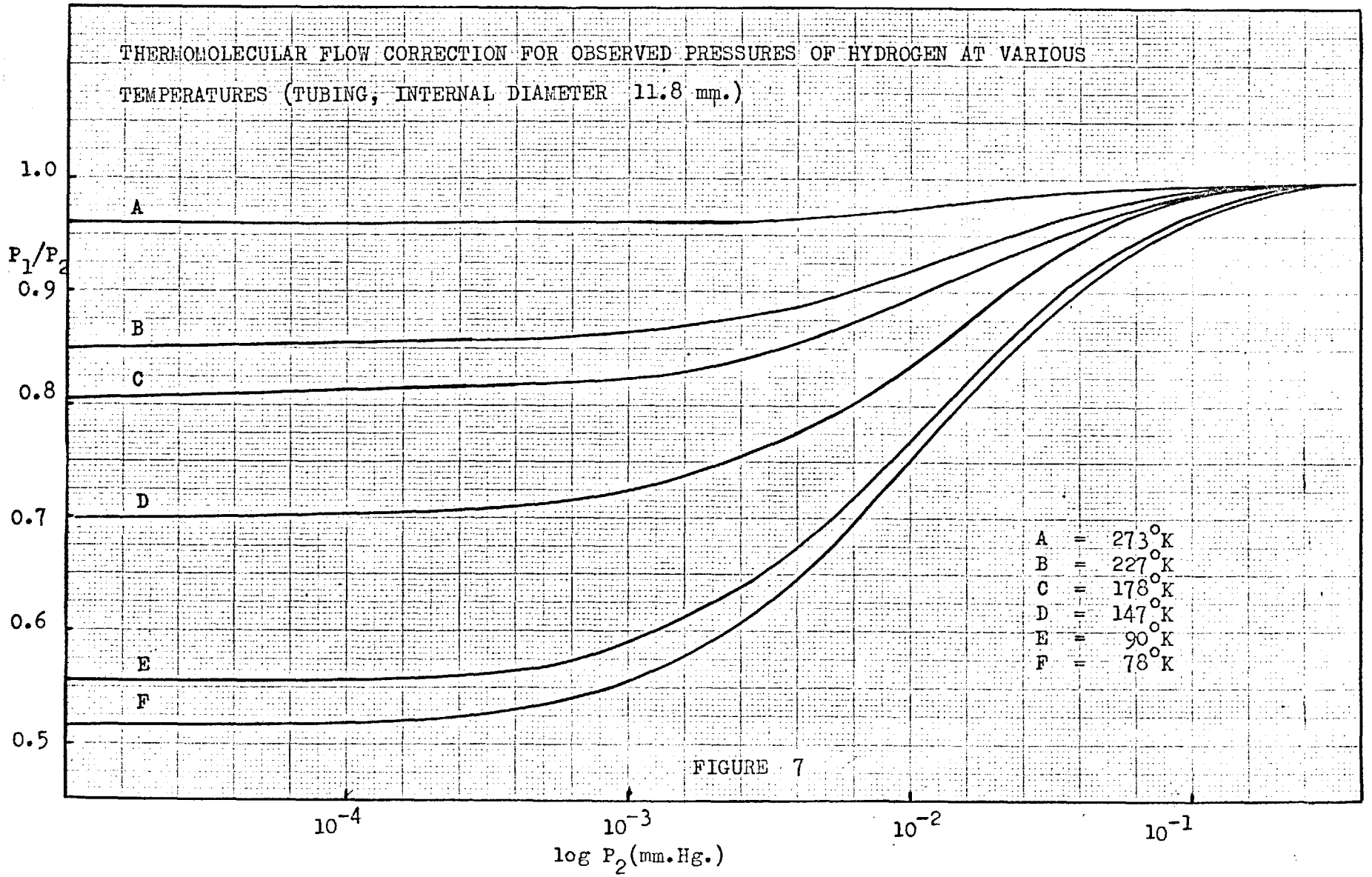
THERMOMOLECULAR FLOW CORRECTION FOR OBSERVED PRESSURES OF HYDROGEN AT VARIOUS TEMPERATURES (TUBING, INTERNAL DIAMETER 11.8 mm.)
1.0
0.9
0.8
0.7
0.6
0.5
P_1/P_2
A
B
C
D
E
F
A = 273°K
B = 227°K
C = 178°K
D = 147°K
E = 90°K
F = 78°K
10^{-4}
10^{-3}
10^{-2}
10^{-1}
log P_2(mm.Hg.)

FIGURE 7

α_{He} = $3.70(1.70 - 2.6 \times 10^{-3} T)^{-2}$ where $T = T_2 - T_1$.

β_{He} = $7.88 (1 - R_M)$, for $R_M \leq 1$.

ϕg = the pressure shifting factor which depends on the gas and is defined such that $\phi_{He} = 1$.

ϕg calc. = may be calculated from the collision diameter, r_o, using the relationship

$\log r_o = 0.43 + 0.24 \log \phi g$[96,97]

r_o = the equivalent elastic sphere diameter calculated from viscosity data using the Lennard-Jones 12:6 potential function.

The calculated values for P_1/P_2 are plotted against log P_2 for hydrogen and krypton in FIGURES 7 and 8 respectively. (Internal diameter of tubing, 11.8 mm.).

The total number of molecules in the gas phase, Ng, was calculated from:

$$Ng = \frac{P_1V_1}{RT_1} + \frac{P_2V_2}{RT_2} + \frac{P_3V_3}{RT_3} + \frac{P_4V_4}{RT_4} \quad \ldots\ldots\ldots \quad (3.2)$$

where the subscripts 1, 2, 3, 4 refer in turn to the cell, the part of the system at room temperature, the Pirani head and the cold traps respectively.

8. Surface Area Measurements

The surface area of the metal has been determined using krypton as the adsorbate at liquid nitrogen temperature. The surface area is then estimated by multiplying the number of krypton atoms required to form a monolayer by the area of a krypton molecule[98] (19.5 sq.^{o}A).

It has been/...

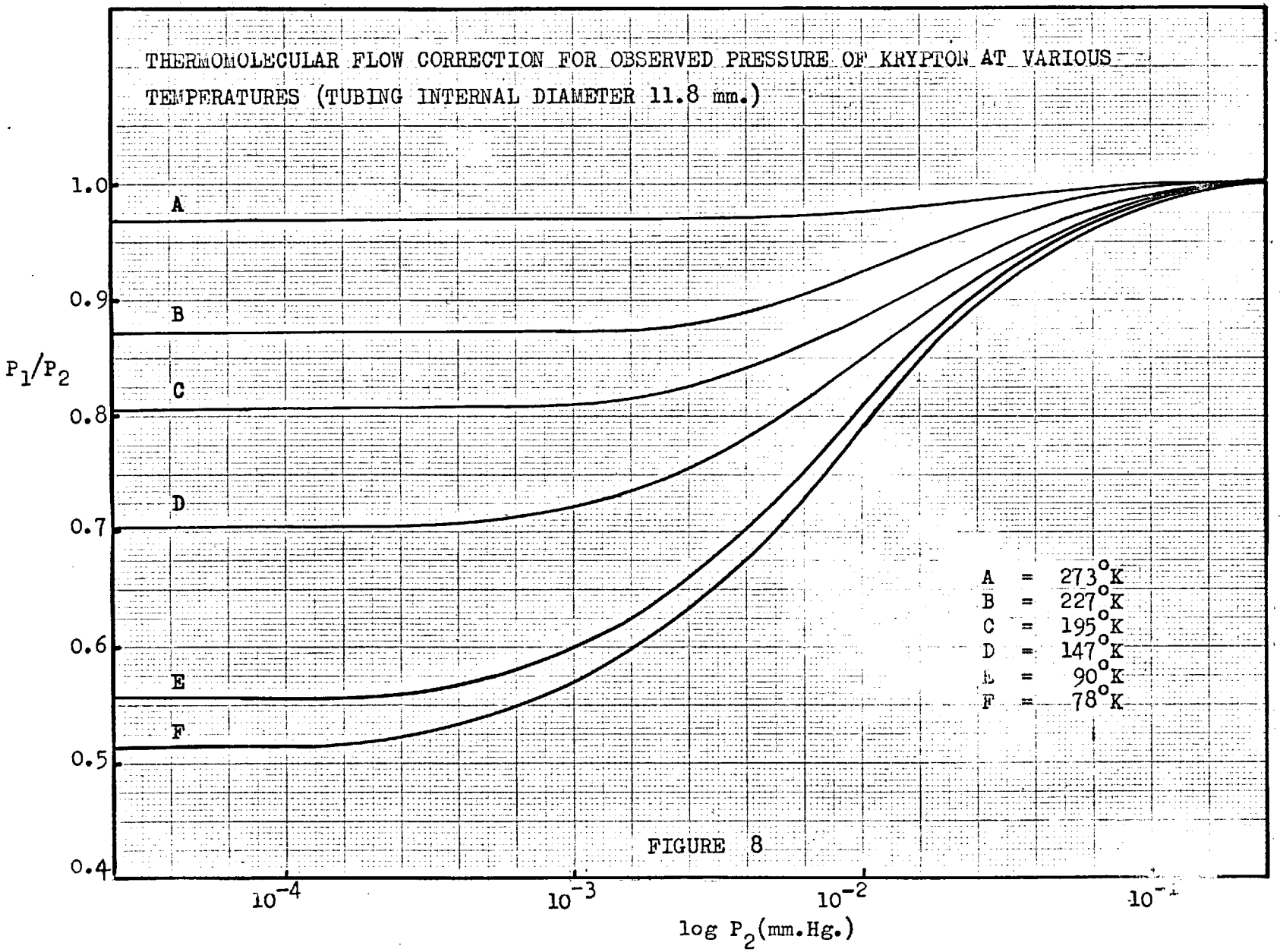
THERMOMOLECULAR FLOW CORRECTION FOR OBSERVED PRESSURE OF KRYPTON AT VARIOUS TEMPERATURES (TUBING INTERNAL DIAMETER 11.8 mm.)
1.0
0.9
0.8
0.7
0.6
0.5
0.4
P_1/P_2
A
B
C
D
E
F
A = 273°K
B = 227°K
C = 195°K
D = 147°K
E = 90°K
F = 78°K
10^{-4}
10^{-3}
10^{-2}
log P_2(mm.Hg.)

FIGURE 8

It has been shown recently by Graham[99] that V_m, the monolayer capacity, obtained from the point B method and the B.E.T. equation do agree well at intermediate relative pressures but at higher values no sharp point B was available. In some cases, at low relative pressures, the B.E.T. plots were not linear thereby reflecting a more complex mechanism of the krypton adsorption than that assumed in the B.E.T. theory. Similar curvature of the plots of the B.E.T. equation;

$$\frac{P}{V_o(P_o - P)} = \frac{1}{V_m C} + \frac{(C - 1)P}{V_m P_o} \quad \ldots\ldots\ldots \quad (3.3)$$

where P_o = saturated vapour pressure of krypton at the temperature at which the adsorption was carried out (taken as 2.0 mm.Hg.)[100]

V_o = Volume of krypton adsorbed at pressure P.

V_m = Volume of gas required to form a monolayer.

C = a constant, depending on the nature of the adsorbent and adsorbate,

was found in the present work. However, at the low relative pressures under consideration the point B method has provided an adequate approximation of the extent of the surface.

The maximum number of sites available for adsorption per sq.cm. (assuming one adatom per site) depends on the crystal structure of the metal[101] and was calculated using the equations given below:-

Number of sites for a f.c.c. metal $= \frac{1.91}{a^2} \times 10^{16}$ ..... (3.4)

Number of sites for a h.c.p. metal $= 2/3\left(\frac{1}{\sqrt{3a^2}} + \frac{1}{ac} + \frac{2}{a\sqrt{3a^2+4c^2}}\right) \times 10^{16}$ ..(3.5)

The calculated/...

The calculated values for the various metals are given in TABLE 4 below. The lattice parameters are taken from F.Seitz: "Modern Theory of Solids", McGraw Hill, N.Y. (1940).

TABLE 4

Metal	Crystal type	a(A^o)	c(A^o)	Sites per sq.cm. ($\times 10^{15}$)
Nickel	f.c.c.	3.52	-	1.54
Cadmium	h.c.p.	2.98	5.62	1.01
Zinc	h.c.p.	2.67	4.95	1.27
Copper	f.c.c.	3.61	-	1.47
Silver	f.c.c.	4.08	-	1.15
Gold	f.c.c.	4.07	-	1.15

4. RESULTS

4.1 Glass

The use of Pyrex glass as an effective "sink" for the adsorption of hydrogen atoms produced from an incandescent tungsten filament was investigated by Langmuir[66] and Bryce[73]. Bryce[73] and later Mochan[71] showed that results obtained with glass even when cooled in liquid nitrogen are unreliable. Bryce then repeated Langmuir's early work using an evaporated molybdenum oxide film as a hydrogen atom trap. He obtained for pressures of 10^{-2} - 10^{-3} mm.Hg. in the temperature range (1200-1400)°K. of the tungsten filament the following rate equation for the atomisation of hydrogen:- (atoms.sq.cm.$^{-1}$ sec.$^{-1}$)

$$a = 2.5 \times 10^{24} (P.mm.)^{\frac{1}{2}} \exp.(-45,000/RT) \quad \ldots\ldots\ldots \quad (4.01)$$

while Ivanoiskaya and Mochan[70] obtained 43.4 kcal.mole.$^{-1}$ for the activation energy using an evaporated film of potassium as the "sink", although, as pointed out by Brennan[74], no correction for the effect of cooling on the filament end was taken into account.

Using essentially the same technique as Bryce, i.e. an evaporated molybdenum oxide film but only using the film up to 30% of saturation, Brennan and Fletcher[74] obtained the following rate equation:- (atoms.sq.cm.$^{-1}$sec.$^{-1}$)

$$a = 18 \times 10^{24} (P.mm.)^{\frac{1}{2}} \exp.(-52,600/RT) \quad \ldots\ldots\ldots \quad (4.02)$$

at temperatures below 1400°K. and pressures exceeding 10^{-6} mm.Hg. Unlike Bryce they did not throw a clean oxide film before each determination but regenerated their oxide by baking out at 450°C. for 15 min. between each reaction. They also showed that an activation energy of 44.5 kcal.mole.$^{-1}$ resulted on removal of a cold trap between the taps and the cell, although

contamination of/...

contamination of the filament with ethylene and oxygen produced identical activation energies to those found for the clean film.

It was therefore of interest to compare our results for the adsorption process with those obtained above. We have observed the uptake rates for an initial dose ($\sim 3 \times 10^{17}$ molecules) of hydrogen atoms on Pyrex glass, molybdenum oxide films and on films of copper, silver, gold, zinc, cadmium and nickel, all at 78°K. It was found that for all these films the initial dose would be adsorbed in 120 secs. $\pm$15 secs. Subsequent doses would be adsorbed more slowly depending mainly on the relative coverage of the film, but for our purpose of comparison only the initial dose will be considered.

For a typical dosage:-

The initial pressure, P = 2.41×10^{-3} mm.Hg.

Volume of gas adsorbed = 2.28×10^{17} molecules.

Time for adsorption of whole dose = 120 secs. $\pm$15 secs.

Assuming that the rate of adsorption remains constant

The initial rate, (molecules/sec.) = $\frac{2.28 \times 10^{17}}{120}$

i.e. The rate of uptake = 1.90×10^{15} molecules/sec.

The length of wire in tungsten helix = 25.0 cms.

Diameter of tungsten wire = 0.01 cm.

∴ Surface area of wire (πdl) = 0.789 sq.cm.

Bryce

$$a = 2.5 \times 10^{24} (2.41 \times 10^{-3})^{\frac{1}{2}} \exp(-45{,}000/R1373)$$

$$= 2.5 \times 10^{24} \times 4.91 \times 10^{-2} \times 10^{-7.188}$$

$$= 7.970 \times 10^{15} \text{ atoms/sq.cm./sec.}$$

$$= 6.288 \times 10^{15} \text{ atoms/sec.}$$

$$= 3.144 \times 10^{15} \text{ molecules/sec.}$$

Brennan/...

Brennan

$$a = 18 \times 10^{24} (2.41 \times 10^{-3})^{\frac{1}{2}} \exp/-52{,}600/R1373)$$

$$= 3.50 \times 10^{15} \text{ atoms/sq.cm./sec.}$$

$$= 2.76 \times 10^{15} \text{ atoms/sec.}$$

$$= 1.38 \times 10^{15} \text{ molecules/sec.}$$

For a sticking probability of unity, the effective uptake rate = the rate of atomisation.

i.e. $\frac{\text{(experimental) rate of uptake}}{\text{rate of atomisation}} = \frac{1.9 \times 10^{15}}{3.144 \times 10^{15}} = 0.61,$

for Bryce or $\frac{1.9 \times 10^{15}}{1.38 \times 10^{15}} = 1.4$

for Brennan.

These results were considered satisfactory since

(1) no cooling corrections were applied to the helical filament

(2) no account was taken of the time lag of the Pirani

(3) the accuracy of the calibration of the filament was ($\pm 50^{\circ}$K.), and

(4) no account was made for the roughness factor of A.C. electrolysed tungsten filament wire.

Glass, however, has often been used as the substrate for studies of surface diffusion and the recombination of hydrogen atoms.[66,106] More recently the interaction between hydrogen atoms and glass surfaces has been studied by de Boer and co-workers[107], Tsu and Boudart[104] and Hickmott[105]. Briefly, the results reported by these authors indicated that at room temperatures hydrogen atoms are chemisorbed on glass to the extent of a complete monolayer showing considerable stability. At lower temperatures further quantities of atomic hydrogen are taken up which are readily desorbable from the glass.

Using an ion/...

Using an ion resonance omegatron Hickmott[105] also studied the residual gases in a glass ultra high vacuum system. He found reproducible surfaces could be obtained by baking out Pyrex glass at 250°C. but prolonged exposure in a flow system to atomic hydrogen produced from molecular hydrogen by an incandescent tungsten filament produced contaminant species (CO, H_2O and CH_4), whose presence may seriously interfere with the study of surface phenomena.

It was thus of interest to study the effect of adsorption of a dose of hydrogen atoms on a clean, thoroughly outgassed, static, Pyrex system. Thus, after the normal outgassing procedure, a normal dose ($\sim 3 \times 10^{17}$ molecules) was rapidly adsorbed on the walls of the cell at 78°K. The filament was switched off and the cell warmed up. The resultant volume desorbed against temperature (°K.) plot is shown in FIGURE 9.

It can be readily seen that for such a dosage no detectable gas will be evolved from the all glass system below 400°K. Thus any subsequent desorption phenomena occurring below this temperature for equivalent dosages may be effectively attributed to the presence of the metallic film and not to that of the glass present.

4.2 Nickel

(i) Preliminary results

In order to effect a study of hydrogen atoms on nickel films, equilibration of the surface with hydrogen molecules is essential before introduction of the atoms. Consequently a film was dosed at 78°K. with approximately equal doses ($\pm 3 \times 10^{17}$ molecules) of hydrogen; the uptake being monitored on a Pirani gauge in the pressure range (10^{-2} - 10^{-6}) mm.Hg. Initial doses were taken up instantaneously while for subsequent doses the

rate of fall/...

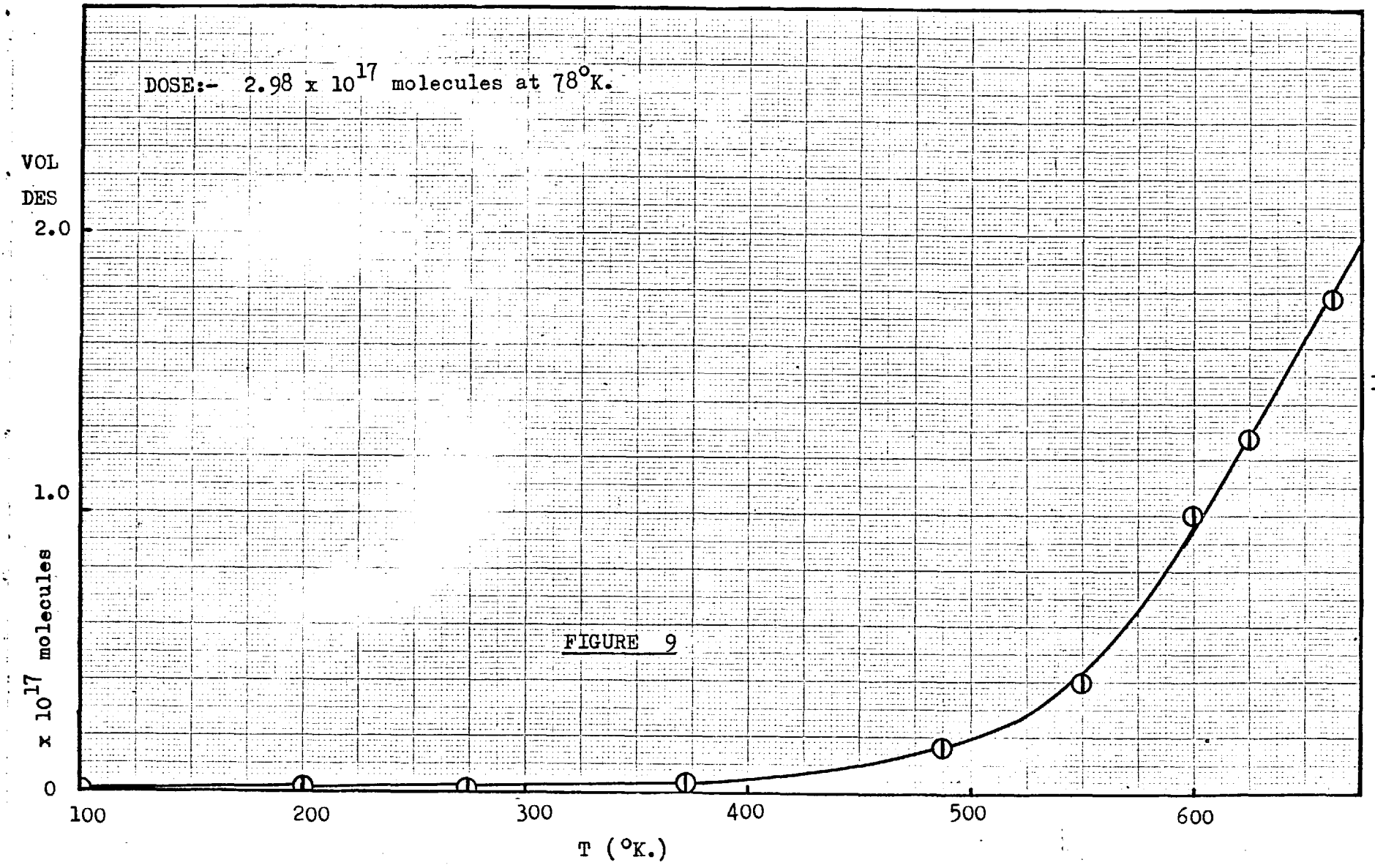
DOSE:- 2.98 x 10^17 molecules at 78°K.
VOL
DES
2.0
1.0
0
x 10^17 molecules
100
200
300
400
500
600
T (°K.)

FIGURE 9

rate of fall in the gas pressure became increasingly slower and the ultimate pressure in pseudo-equilibrium with the film gradually increased. True equilibrium could not be attained as a slow uptake process, similar to that found by Gundry[48] persisted, independent of the pressure and the temperature of the system. When this slow uptake process had taken about 1 hour to remove a dose of $\pm 3 \times 10^{17}$ molecules and the overall pressure in the system had fallen to $\pm 1 \times 10^{-5}$ mm.Hg., the temperature of the film was suddenly raised from 78°K. to 298°K. in the static system.

Desorption occurred as follows:- a slight burst of gas ($\pm 5\%$ of the total volume desorbed) was instantaneously evolved and rapidly readsorbed. This readsorption was then followed by a slightly slower desorption which eventually deteriorated into a slow uptake which persisted at the higher temperature. Approximately 15% of the total gas adsorbed at 78°K. was desorbed at 298°K., neglecting the slow uptake process.

The film was then allowed to remain in contact with additional gas in the gas phase (to facilitate equilibrium: $P = 4 \times 10^{-2}$ mm.Hg.) overnight, at room temperature. Subsequent recooling to 78°K. after this period found a very slow rate of uptake still persisting though less gas was now found to be readsorbable (only 25% of the amount desorbed). Upon turning on the atomising filament a rapid (about 2 minutes) uptake occurred and all the remaining gas was taken up, the pressure decreasing from $\pm 5 \times 10^{-3}$ mm.Hg. to 1×10^{-6} mm.Hg. The filament was then switched off and no desorption was detectable at 78°K. On raising the substrate temperature to 298°K. again, no initial burst of gas resulted, and the rate of desorption was faster than for the second desorption of the hydrogen molecules found initially. However, exactly the same volume as before was desorbable, the slow uptake,

however, now/...

however, now being noticeably absent at this temperature. It thus seemed feasible that sorption of atomic hydrogen could occur on a surface already effectively saturated by equilibration with hydrogen molecules at 78°K.

The slow uptake which was found at all temperatures was probably the activated sorption process reported by Gundry and Tompkins[47]. The initial burst of gas on warming could result from desorption sites associated with surface heterogeneities as occasionally found by Gundry[48]. A rearrangement of the packing of the initially adsorbed atoms to a more likely distribution on warming[108] would result in a further reduction of the available surface area for readsorption.

The more homogenous nature of the surface now produced would account for the disappearance of the initial burst of gas while a faster desorption rate could result from the geometric positioning of the atomised adatoms.

(ii) The effect of substrate temperature on the uptake of atomised hydrogen

A film was dosed with equal doses ($\pm 3 \times 10^{17}$ molecules) of hydrogen at room temperature until the pseudo-equilibrium pressure over the film was approximately 1×10^{-3} mm.Hg. i.e. about 45 minutes sorption of the final dose; the slow uptake still persisting. After a further 30 minutes to characterise the slow uptake ($P = 1 \times 10^{-4}$ mm.Hg.) at this temperature, the atomising filament was switched on at this pressure. Apart from a very slight increase in the adsorption rate the slow uptake process was found to predominate. When the filament was switched off, usually after 10 minutes, no change in the slow uptake rate was observed. This procedure was repeated systematically for lower substrate temperatures; the pressure being maintained in the range 10^{-3} to 10^{-4} by suitable hydrogen molecule dosage, where required. No marked increase in the rate or amount taken up as hydrogen

atoms occurs/...

atoms occurs until 90°K. when a large quantity of hydrogen as atoms are rapidly sorbed (TABLE 5). No desorption occurred on switching off the filament at each of the temperatures listed below.

TABLE 5

Temperature of Substrate °K	Hydrogen molecules taken up (x 10^{17})	Hydrogen molecules adsorbed as atoms (x 10^{17})
273	29.0	0.56
250	2.3	0.38
223	1.7	0.09
178	2.7	0.95
148	3.1	1.25
90	1.7	35.74 *
78	0.3	4.0

* The hydrogen atom sorption rate had not yet approached the slow uptake rate of hydrogen molecules at this temperature.

Thus it would seem that nickel films possess additional sorptive properties for atomised hydrogen as distinct from molecular hydrogen at 90°K. No desorption occurred with all the gas on at 78°K. but on raising the temperature to 90°K. a very slight amount was desorbed (0.01 x 10^{17} molecules). Increasingly large amounts were desorbed at higher temperatures and the most noticeable effect on desorption was the complete absence of the slow uptake rate at these temperatures. A more quantitative investigation into the desorption process will be discussed later.

(iii) Kinetics of the adsorption process

A film was dosed at 148°K. with equal doses of hydrogen molecules ($\pm$3 x 10^{17} molecules) until the final dose took longer than one hour to sorb.

This final/...

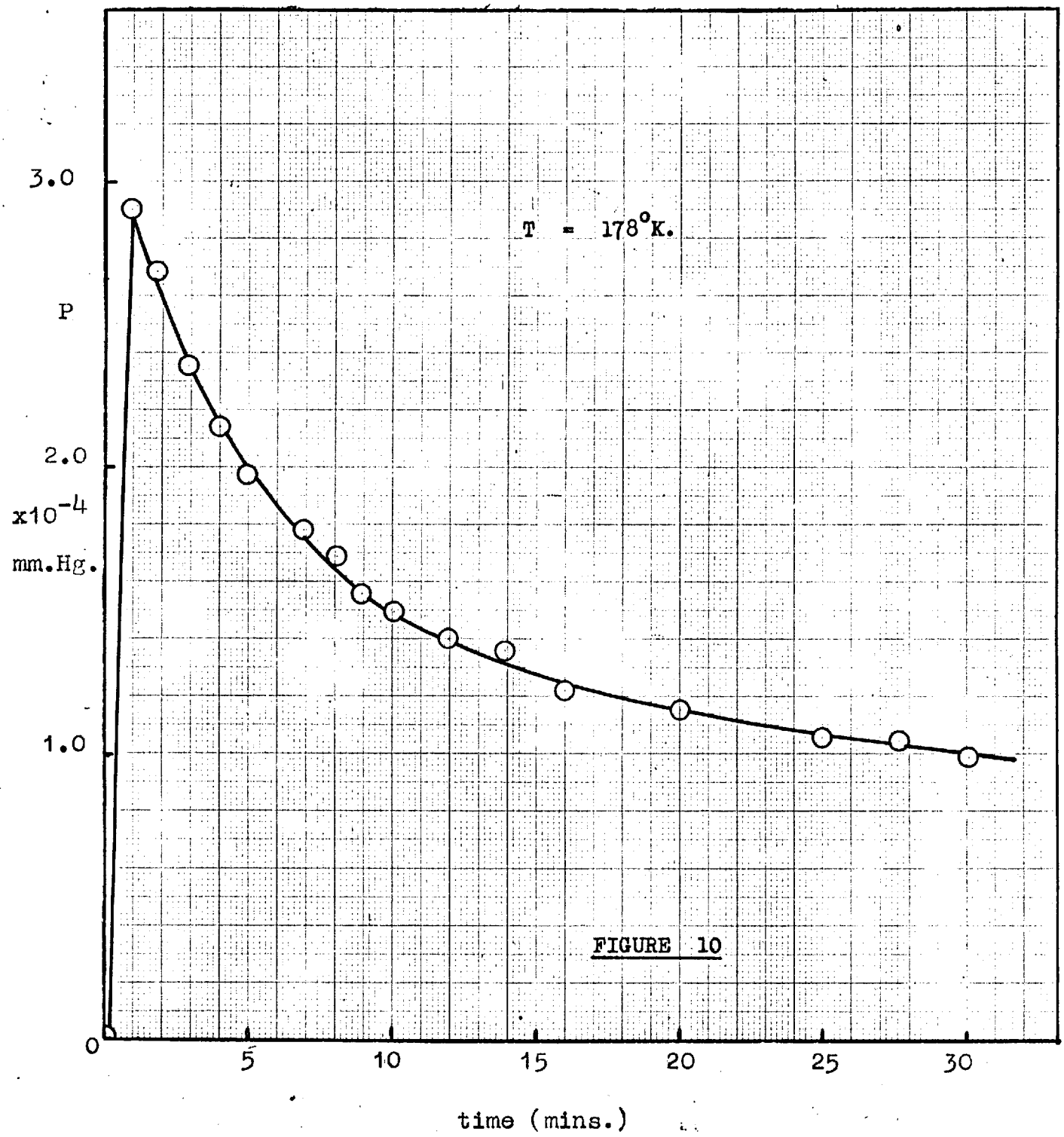

FIGURE 10

This final fall in pressure with time was carefully measured and when all the gas had been sorbed the temperature was raised to 178°K. (FIGURE 10) and the pressure again recorded. After a very rapid desorption, the slow uptake process again predominates and after characterisation of the rate at this temperature, the temperature was reduced to 148°K. The procedure was repeated at correspondingly higher desorption temperatures up to 273°K.

The rate of adsorption, r_s, was determined (millimoles $g.^{-1}$ $min.^{-1}$) by tangential slopes at fixed values of q from the plots of q (total volume adsorbed) against t (min.). Associated with each q value is the corresponding pressure value, p, in mm.Hg. From the Elovich equation, 1.10, it follows that a plot of $\log(r_s/p^{\frac{1}{2}})$ against q should be linear, i.e.

$$\log(r_s/p^{\frac{1}{2}}) = \frac{-C}{2.303RT} q + \text{constant} \quad \ldots\ldots\ldots\ldots \quad (4.03)$$

or substituting in an Arrhenius equation

$$\Delta \log(r_s/p^{\frac{1}{2}}) = \frac{-E(q)}{2.303R\Delta T} \frac{q}{} \quad \ldots\ldots\ldots\ldots\ldots \quad (4.04)$$

Hence knowing q, ΔT and $\Delta \log(r_s/p^{\frac{1}{2}})$, E can be evaluated for various q. FIGURE 11 illustrates a typical plot of $\log \frac{(dq/dt)}{p^{\frac{1}{2}}}$ against q while TABLE 6 shows the resultant variation in E with increasing q for 178°K. and 148°K., the only two temperatures where the q values overlap. This variation is illustrated in FIGURE 12. At 273°K. the slow process was allowed to characterise itself for about an hour and was then interrupted and cooled to 148°K.

TABLE 6

E(kcal.mole.$^{-1}$)	: 1.27	1.36	1.50	1.63	2.01
q(millimoles.g^{-1})	: 0.1006	0.1008	0.1011	0.1014	0.1018

Two sweeps/...

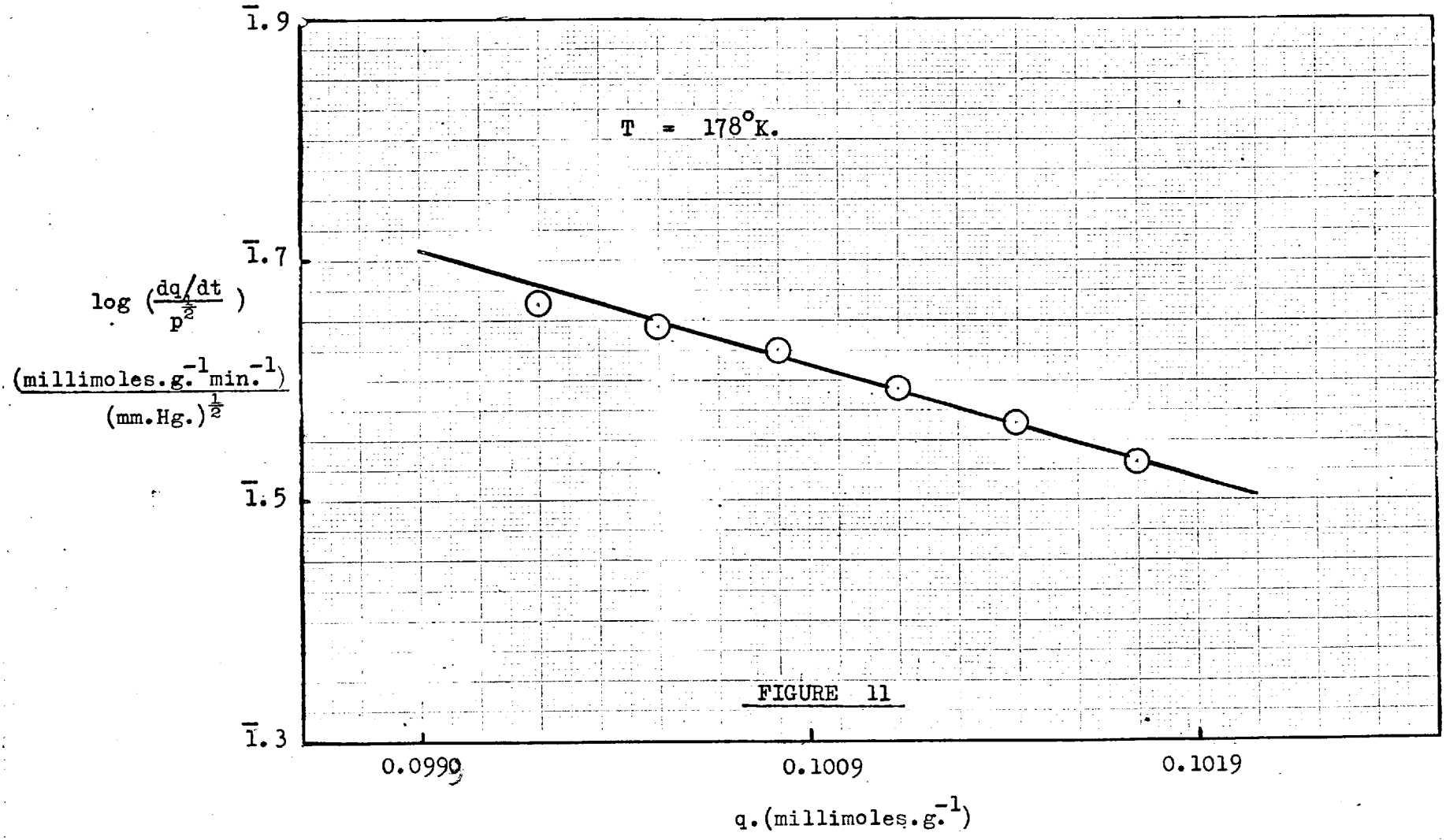
T = 178°K.
$\bar{1}.9$
$\bar{1}.7$
$\bar{1}.5$
$\bar{1}.3$
$\log \left(\frac{dq/dt}{p^{\frac{1}{2}}}\right)$
$\frac{(\text{millimoles.g.}^{-1}\text{min.}^{-1})}{(\text{mm.Hg.})^{\frac{1}{2}}}$
0.0990
0.1009
0.1019
q.(millimoles.g.$^{-1}$)

FIGURE 11

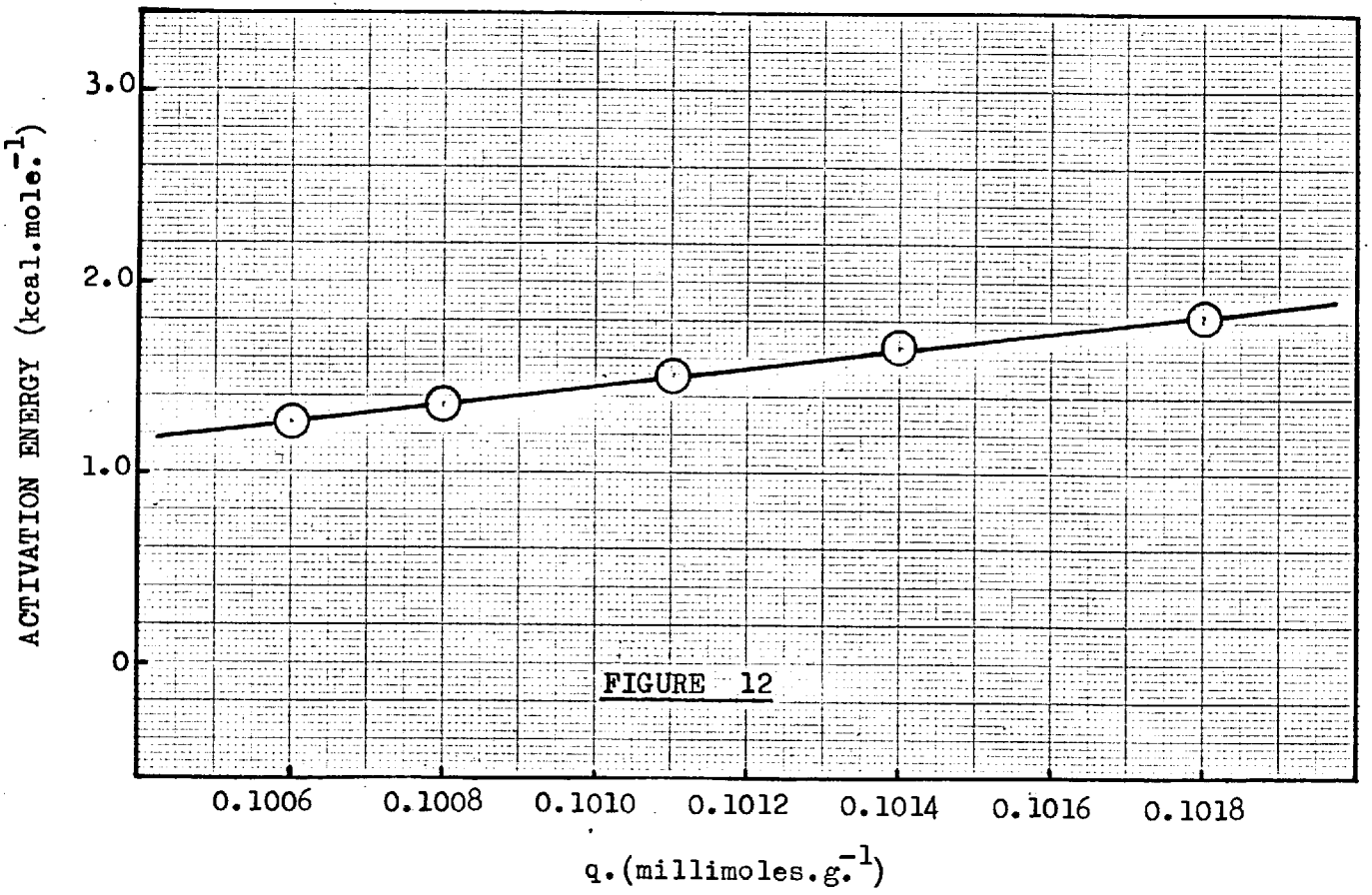
ACTIVATION ENERGY (kcal.mole.$^{-1}$)
3.0
2.0
1.0
0
0.1006
0.1008
0.1010
0.1012
0.1014
0.1016
0.1018
q.(millimoles.g.$^{-1}$)

FIGURE 12

Two sweeps in temperature were then made directly from 148°K. to 273°K. and in each case the rate of uptake at the higher temperature characterised for about 30 minutes. The overall exponential fall of pressure with time at 273°K. was merely interrupted by these sweeps and was found to continue to proceed decreasingly slower.

The film was eventually cooled to 78°K. and when the rate had been measured for about an hour no further addition of gas was introduced. The total volume of hydrogen molecules added up to this stage was taken as equal to full surface coverage, $\theta = 1.0$, the slow uptake process now taking longer than 90 minutes to remove a dose of 2×10^{17} molecules from the gas phase.

(iv) The kinetics of the desorption process

The substrate was then dosed with atomic hydrogen to a total dosage of $\theta = 1.27$ at 78°K. Upon switching off the filament no desorption occurred at this temperature. On raising the temperature to 90°K. desorption occurred followed by a slight, almost negligible, readsorption. On re-cooling to 78°K. and desorbing at temperatures greater than 90°K. (each preceded by a recooling and readsorption at 78°K.) desorption was found to occur with no readsorption at all.

Upon dosing with hydrogen atoms until the same uptake rate for hydrogen molecules was attained i.e. until a dose of 3×10^{17} molecules (as atoms) at 78°K. took longer than 90 minutes to become adsorbed, the total hydrogen molecule concentration on the film was now found to be $1.93\ \theta$ where $\theta = 1$, as defined above. No detectable desorption occurred upon switching off the filament at 78°K. Upon desorption from 78°K. (in each case) to higher temperatures no readsorption occurred (FIGURE 13). It was noted, however,

that now/...

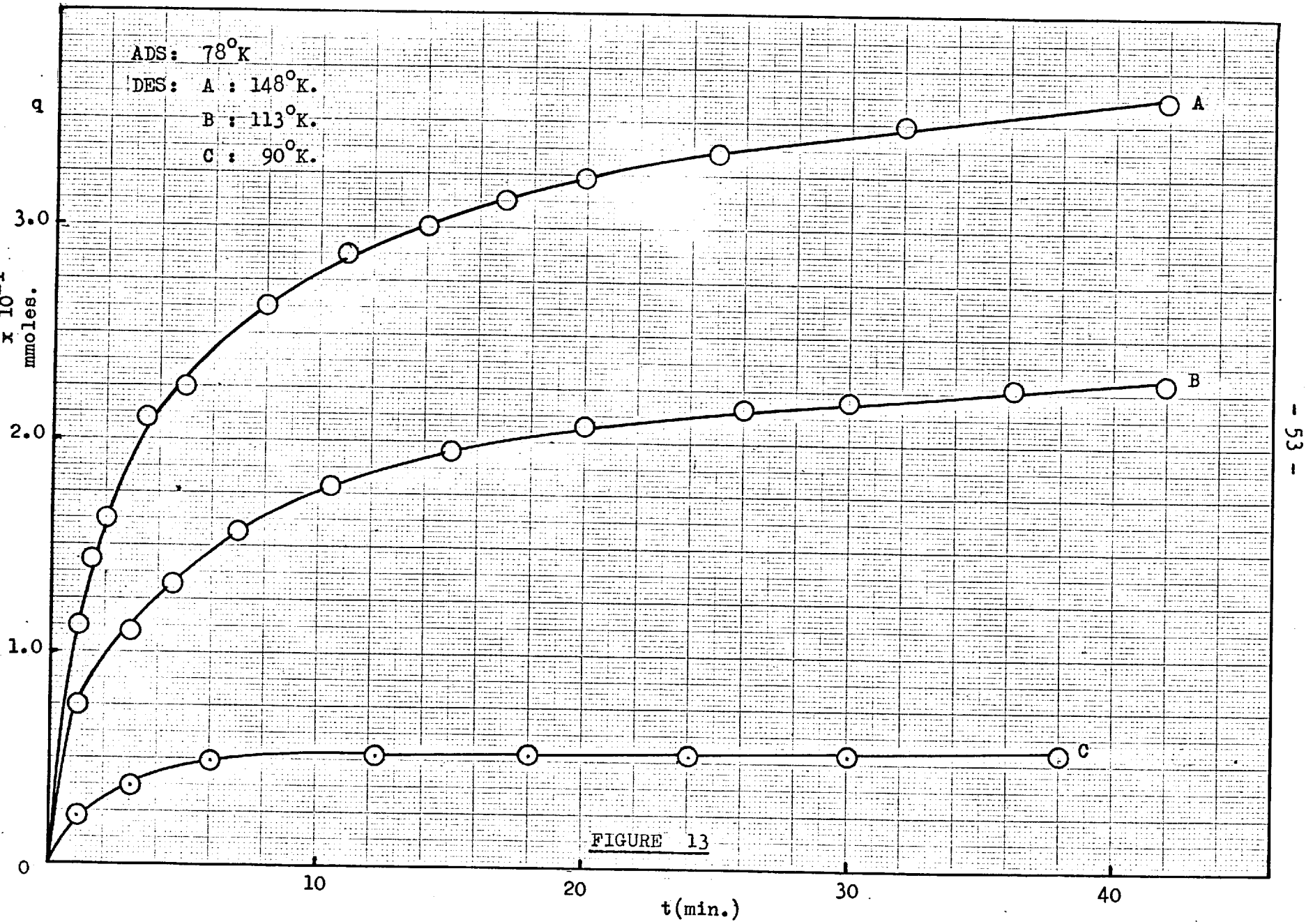
ADS: 78°K
DES: A : 148°K.
B : 113°K.
C : 90°K.
q
x 10⁻¹ mmoles.
3.0
2.0
1.0
0
10
20
30
40
t(min.)
A
B
C

FIGURE 13

that now equilibrium was only attained in some instances after a lengthy slow desorption rate which followed the comparatively rapid initial desorption. This very slow rate of desorption, where present, was extrapolated to $t = \infty$ for the subsequent kinetic analyses of the rate plots.

All the measurable rate plots in the temperature range studied (113-148°K.) were best fitted by the equation for a 2nd order process i.e.

$$1/(a-x) = k_1 t + c \qquad \ldots\ldots\ldots\ldots\ldots\ldots\ldots\ldots \quad (4.05)$$

where a = the concentration of hydrogen molecules in the gas phase at $t = \infty$ and x = the concentration of hydrogen molecules in the gas phase at time t. FIGURE 14 illustrates a typical rate plot and the corresponding kinetic analysis.

Although the rates of evolution of hydrogen molecules at a fixed temperature do vary considerably from film to film, for one particular film the reproducibility is satisfactory enough to warrant the estimation of the apparent activation energy for desorption over this temperature range.

Thus, to investigate the effects of variable concentration of hydrogen atoms sorbed at 78°K. on the subsequent rates of desorption and on the volume of gas desorbable from the substrate at $78 \leq T°K. \leq 273$, a new film was dosed with hydrogen molecules at 78°K. and thermally cycled to 273°K. until the sorption of a dose at 78°K. ($\pm 3.0 \times 10^{17}$ molecules) took about 90 minutes. Upon sorption of the whole dose, a dose of 0.5×10^{17} molecules as atoms was introduced on to the film and instantaneously adsorbed. Upon desorption at 90°K. the slow readsorption process was still found to be present. However, after a subsequent dose no slow uptake was observed at any temperature and it was possible to measure the rates of desorption

in the temperature/..

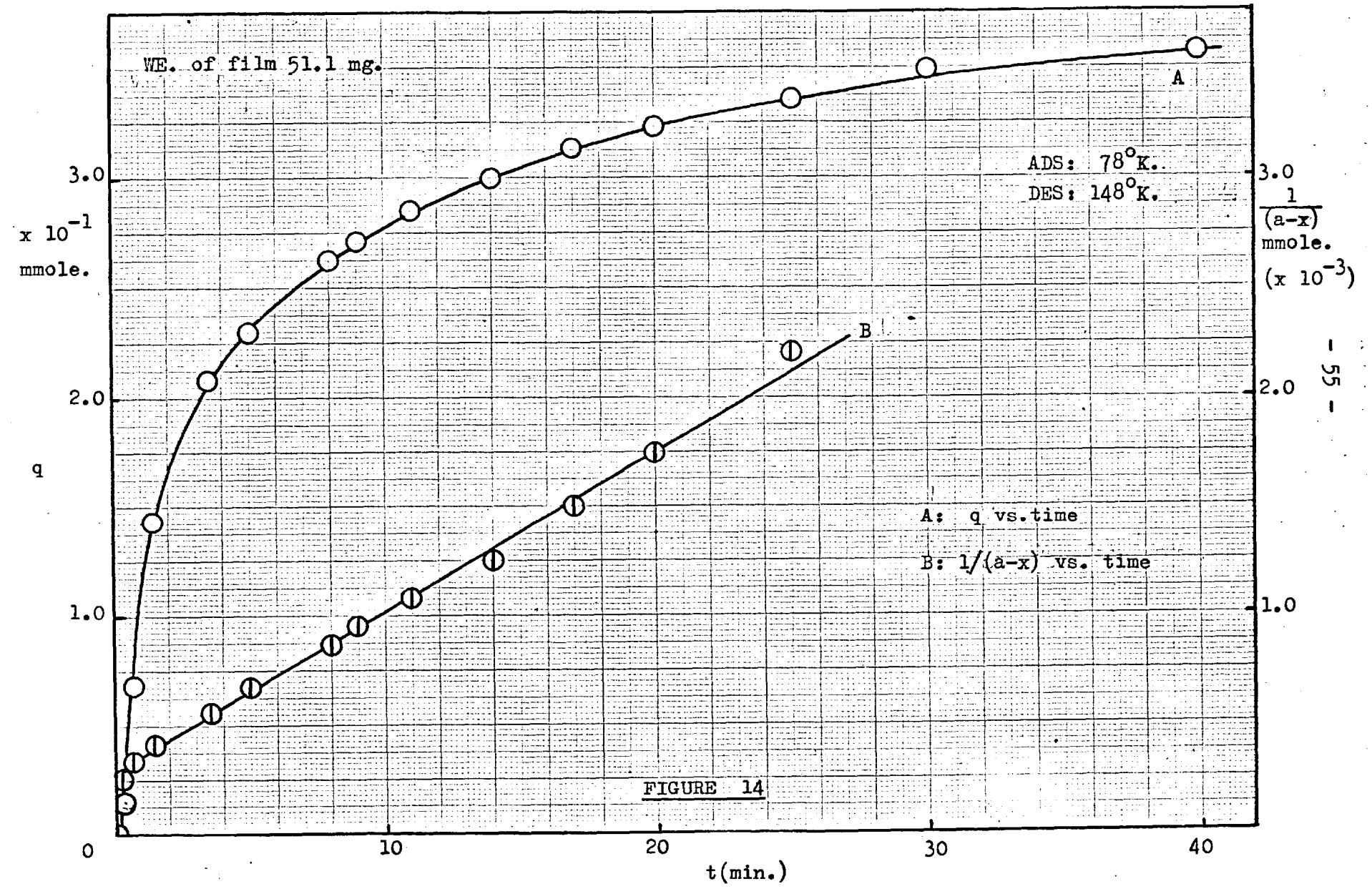
WE. of film 51.1 mg.
A
B
ADS: 78°K.
DES: 148°K.
A: q vs.time
B: 1/(a-x) vs. time
3.0
2.0
1.0
0
x 10⁻¹
mmole.
q
10
20
30
40
t(min.)
3.0
2.0
1.0
1/(a-x)
mmole.
(x 10⁻³)

FIGURE 14

in the temperature range (113-148) ^{o}K; the amount of gas evolved at 90^{o}K. being too small for accurate rate measurements and the rate of evolution above 148^{o}K. being too fast to be accurately recorded. The rate plots were best fitted by a 2nd order relationship and the resulting rate constants are tabulated below in TABLE 7.

TABLE 7

Species sorbed	Total dose molecules x 10^{17}	θ	k_1 (10^6 moles.$^{-1}$ q.min.$^{-1}$) 113^{o}K.	142^{o}K.	148^{o}K.
molecules	36.80	1.00	slow uptake present		
atoms	0.96	1.026	0.0325	0.1077	0.1886
"	1.56	1.042	0.0450	0.0615	0.2707
"	2.71	1.073	0.0850	0.1818	0.2837
"	4.69	1.127	0.0883	0.2147	0.3139
"	8.48	1.230	0.1383	0.2073	0.3773
"	14.88	1.404	0.0678	0.1704	0.2362
"	27.68	1.752	0.0693	0.1334	0.4042

Although variations in the rate constant at a fixed temperature are apparent, from the subsequent Arrhenius plots the results lie within the range of activation energies 1.2 $\pm$ 0.4 kcal.mole.$^{-1}$

The amounts desorbed at each temperature for varying dosages of hydrogen atoms are tabulated below in TABLE 8, the volumes all corrected to 78^{o}K., the dosing-in temperature. FIGURE 15 illustrates the number of hydrogen molecules desorbed at various temperatures as a function of the total amount of hydrogen (atoms and molecules) on the film at 78^{o}K. FIGURE 16 shows the plot of the volume remaining on the surface as a function of the temperature of desorption for various doses of hydrogen atoms.

TABLE 8/...

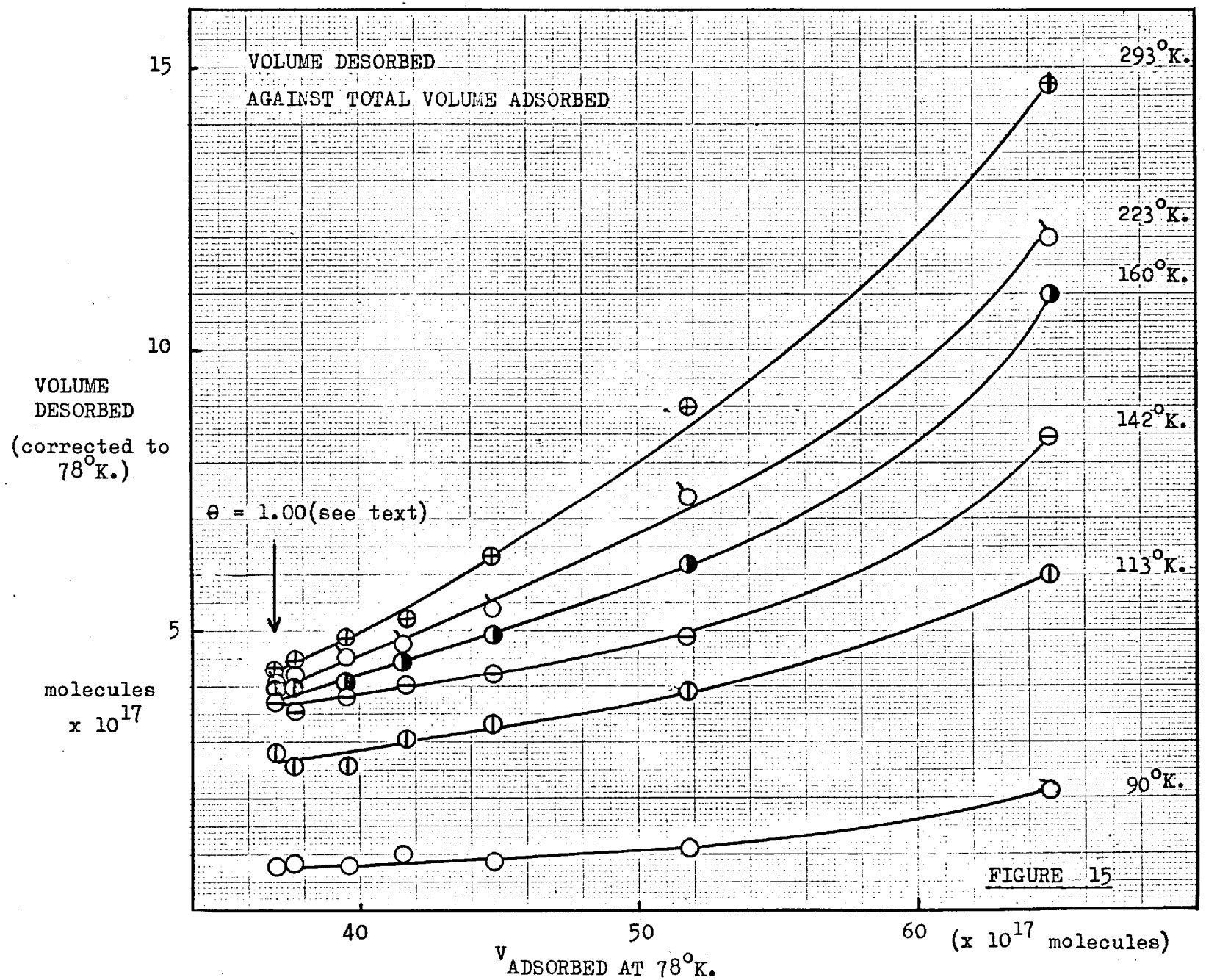
VOLUME DESORBED
AGAINST TOTAL VOLUME ADSORBED
293°K.
223°K.
160°K.
142°K.
113°K.
90°K.
θ = 1.00(see text)
15
10
5
VOLUME DESORBED (corrected to 78°K.)
molecules x 10^17
40
50
60
(x 10^17 molecules)
V ADSORBED AT 78°K.

FIGURE 15

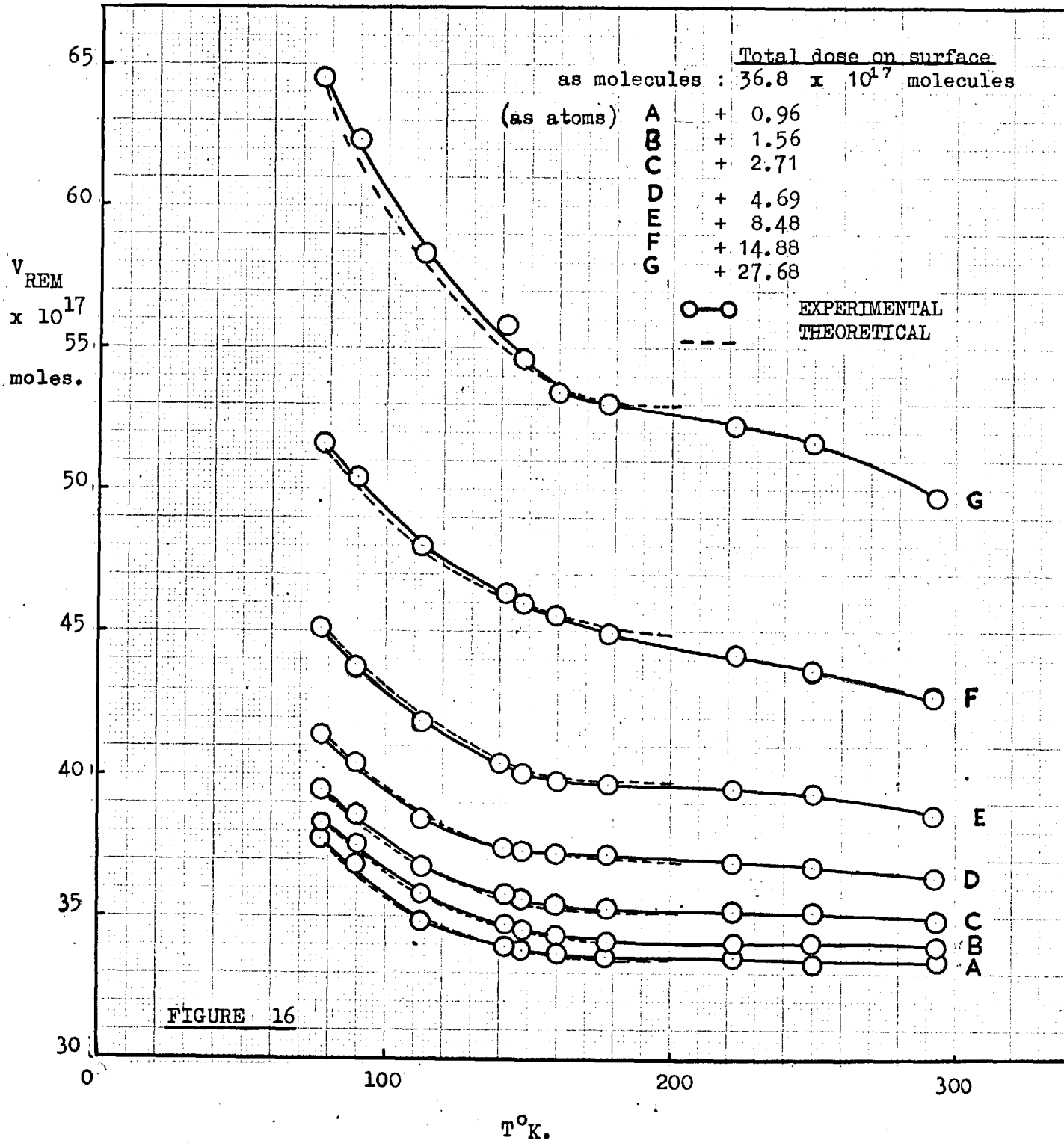
Total dose on surface
as molecules : 36.8 x 10^17 molecules
(as atoms)
A + 0.96
B + 1.56
C + 2.71
D + 4.69
E + 8.48
F + 14.88
G + 27.68
EXPERIMENTAL
THEORETICAL
V_REM x 10^17 moles.
65
60
55
50
45
40
35
30
0
100
200
300
T°K.
G
F
E
D
C
B
A

FIGURE 16

TABLE 8

Hydrogen molecules on film at 78°K.: 36.80 x 10^{17}										
Total Volume on film at 78°K. (molecules x 10^{17})	θ	Total molecules desorbed (x 10^{17}) corrected to 78°K.								
		90°K	113°K	142°K	148°K	160°K	178°K	223°K	250°K	293°K
37.76	1.026	0.78	2.79	3.72	3.87	4.01	4.14	4.08	4.03	4.15
38.36	1.042	0.85	2.56	3.52	3.72	3.98	4.18	4.22	4.36	4.47
39.51	1.073	0.73	2.57	3.86	3.87	4.08	4.21	4.40	4.45	4.89
41.49	1.127	0.99	3.03	3.98	3.95	4.11	4.30	4.64	4.56	5.21
44.28	1.230	0.82	3.36	4.21	4.57	4.81	5.00	5.22	5.44	6.39
51.68	1.404	1.13	3.89	4.83	5.06	6.20	6.78	7.41	8.05	9.10
64.48	1.752	2.14	5.99	8.49	9.69	11.00	11.35	12.04	12.74	14.56

(v) The effect of mercury vapour

If the cold traps, normally cooled in liquid nitrogen, were allowed to warm up, mercury vapour distilled over on to the film. TABLE 9 indicates the amount of gas evolved at each temperature on warming a dosed film from 78°K. with the cold traps at room temperature. The substrate was allowed to remain at each desorption temperature for thirty minutes and then re-cooled, together with the cold traps to 78°K. and the volume of gas desorbed measured. No rate measurements were taken and the cold traps were always warmed to room temperature before each desorption. The film was dosed with molecules as before up to 1.0 θ at 78°K. and a further dose of 0.3 θ hydrogen molecules as atoms added. The total volume sorbed was 1.3 θ.

It is interesting to note that even the hydrogen atoms taken up at 78°K. were desorbed by this process. Similar effects for hydrogen molecules on metal films were reported by Porter and Tompkins[6], Gundry and Tompkins[47] and Campbell/...

and Campbell and Thomson.[109]

TABLE 9

$T^{\circ}K$	78	90	178	223	273	303
% of 1.3 θ desorbed	no desorption	$\angle 1$	19.5	53.2	74.8	95.0

(vi) Discussion

Hydrogen molecule adsorption

Early work relevant to this discussion can be briefly summarised as follows:- Beeck et al[14,110,111,112] from their studies on nickel and other metal films concluded that

(1) There is no activation energy for the adsorption of hydrogen.

(2) Complete monolayers are formed under the following arbitrarily defined conditions:-

(a) the adsorption of hydrogen within 15 secs. of addition at $78^{\circ}K$. or

(b) the hydrogen adsorption at $296^{\circ}K$. and 10^{-1} mm.Hg.

(3) Slow adsorption of hydrogen by metals in solution or absorption into the metal lattice. This is dependent only on the mass of the film and not on the area. In some cases hydrogen can induce sintering of the film.

Rideal and Trapnell[2] have indicated that the extent of the monolayer assumed by Beeck for tungsten films is 20% too low. This new monolayer was based on the fast oxygen adsorption at low pressures.

It has been realised for some time[6,47,49] that Beeck's view that the slow process at high coverage is due to adsorption is incorrect; the process at present being regarded as a surface phenomenon. This is made quite evident in the present investigation where the hydrogen was adsorbed

at the lower/...

at the lower temperature (148°K.) and the temperature then raised quickly to a higher constant value with the adsorption system closed. There occurred a very rapid desorption followed by a re-adsorption (FIGURE 10), a phenomenon characteristic of a heterogenous surface. The analysis of the plots requires the rate of uptake (dq/dt) at constant pressure p and constant surface coverage q. Therefore at a constant temperature, dq/dt is obtained for constant q's and then, since it has been previously shown that the rate of slow uptake is proportional to $p^{\frac{1}{2}}$, [47] $(dq/dt.p^{\frac{1}{2}})$ is evaluated for a series of constant q values at the given temperatures (FIGURE 11). The plots at constant T for varying q strictly obey the Elovich equation:

$$dq/dt = a'p^{\frac{1}{2}} \exp(-bq) \quad \ldots\ldots\ldots\ldots\ldots\ldots\ldots \quad (1.12)$$

where a' and b are constants.

The activation energies E when plotted as a function of q are linear (FIGURE 12) with the increase of q such that

$$E = 450q - 44.0 \text{ kcal.mole.}^{-1} \quad \ldots\ldots\ldots\ldots\ldots\ldots\ldots \quad (4.06)$$

(cp. Gundry[51] $E = 462q - 39.1$ kcal.mole.$^{-1}$)

(cp. Porter[51] $E = 470q - 61.0$ kcal.mole.$^{-1}$)

where q is in millimoles H_2/g.Ni.

The linear dependence of E on q determines the form of the Elovich equation and hence is here obeyed experimentally.

At these coverages, Gundry[48] finds that $-\Delta H$, the heat of adsorption, decreases linearly with q, so that, using $\Delta E \sim V_D + \Delta H$, ΔE increases linear with q provided V_D is constant or decreases more slowly than linearly as ΔH decreases. Ehrlich's[44] suggestion of the origin of the activation energy of the slow process may therefore be used to give the

correct magnitude/...

correct magnitude and the correct variation with coverage.

However, kinetically difficulties arise. Two adjacent empty sites on the surface are a prerequisite for chemisorption; when these are hit by a bombarding hydrogen molecule with the necessary activation energy, adsorption proceeds, but the rate, from the Herz-Knudsen equation, should be proportional to p and not $p^{\frac{1}{2}}$. Furthermore, since the mobility of adatoms requires an energy of $\sim$7 kcal., the formation of surface divacancies would superficially appear to be the rate-determining step since, experimentally, ΔE is $\pm$2 kcal. only. It is therefore essential from the present viewpoint for the rate of formation of divacancies to exceed the rate of collision of hydrogen molecules from the gas phase with these divacancies. Now this collision rate per $cm.^2$ per sec. at a representative pressure of 1.05×10^{-4} mm.Hg. and T = 148°K. is

$$r_b = \frac{P}{(2\pi mkT)^{\frac{1}{2}}}(1-\theta_V) \qquad \ldots\ldots\ldots\ldots\ldots\ldots\ldots\ldots (4.07)$$

where P = 1.05×10^{-5} cm.Hg.

m = 3.354×10^{-24}

k = 1.38×10^{-16}

= $2.13 \times 10^{17}\ \theta_V$ molecules/sec.

where θ_V represents the fraction of the surface covered with vacancies. At this pressure we have adsorbed 1.002×10^{-1} millimoles.g^{-1} of gas and we can adsorb a total of 1.228×10^{-1} millimoles.g^{-1}. Therefore 81.6% of the surface is covered, i.e. θ_V = 81.6%. The total uptake is 3.698×10^{18} molecules and since the number of sites available is 1.54 sites/sq.cm. and we assume 1 atom/site we have an available area of 4802 sq.cms. The area covered is 81.6% i.e. 883.6 sq.cms. are left.

Since/...

Since θ_V = 82% it is assumed that all the vacancies present are present as divacancies to obtain an order of magnitude value, where r_b, the maximum rate of bombardment of the divacancies is $2.13 \times 10^{17}/883.6$ molecules/$cm.^2$sec., i.e. 2.4×10^{14} molecules.$cm.^{-2}sec.^{-1}$ This has to be compared with the rate of formation of the divacancies. This rate is essentially the bimolecular collision rate of mobile hydrogen adatoms since these move into vacancies and leave vacancies behind on movement. Such a rate is given by

$$r_c = \sqrt{2}\left(\frac{n^2}{N}\right) \nu_m \, e^{-V_D/RT} \qquad \ldots\ldots\ldots\ldots\ldots\ldots (4.08)$$

where N = the total number of sites available/sq.cm. = 1.54×10^{15}.

and n = the maximum number of single vacancies available/sq.cm.

= 18.4% x 1.54×10^{15} = 2.83×10^{14} vacant sites/sq.cm.

ν_m = the jump frequency = 10^{13}.

V_D = the mobility energy for a single recombination[44] = $\pm$7 kcal.$mole.^{-1}$

Thence:-

r_c = 2.8×10^{16} or divacancies are formed at a rate $\pm$100 times faster than the collision of hydrogen molecules with divacancies. At higher coverages r_c decreases but r_b, because of the increasing activation energy for adsorption with coverage, decreases more rapidly. Hence this conclusion is valid at all θ.

The $p^{\frac{1}{2}}$ dependency is, however, still unexplained. It is therefore assumed that the filling up of a divacancy proceeds from hydrogen molecules physically adsorbed on the chemisorbed layer (so call second-layer), and that the adsorption isotherm can be expressed as a Freundlich equation;

e.g. $\theta = k_3 p^{\frac{1}{2}}$ ..... (4.09)

the chemisorption/...

the chemisorption rate is then proportional to θ or $p^{\frac{1}{2}}$. The assumption, however, requires maintenance of the adsorption equilibrium, i.e. the rates of both adsorption and desorption on top of the chemisorbed layer must well exceed the rate of the slow chemisorbed uptake. An evaluation of this desorption requires a knowledge of the heat of adsorption, $-\Delta H_2$, and this may be estimated by fitting a Langmuir isotherm to the Freundlich plot - this is possible with good accuracy[113] up to $\theta = 0.70$ i.e.

$$\theta = k_1 p/(k_2 + k_1 p), \text{ where } k_1 p = S.P/\sqrt{2\pi mkT} \quad \ldots\ldots\ldots\ldots\ldots (4.10)$$

molecules/cm.^{2}sec. for the rate of adsorption, and

$$k_2 = \exp(-\Delta H_2/RT)$$

The sticking probability, S, is assumed unity, and θ_2 is taken as 0.1. Hence for a measured rate of uptake of 1.02×10^{13} molecules/cm.^{2}sec. $-\Delta H$ is 1.07 kcal./mole., a reasonable value as will be shown later. (It is assumed that equilibrium is maintained if the desorption rate is 10 times faster i.e. 1×10^{14} molecules/cm.^{2}sec.).

Summarising therefore: assuming that the activation energy of the slow process is due to the decrease in the heat of adsorption in the first layer and the fact that the hydrogen molecule in the unperturbed state cannot attain its final energy of binding, the following phenomenon can be explained:-

(1) the magnitude of ΔE and its variation linearly with coverage above a critical θ value,

(2) the variation of rate as $p^{\frac{1}{2}}$ by the adsorption of hydrogen molecules in a second, physically adsorbed on top of the first, chemisorbed layer, provided this adsorption follows the Freundlich equation,

(3) despite the/...

(3) despite the greater mobility energy of the adatoms ($\sim$7 kcal.mole.$^{-1}$) compared with $\Delta E \sim 2$ kcal. for desorption, the slowest (rate-determining) process is in fact shown to be the activated adsorption of hydrogen molecules from the physically adsorbed second layer into adjacent divacancies in the first chemisorbed layer.

It is also of note that the explanation put forward by Gundry and Tompkins in 1956[47] remains an acceptable alternative. Here, it was assumed that the final chemisorbed state, C_f, is attained only by passing from an initial chemisorbed state, C_i, of higher potential energy, the latter involving solely d-orbitals while the former involved the stronger hybridised bonds of the dsp-type. The readjustment of surface metal-sorbate and metal-metal bonds to attain minimum free energy of the final surface complex then requires a small activation energy, ΔE. The hydrogen adsorbed in the C_i state is dissociative but the $-\Delta H$ of adsorption is small and thus the extent of the adsorption is small and the isotherm is always in the Henry's law regime - thus the $p^{\frac{1}{2}}$ dependence is followed. The unimolecular transformation (rehybridisation) is slow compared with the rates of adsorption and desorption from the van der Waals layer (which equilibrium is set up rapidly and remains substantially unchanged throughout) as soon as $E'(q)$ increases above zero.

Thus the essential difference between the use of Ehrlich's[44] fundamental equation above and that of Gundry and Tompkins[51] is that in the former the rate of chemisorption of hydrogen molecules from the physical adsorbed layer into the divacancies is the activated rate-determining process, whereas in the latter the rate of transformation of an H-adatom from the C_i to the C_f state is the activated process. The latter does not

depend on/...

depend on the mobility concept - both however are essentially associated with - ΔH decreasing with θ.

Recombination

In the recombination process, the concentration of atoms on the surface at any fixed time is governed by the rate at which atoms are lost by surface recombination or through direct collision with atoms in the gas phase or are removed by reflection of gas atoms from the surface or are evaporated directly from the surface. Sorption or removal of the adatoms by absorption or "solution" into the bulk of the solid will not be considered at this stage although it will certainly take place to some extent.

As the desorption process is always carried out with the filament off and the overall pressure in the system about 1×10^{-5} mm.Hg., i.e. atom pressures of the order of 10^{-9} mm.Hg., direct collision with gas atoms and reflections from the surface are processes which are not significant in the present discussion. Thus evaporation directly from the surface or a recombination process on the surface are the only available methods whereby atoms may be removed from the surface. Evaporation of atoms directly from the surface at these low temperatures may be considered negligible or very slow in this case and thus the recombination process becomes a problem predominantly of collision between adatoms on the surface.

As discussed previously, strong attractive interactions are possible everywhere between the surface and the atoms and "sites" as such merely constitute localised regions of a continuous distribution where such interactions are possible. In moving over the surface there is thus a continuous interaction process occurring between the adatom and the metal regardless of its location. Associated with this adatom movement over

the surface/...

the surface at a particular temperature will be a corresponding adatom-adatom interaction.

Neglecting any influence the surface may have on the recombination process we may consider the adatom collision rate as the same as that occurring in a two dimensional collision between atoms of a monatomic ideal gas. The collision frequency, ν, is given by

$$\nu = \sqrt{2}\ n^2 \sigma \Omega \quad \text{where} \qquad \ldots\ldots\ldots\ldots\ldots\ldots\ldots\ldots \quad (4.11)$$

n = the number of atoms involved in the desorption

σ = the interatomic distance

and $\Omega = \left(\frac{\pi kT}{2m}\right)^{\frac{1}{2}} \qquad \ldots\ldots\ldots\ldots\ldots\ldots\ldots\ldots\ldots\ldots\ldots\ldots \quad (4.12)$

where k = Boltzman's constant

T = $^{o}K.$

and m = atomic weight of the gas.

$$= \left(\frac{3.154 \times 1.38 \times 10^{16} \times 113}{2 \times 1.673 \times 10^{-24}}\right)$$

$$= 1.21 \times 10^{-5} \text{ cm./sec.}$$

n = 2.8×10^{17} molecules from film (area $\approx$ 4000 sq.cm.)

$= 0.7 \times 10^{14}$ molecules/sq.cm.

$= 1.4 \times 10^{14}$ atoms/sq.cm.

$\therefore$ $= 1.414(1.4 \times 10^{14})^2 \times 0.5 \times 10^{-8} \times 1.21 \times 10^{5}$ collisions $cm.^{-2} sec.^{-1}$

$= 1.68 \times 10^{25}$ collisions $cm.^{-2} sec.^{-1}$

The recombination process or the adatom-adatom interaction was found to be a second order rate process with an apparent activation energy of $1.2(\pm 0.5)$ kcal.$mole.^{-1}$ in the temperature range $113^{o}K.$-$148^{o}K.$ A reasonable conclusion is that the activation energy is the surface mobility energy of

the hydrogen adatoms./...

the hydrogen adatoms.

In the temperature range under consideration (113°K.-142°K.) the initial rate is obtained from the expression

rate of recombination = $k(a-x)^2$ ..... (4.13)

for a bimolecular process where

k = the rate constant

a = the total volume of gas evolved at the relevant temperature

x = the volume of gas evolved at time, t.

At t = 0,

rate = ka^2

These initial rates for nickel between 113°K.-142°K. are all of the order of 10^{11} - 10^{12} atoms $cm.^{-2}sec.^{-1}$ i.e. very much lower than a simple two dimensional monatomic ideal gas collision theory would predict.

It would thus seem feasible that surface-adatom interactions are important and for the removal of the adatom some inherent mobility must be accepted at these temperatures. We may thus ascribe to any particular temperature a mobility energy sufficiently large to denude all the sites possessing interaction energies up to and including this value. The locality of these sites is distributed throughout the adatom population on the surface. Following Ehrlich[44] the rate of surface recombination can be calculated from

$$r_D = \sqrt{2}\ \left(\frac{n^2}{N}\right)\ \nu_m\ K_m \exp -V_D/kt \quad \text{..... (4.08)}$$

where n = the total number of mobile hydrogen adatoms or the number desorbed as molecules at the temperature T (113°K.)

ν_m = the frequency factor for M-H vibrations and is about $10^{13}sec.^{-1}$

N = the total/

N = the total number of sites/cm.^{2} at full coverage (evaluated from the surface area, krypton B.E.T. at 78°K., and the average lattice spacing on the Ni (100), (110), (111) faces

and K_m = a steric factor for the recombination process

= $1/10^{(44)}$

Thus $r_D \approx$ 1-2 x 10^{20} collision cm.$^{-2}$sec.$^{-1}$

There is therefore a discrepancy of $\sim 10^8$ between r_D above and the measured rate of hydrogen evolution (10^{11} - 10^{12} atoms cm.$^{-2}$sec.$^{-1}$). This suggested that, as in the gas phase, H + H adatom recombination requires an effective third body collision for H_2 production - or, in other words, recombination over the main bulk of the surface does not take place; this only occurs at specific active centres, which are sparsely scattered over the film.

Let $[M]$ be the number of active centres/cm.^{2}, then the process may be formulated as:-

$$H + M \underset{k_2}{\overset{k_1}{\rightleftharpoons}} H\,M \qquad \ldots\ldots\ldots\ldots\ldots\ldots\ldots\ldots\ldots\ldots \quad (4.14)$$

$$H\,M + H \longrightarrow M + H_2 \qquad \ldots\ldots\ldots\ldots\ldots\ldots\ldots \quad (4.15)$$

Provided $k_3 \,//\, k_1$, $k_2 [H\,M] = \frac{k_1}{k_2}[H][M]$ ..... (4.16)

i.e.

$$d[H_2]/dt = \frac{k_1 k_3}{k_2}[H]^2[M]$$

$$= C \exp\left[(-E_1 - E_3 + E_2)/RT\right][H]^2[M] \qquad \ldots\ldots \quad (4.17)$$

where $E_A = E_1 + E_3 - E_2 \sim 2$ kcal.mole.$^{-1}$

From the experimental rate and E_A, the maximum value of $[M]$ is found

to be/...

to be $10^7/cm.^2$ or 1 in 10^8 sites are 'active'. These sites can be identified with (a) emergence of dislocations at the surface - a typical density is $10^7/cm.^2$ - or (b) to the presence of surface vacancies whose concentration at the m.p. is often 1 in 10^5, so that a frozen-in density of $10^7/cm.^2$ at the surface is feasible, or (c) to sites at the edges of the small crystallites, the ratio of these to the total number of all surface sites being again about 1 in 10^8. Particularly at the edges or at dislocation emergences, the binding energy M-H is less and therefore H + H recombination and H_2 evolution would be encouraged. The main conclusion would then be that the normal flat surface is completely ineffective as a third body for removing the excess energy of recombination; however, this mechanism involves a paradox - the amount of H_2 evolved increases with temperature for the same loading. The mechanism suggested cannot account for this because there is no means of stopping total gas evolution once a sufficiently high temperature for evolution has been attained. A reasonable explanation is possible only if E_A is not related directly with the mobility energy.

The procedure of calculation has therefore been reversed. If it is assumed that we are dealing with a heterogeneous surface and that atoms deposited from the beam are adsorbed randomly ($S \approx 1$) at $78^oK.$, on warming the composite surface the adatoms will become mobile on the most weakly held sites. For a very dilute surface concentration and a coarse-grained heterogeneity, such adatoms either migrate to sites of stronger binding energy or encounter similar mobile adatoms or combine and evaporate as hydrogen molecules. For more concentrated layers and a fine-grained patch-wise surface, the second process predominates. We use this simpler

state of/...

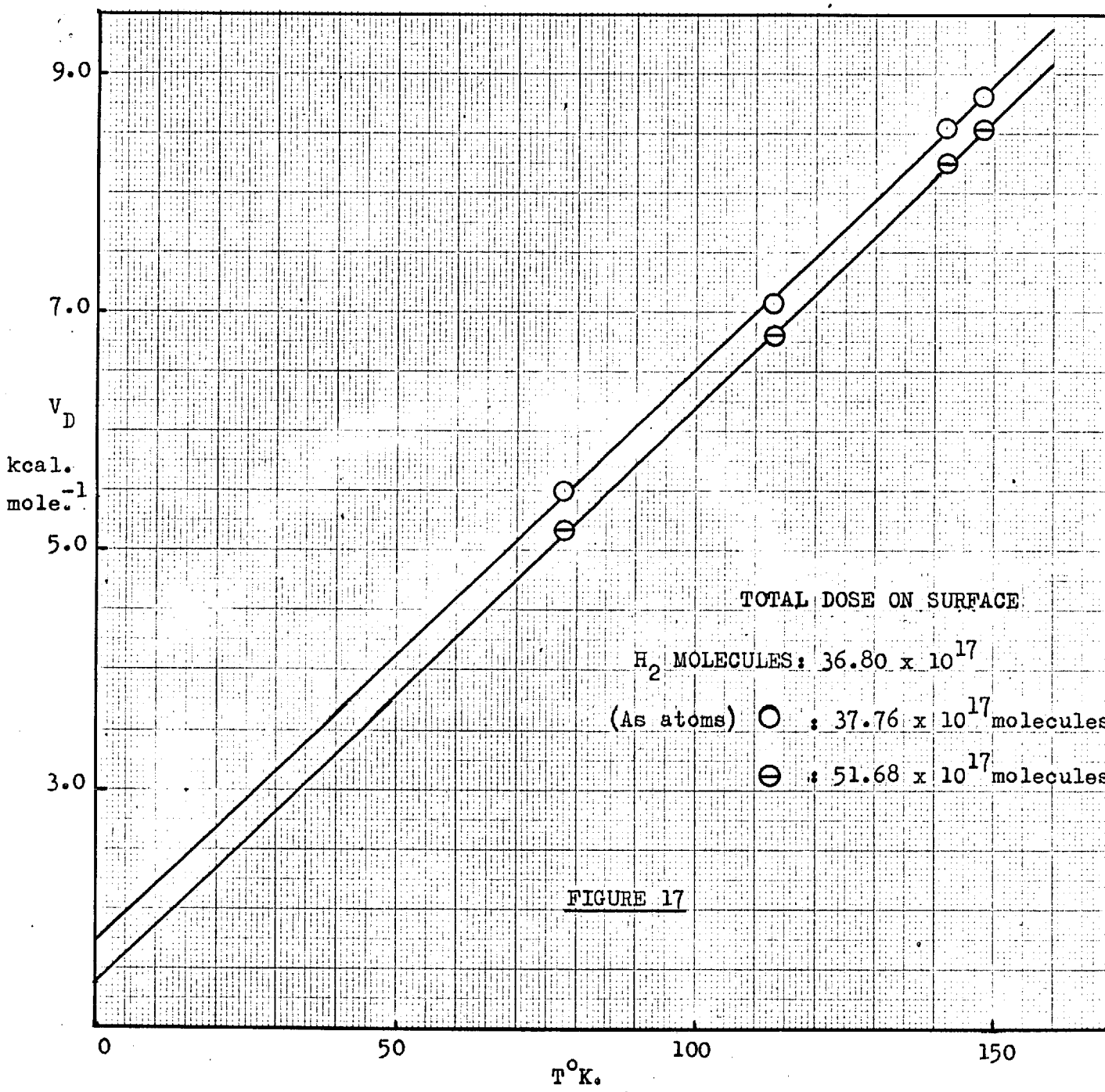
9.0
7.0
V_D
kcal.
mole.$^{-1}$
5.0
3.0
0
50
100
150
T°K.
TOTAL DOSE ON SURFACE
H_2 MOLECULES: 36.80 x 10^{17}
(As atoms) O : 37.76 x 10^{17} molecules
⊖ : 51.68 x 10^{17} molecules

FIGURE 17

state of affairs and from the rate of evolution and the concentration of adatoms, the mobility energy necessary to account for the low rate of evolution is calculated using the formula

$$r_c = \sqrt{2}\ (n^2/N)\ \nu_m\ K_m \exp(-V_D/RT) \quad \ldots\ldots\ldots\ldots\ldots\ (4.08)$$

Evolution is possible only when adatoms are mobile. Thus, if $V_D = V_D'$ on patch A and $V_D = V_D''$ on patch B, then at a particular temperature T', we have for A : $akT' \geq V_D'$; but for B, $akT' < V_D''$ where a is a constant. Hence gas evolution proceeds rapidly from A, but very slowly from B. However when the temperature is raised to T'' where $akT'' \geq V_D''$ rapid evolution from B ensues. Hence, the hydrogen molecules are evolved in steps and from such steps the variation of V_D (and $-\Delta H$) over the surface can be deduced. The plots of V_D against T for a high (1.40 θ) and low loading (1.026 θ) are linear (FIGURE 17) i.e.

$$V_D = akT + W_L \quad \ldots\ldots\ldots\ldots\ldots\ (4.18)$$

where ak = a constant independent of loading

and W_L = a constant, dependent on loading.

Thus, at the low loading at 78, 113, 142 and 148°K., V_D = 5.0, 7.0, 8.25 and 8.50 kcal./mole. respectively, and

$$V_D = 50T + 1{,}650 \text{ calories} \quad (\theta = 1.026) \quad \ldots\ldots\ldots\ (4.19)$$

$$V_D = 50T + 1{,}400 \text{ calories} \quad (\theta = 1.40) \quad \ldots\ldots\ldots\ (4.20)$$

The constant term (ak) is essential in order to obtain a constant E_A of 1-2 kcal. from the velocity constants of the bimolecular evolution curves. Thus from the rate curves, E_A is obtained via:-

$$\log(k_1/k_2) = \frac{E_A}{R}\left(\frac{1}{T_1} - \frac{1}{T_2}\right) \quad \ldots\ldots\ldots\ldots\ldots\ (4.21)$$

but k has/...

but k has the form $k_1 = C \quad e^{-V'_D/RT_1}$

where $V'_D = akT + W$

hence $k_1/k_2 = \exp\left\{\frac{1}{R}\left(-\frac{V'_D}{T_1} + \frac{V''_D}{T_2}\right)\right\}$ ..... (4.22)

whence $E_A = W$ as is found experimentally.

The significance of W

The rate of recombination, as discussed earlier, is the slowest and therefore the rate determining step in the process of H_2 evolution. It would now seem that, while sufficient potential energy is supplied to raise the adatom from its potential well to an adjacent potential hill, not all the energy is supplied thermally. The residual energy is potential energy associated with the adatoms themselves. As two hydrogen atoms approach each other some attractive interactions could occur as they approach their stable equilibrium position in the molecule. It is probable that such an interaction may account for W. Assuming a sinusoidal barrier energy variation over the surface of height akT and spacing between peaks of 2.5A^o, then for an unperturbed H-H distance of 0.75A^o, the H-H atoms can recombine when about 1.7 kcal. below the maximum value. This magnitude can vary only slightly for the small variation in V_D and is essentially W.

It has been shown that the mobility energy decreases for high loading. This effective decrease in V_D is reflected in an increase in the value of the rate constants for a given temperature at higher loading. This overall decrease in V_D with larger doses of hydrogen atoms may be explained as follows: the small, initial doses of hydrogen atoms on the nickel film completely fill the sites available for adsorption in the second layer i.e.

no slow/...

no slow uptake will now occur. Subsequent adsorption of the hydrogen atoms will only proceed by absorption into the bulk of the metal.

It is assumed that the equilibrium established between the first layer (chemisorbed from hydrogen molecules) and the bulk is maintained throughout the desorption process. Furthermore, the deposited hydrogen atoms will distribute themselves in such a manner as to fill the second layer even for the smallest dosage used and the excess atoms will be deposited in the bulk. If the ratio of the heat of solution to the heat of adsorption is such that desorption from the surface layer will proceed more quickly for the initial doses than from the bulk then as the dosage proceeds there is every likelihood of the bulk distribution of the atoms being concentrated just below the surface and more atoms from the bulk will participate in the desorption process as is shown in FIGURE 15.

Hydrogen atoms on nickel, in the second layer, are likely to be held by relatively weak metal hybrid orbitals because a large part of the bonding power of the metal will be concerned with the first layer. Eley[114] has associated the metal-hydrogen bond with the atomic d-electrons. It would thus seem feasible that increased sorption of hydrogen by the bulk metal would tend to saturate the d-bands near the surface and consequently the free energy of the surface and the adatom would be lowered. This decrease in free energy would in turn be reflected in a drop in the value of the mobility energy. This lower value of the mobility energy at a given temperature for higher loading is not, however, of primary importance in determining whether an increase in the number of molecules desorbed will occur. The explanation for the latter effect is as follows:-

The V_{REM} against T plots were fitted mathematically by a series of

successive/...

successive approximations yielding a plot of the form

$$(V_{REM} - V_b) = (V_{ADS} - V_b)\ (1 - e^{-C/T-78}) \quad \ldots\ldots\ldots\ldots \quad (4.23)$$

where

V_b is the volume of gas remaining on the surface at $T = \infty$ if the initial burst of gas was the only desorption process occurring.

V_{REM} is the measured volume remaining on the surface at temperature, T, and

V_{ADS} is the total volume on the surface at $T = 78^{o}K$.

C is a constant ≈ 10.

We have previously shown that

$$V_D = akT + E \quad \ldots\ldots\ldots\ldots\ldots\ldots\ldots\ldots \quad (4.18)$$

But as the experiments were carried out above $78^{o}K$. an arbitrary limit was imposed on the system at this temperature i.e.

$$V_D = ak(T - 78) + E' \quad \ldots\ldots\ldots\ldots\ldots\ldots\ldots \quad (4.24)$$

i.e. $(T - 78) = \dfrac{V - E'}{ak}$

where E' is the activation energy at $78^{o}K$.

Now, if

$$(V_{REM} - V_b) = N_R, \quad \ldots\ldots\ldots\ldots\ldots\ldots\ldots\ldots \quad (4.25)$$

= the total number of sites remaining on the surface with mobilities down to and slightly greater than V_D

and $(V_{ADS} - V_b) = N_T, \quad \ldots\ldots\ldots\ldots\ldots\ldots\ldots\ldots \quad (4.26)$

= the total number of sites with mobility up to and including V_m, the maximum mobility associated with the complete clearance of sites at the highest temperature, T_m.

N_T is a maximum/...

N_T is a maximum at 78°K. since we have arbitrarily chosen no mobility at this temperature.

Hence,

$$N_R = N_T (1 - e^{-C/T-78}) \quad \text{.... from} \quad \text{.....} \quad (4.23)$$

$$= N_T (1 - \exp[-Cak/(V-E')]) \quad \text{.....} \quad (4.27)$$

or $N_R/N_T = (1 - \exp[-b/(V-E')]) \quad \text{.....} \quad (4.28)$

where $b = Cak.$

Therefore $1 - (N_R/N_T) = \exp[-b/(V-E')] \quad \text{.....} \quad (4.29)$

i.e. $$\frac{N_T - N_R}{N_T} = \exp[-b/(V-E')] \quad \text{.....} \quad (4.30)$$

Now $N_T - N_R$ = the volume of gas desorbed

= the number of sites possessing mobility energies up to and including, V, the mobility energy for desorption at this temperature

= N

i.e.

$$N/N_T = \exp[-b/(V-E')] \quad \text{.....} \quad (4.31)$$

Now, if we assume an initial random distribution of the atoms over the surface,

$$N/N_T = \int_0^{V_{max}} D_V \, \theta_V \, d_V \quad \text{where} \quad \text{.....} \quad (4.32)$$

θ_V = C^*, a constant

and D_V = the distribution function of some functional form relating the distribution of sites on the surface to the mobility energy, V.

i.e. $$N/N_T = C^* \int_0^{V_{max}} D_V \, dV \quad \text{.....} \quad (4.33)$$

Therefore/...

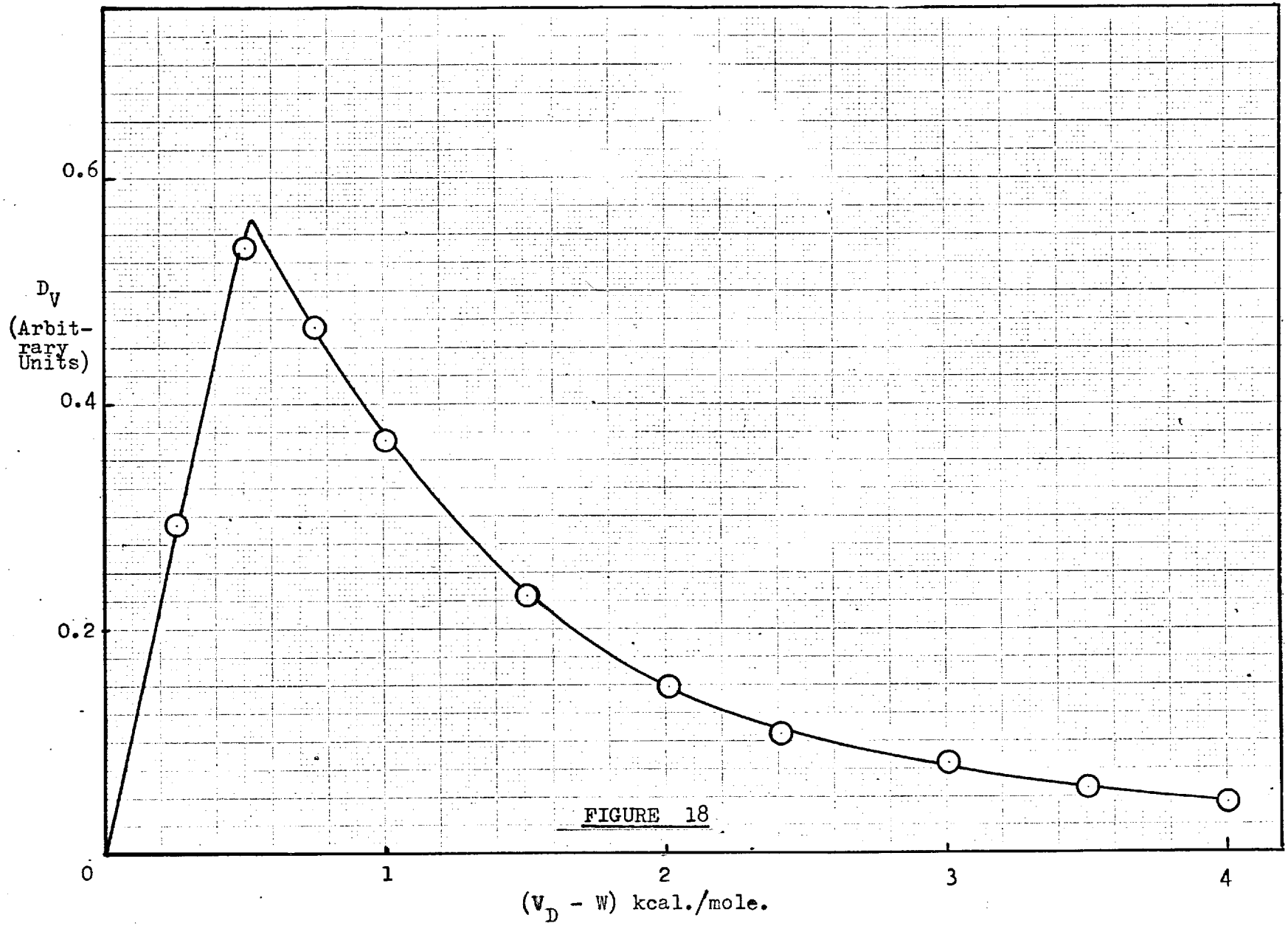

FIGURE 18

Therefore,

$$C^{*} D_V = \frac{dN}{dV} \cdot \frac{1}{N_T} = \frac{d}{dV} \exp\left[-b/(V-E')\right] \quad \ldots\ldots\ldots\ldots\ldots \quad (4.34)$$

$$= \frac{b}{(V - E')^2} \cdot \exp\left[-b/(V-E')\right] \quad \ldots\ldots\ldots\ldots\ldots\ldots \quad (4.35)$$

or $$D_V = \frac{b}{C^{*}} \cdot \frac{\exp\left[-b/(V-E')\right]}{(V - E')^2} \quad \ldots\ldots\ldots\ldots\ldots\ldots\ldots \quad (4.36)$$

The plot of D_V, against (V-E') kcal. is shown in FIGURE 18; and resembles a skew-type probability curve. Here E' is the value of V_D at 78°K.

Although an increase in dosage will decrease V_D, the change in the relationship $V_D = akT + E$ is a change in E i.e. V_D-E will increase with dosing and the distribution function will shift incrementally along the V_D-E axis by this amount to the region of less gas off at the same temperature. Thus it is postulated that on dosing the whole distribution plot is altered to increase the number with lower mobility. Such an increase may be effected by a variation in N_T with temperature or may be associated with some smoothing out of the potential wells and hills by the gas inside the solid.

4.3 Copper

(i) Adsorption

(a) Hydrogen molecules

No appreciable adsorption ($\lesssim$ 1%) of molecular hydrogen occurred on exposure of a copper film to the gas in the temperature range 78°K. to 273°K.

(b) Hydrogen atoms

As no appreciable adsorption of molecular hydrogen occurred on the film at 78°K., adsorption of hydrogen atoms was carried out at this

temperature./...

temperature. Doses of approximately 3.0×10^{17} molecules were introduced on to the film as atoms and, initially, were taken up instantaneously. This is in accord with results already reported[78,79,80,82]. The rate of uptake of progressive doses becomes slower, the time to adsorb equal doses gradually increases as does the pressure in pseudo-equilibrium with the film. When the rate of uptake became slow i.e. when the sorption of a dose of approximately 3×10^{17} molecules had taken about two hours and the pressure in the system had decreased to about 5×10^{-5} mm.Hg., dosing was usually terminated although this by no means represented the complete sorptive capacity of the film. (For instance, a 30.0 mg. copper film was dosed continuously for a period of 12 days at 78°K. to attempt saturation and, with a very slow uptake rate still persisting, the ratio of adsorbent: adsorbate was 5 copper atoms: 1 hydrogen atom throughout the whole film.)

(ii) Desorption

Upon switching off the filament at this point no desorbed gas was detected. Repetition of the adsorption procedure at 78°K. and the subsequent desorption at higher substrate temperatures resulted in a slight amount of gas being desorbed up to 220°K. while above this temperature the amount desorbed after switching off the filament and raising the temperature increased until at 273°K. about 75% of the total amount adsorbed at 78°K. was desorbable. Even at the highest temperature (310°K.) not all the gas was desorbed.

If the adsorption temperature of the substrate is raised from 78°K. to somewhere below 220°K., say 150°K., no appreciable desorption occurs upon switching off the filament although, approaching 220°K. some gas evolution

is detected/...

is detected. However, above 220°K., adsorption occurs as usual but on switching off the filament desorption occurred. (see later). These temperatures are not well defined for every film but satisfactory agreement to within ±10°C. over the whole series of experiments was obtained.

At every temperature the rate of desorption decreased with time but was still finite even after a period of several hours. For practical purposes, where possible, the rate was extrapolated to an "infinite time" value. Similar characteristics were exhibited on the desorption of hydrogen atoms from germanium films.[115]

(iii) The kinetics of the desorption process

Experiments were carried out to determine the order of the desorption reaction and the apparent activation energy for this process. A pre-sintered, clean copper film was dosed with hydrogen atoms at 78°K. and when the rapid adsorption was complete, the filament was switched off and the substrate temperature rapidly raised to the required desorption temperature (the process took no longer than 30 secs.) and the desorption rate measured. Upon completion of the rate measurements the substrate was recooled to 78°K. and the volume of gas desorbed, noted. Hence, as well as the rates of desorption, the volumes of gas desorbed at each temperature were noted and are tabulated below in TABLE 10.

As the desorption temperature increased, the volume of gas desorbed at each temperature increased, up to room temperature (FIGURE 19). Also, as the dosage increased, the volume desorbed was also found to increase at the various temperatures and the desorption rates at lower temperatures (restricted by the small amount desorbed for lower dosages) could be measured.

TABLE 10/...

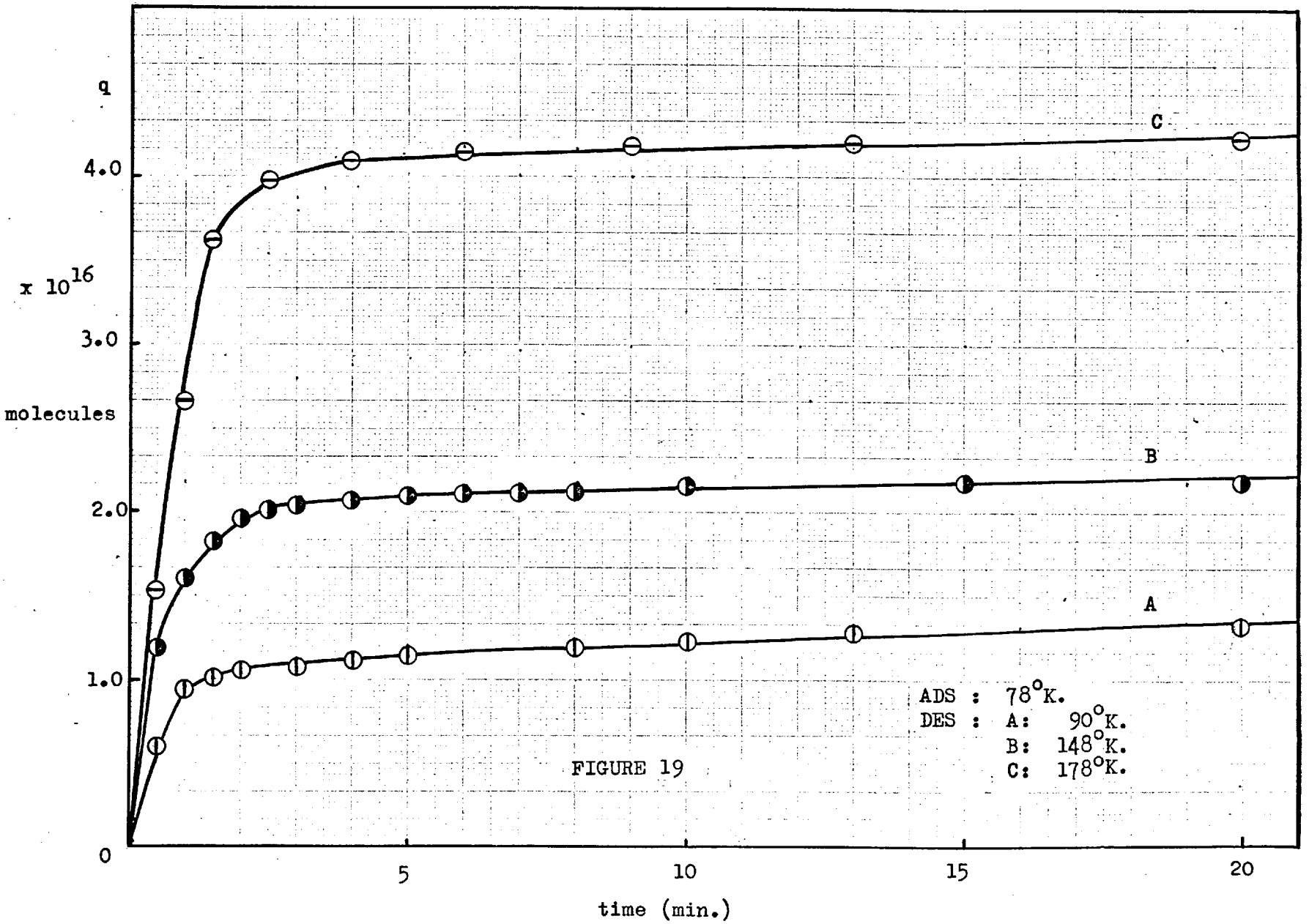
q
4.0
x 10^16
3.0
molecules
2.0
1.0
0
5
10
15
20
time (min.)
C
B
A
ADS : 78°K.
DES : A: 90°K.
B: 148°K.
C: 178°K.

FIGURE 19

TABLE 10

Wt. of film:- 19.0 mg.

Total Volume of hydrogen on film at 78°K. (molecules x 10^{17})	Volume desorbed (molecules x 10^{17}) (corrected to 78°K.)						
	90°K.	148°K.	178°K.	223°K.	250°K.	273°K.	294°K.
0.2997	0.002867	0.00430	0.00459	0.005733	0.02007	0.1282	0.1605
0.8836	0.008887	0.01577	0.01404	0.02322	0.06452	0.2983	0.3017
1.7221	0.01377	0.03096	0.02954	0.03441	0.1064	0.4433	0.5091
2.774	0.01414	0.03210	0.03083	0.03728	0.1514	0.6255	0.7589
2.774	0.01450	0.03228	0.03109	0.03759	0.1534	0.6276	0.7603
2.774	0.01426	0.03202	0.03096	0.03771	0.1544	0.6283	0.7573
3.967	0.03008	0.04737	0.06309	0.08513	0.1953	1.081	1.157
5.053	0.03169	0.05681	0.06900	0.09817	0.2047	1.101	1.233
6.942	0.03500	0.05830	0.07804	0.1047	0.3797	1.589	1.717
8.855	0.03441	0.08660	0.09831	0.1240	0.4176	1.687	1.997

Reproducibility is satisfactory; three desorption rates for the same dosage and temperature on the same film were almost identical; the resulting rate constants agree to within 5%. A typical desorption plot is shown in FIGURE 20.

(iv) Mathematical analyses of the rate plots

The resulting q against time plots were found to obey a second order equation,

$$1/(a - x) = k_1 t + c \quad \ldots\ldots\ldots\ldots\ldots\ldots\ldots \quad (4.05)$$

where a = the concentration of hydrogen molecules in the gas phase, extrapolated to "infinite time" and

x = the/...

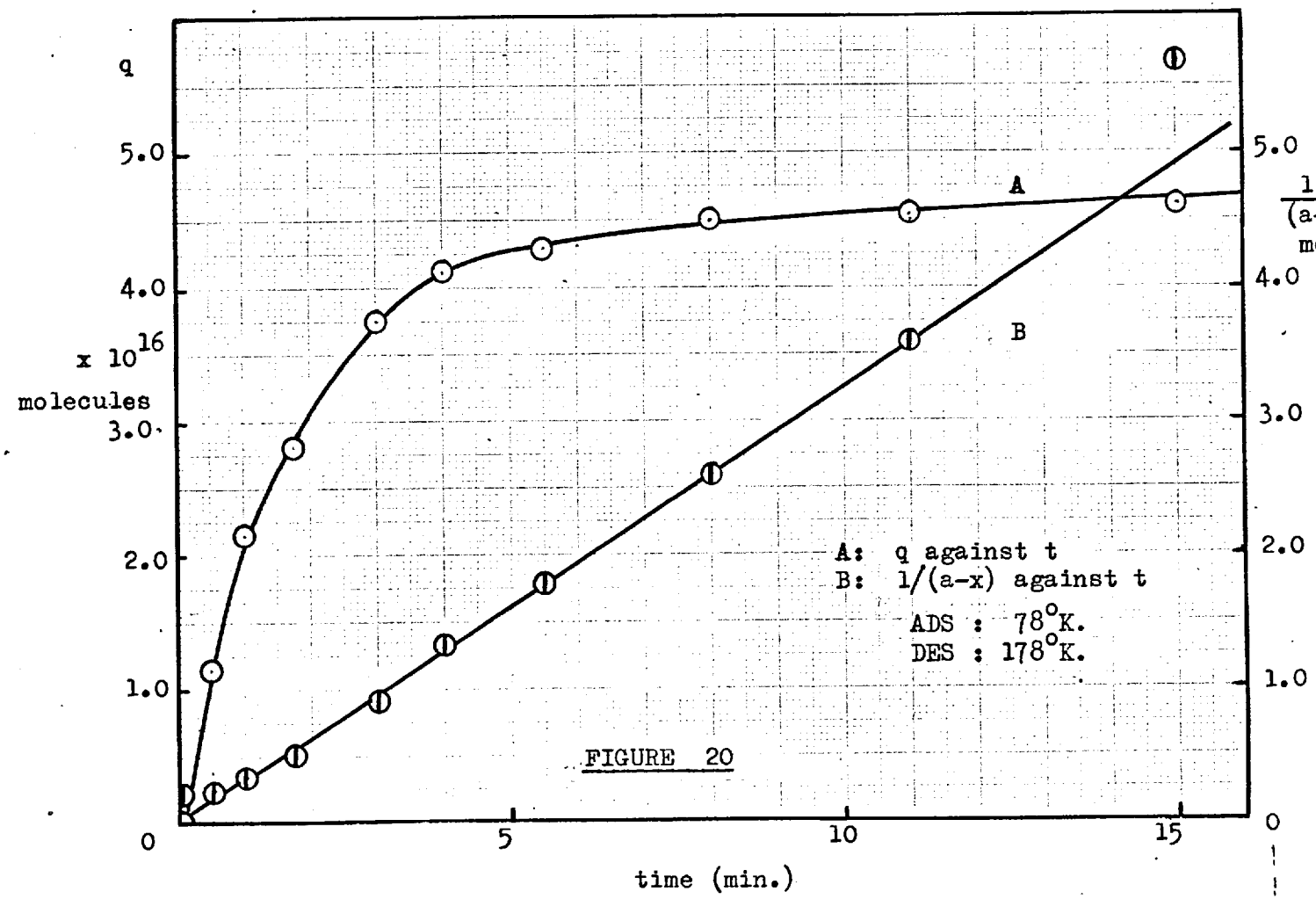
q
5.0
4.0
x 10^16
molecules
3.0
2.0
1.0
0
5
10
15
time (min.)
A
B
A: q against t
B: 1/(a-x) against t
ADS : 78°K.
DES : 178°K.
5.0
4.0
3.0
2.0
1.0
0
1/(a-x) x 10^-16
molecules^-1

FIGURE 20

x = the concentration of hydrogen molecules in the gas phase at time, t.

A typical plot is shown in FIGURE 20. The measurable rate constants (listed below in TABLE 11) were restricted to the temperature range governed by the desorbable volume which could be measured accurately. The latter varied with dosage (see TABLE 10) and hence only the rate constants below could be determined.

The subsequent Arrhenius plots yield apparent activation energies which decrease from 2.6 kcal.mole.$^{-1}$ to 0.1 kcal.mole.$^{-1}$ ($\pm$0.4 kcal.mole.$^{-1}$) with increasing dosage.

TABLE 11

Weight of film: 19.0 mg.

Total volume of hydrogen on film (molecules x 10^{17})	Rate constants, k_1 (x 10^{-17} molecules.$^{-1}$ min.$^{-1}$)					
	148°K.	178°K.	223°K.	250°K.	273°K.	294°K.
0.2997	-	-	-	-	0.00056	0.00108
0.8836	-	-	-	-	0.00176	0.00207
1.7221	-	-	-	0.00066	0.00241	0.00289
2.7735	-	-	-	0.00122	0.00516	0.0101
2.7735	-	-	-	0.00120	0.00535	0.0107
2.7735	-	-	-	0.00118	0.00524	0.0104
3.9667	-	-	-	0.00206	0.00762	0.0126
5.0530	-	-	-	0.00269	0.00796	0.0290
6.9423	-	-	0.00639	0.00848	0.01340	0.1364
8.8552	0.01610	0.0241	0.02665	0.02958	0.02989	-

(v) Surface area

After completion of the experiment the film was pumped at room temperature to remove all the desorbable gas. The surface area of the film was

then determined/...

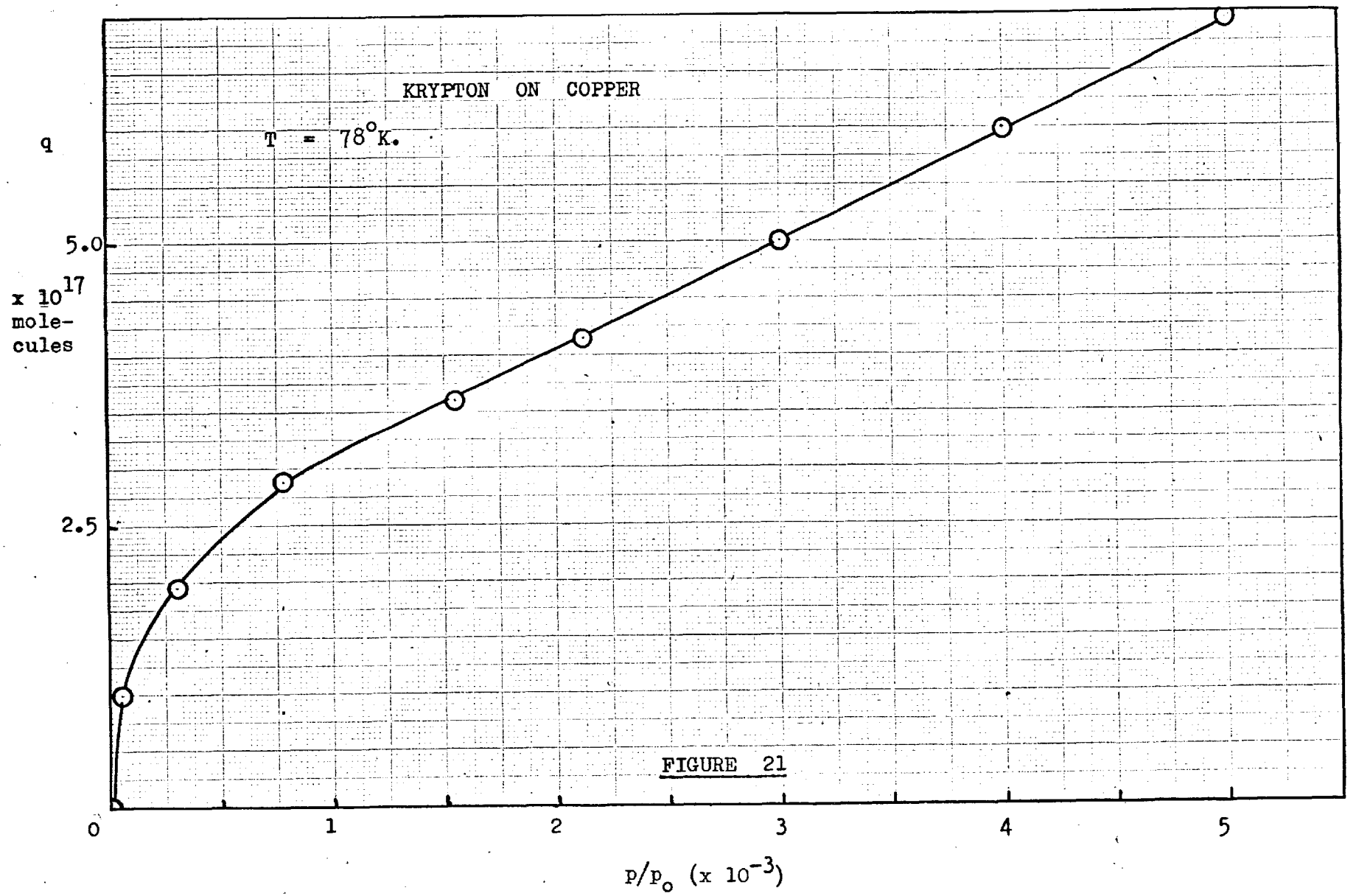
KRYPTON ON COPPER
T = 78°K.
q
5.0
x 10^17 molecules
2.5
0
1
2
3
4
5
p/p_o (x 10^-3)

FIGURE 21

then determined at 78°K. using krypton and the "point B" method (FIGURE 21). The resulting surface area was 530 sq.cm. (Geometric area ± 200 sq.cms.)

(vi) Discussion

Kinetic measurements on copper films below room temperature are rare. Between 108°C. and 148°C. Eley et al[116] have determined the rates of parahydrogen conversion on copper wires. They found $-\Delta H = 8$ kcal.mole.$^{-1}$ and an activation energy of chemisorption of 5 kcal.mole.$^{-1}$ Bond[35] has examined the rates of the parahydrogen conversion using Eley and Rossingtons results[114] for copper films in the same temperature range and found an absolute value of 13.0 kcal.mole.$^{-1}$ for the activation energy.

Pritchard[80,82] in his investigation of the correlation between surface potential and coverage on the chemisorption of hydrogen by copper films determined the activation energy for the desorption process in the temperature range -30°C. to 27°C. He adsorbed measured quantities of hydrogen ($\approx 2 \times 10^{17}$ molecules) and found rapid and complete adsorption resulted at low temperatures. He found this adsorption to be weak, enabling clean surfaces to be regenerated simply by pumping at 60°C. At higher temperatures or with comparatively large quantities of hydrogen the rapid uptake was incomplete; the fast adsorption being followed by a slow adsorption. This could not be removed completely until above 100°C.

Experimentally the procedure was as follows:- initially he adsorbed hydrogen at 195°K. and desorbed at 333°K., four times to stabilize the films; no volumetric measurements were mentioned, however, during this period. Subsequent quantitative determinations were then carried out in the required temperature range. After sorption of the given dose at a fixed substrate temperature, the filament was switched off and the pressure

increase in the/...

increase in the system recorded as a function of time. Desorption rates were subsequently measured over a five minute period. Repetition of the above at various temperatures and dosages enabled a calculation of the rates of adsorption to be made. At a particular coverage, the tangential rate was obtained from the coverage against time plots for use in the Arrhenius equation. He found an apparent activation energy for desorption which varied from 24.0 kcal.mole.$^{-1}$ to 8 kcal.mole.$^{-1}$ with increasing coverage. No mention was made of the order of the reaction although in an earlier paper a second order process was envisaged.[117]

However, at the temperatures under consideration above, it is evident that desorption is incomplete. Considerable variations in the volume desorbed with temperature also occur in the temperature range discussed above (see FIGURES 22 and 23). No normalisation of the rate curves was carried out and thus any variation in the amount desorbed with temperature will be reflected in the activation energy plots. The comparatively large apparent activation energies seem to conflict with the value (2.6 - 0.1) kcal.mole.$^{-1}$ obtained above. However, Pritchards experiments do differ from those above in that the adsorption and desorption were carried out at the same substrate temperature and in a higher temperature range. Thus a series of experiments were carried out to determine whether the temperature of adsorption or the temperature range of desorption in any way affected the nature of the desorption process.

A comparatively large dose of 8.78×10^{17} molecules was adsorbed on the film rapidly at 78°K. and the desorption rates and volumes desorbed characterised at the lower temperatures (90 - 178)°K. whereupon the adsorption temperature of the film was raised to 273°K. The rates of desorption

and the volumes/...

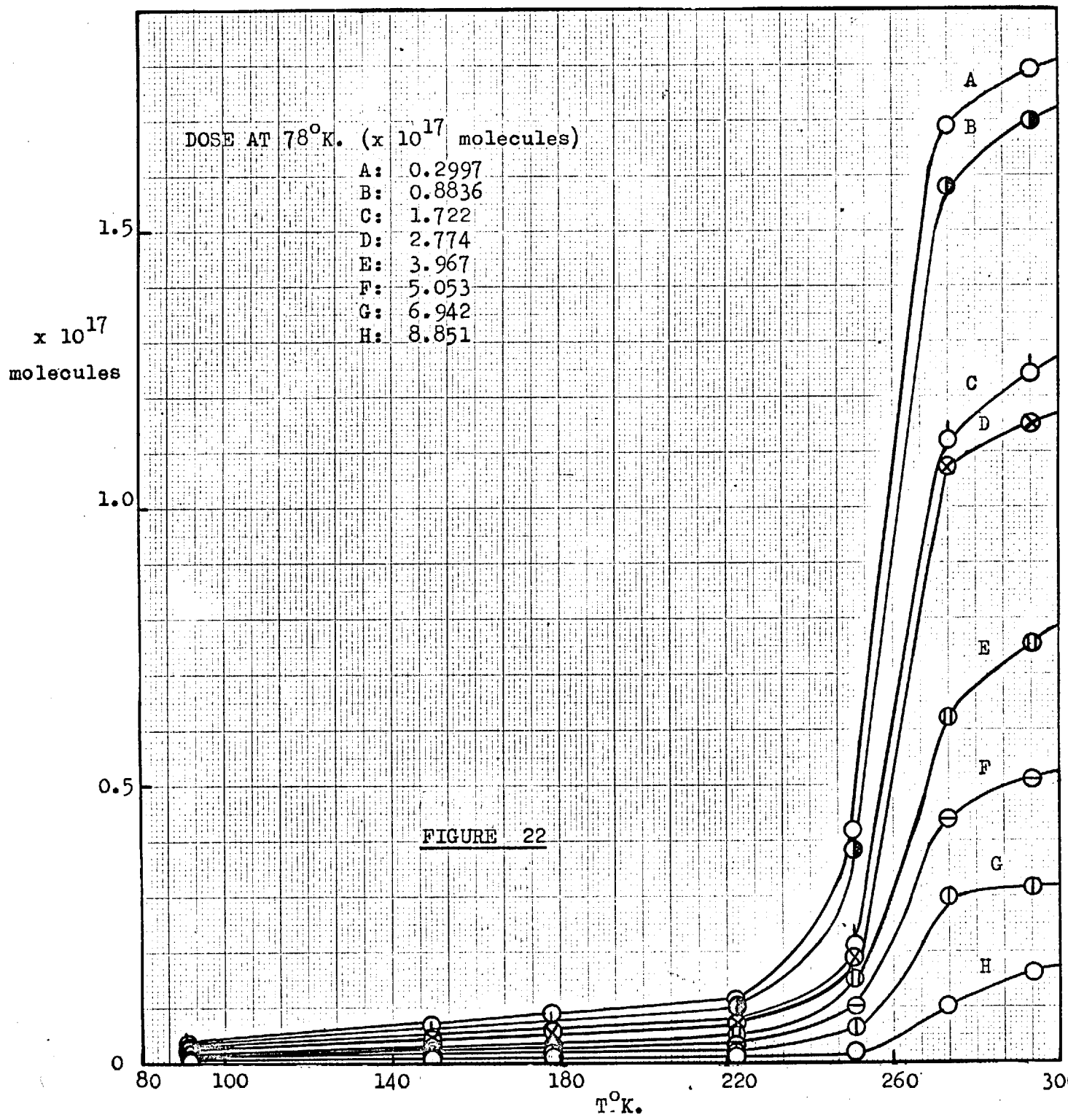
DOSE AT 78°K. (x 10^17 molecules)
A: 0.2997
B: 0.8836
C: 1.722
D: 2.774
E: 3.967
F: 5.053
G: 6.942
H: 8.851
x 10^17 molecules
1.5
1.0
0.5
0
80
100
140
180
220
260
300
T°K.
A
B
C
D
E
F
G
H

FIGURE 22

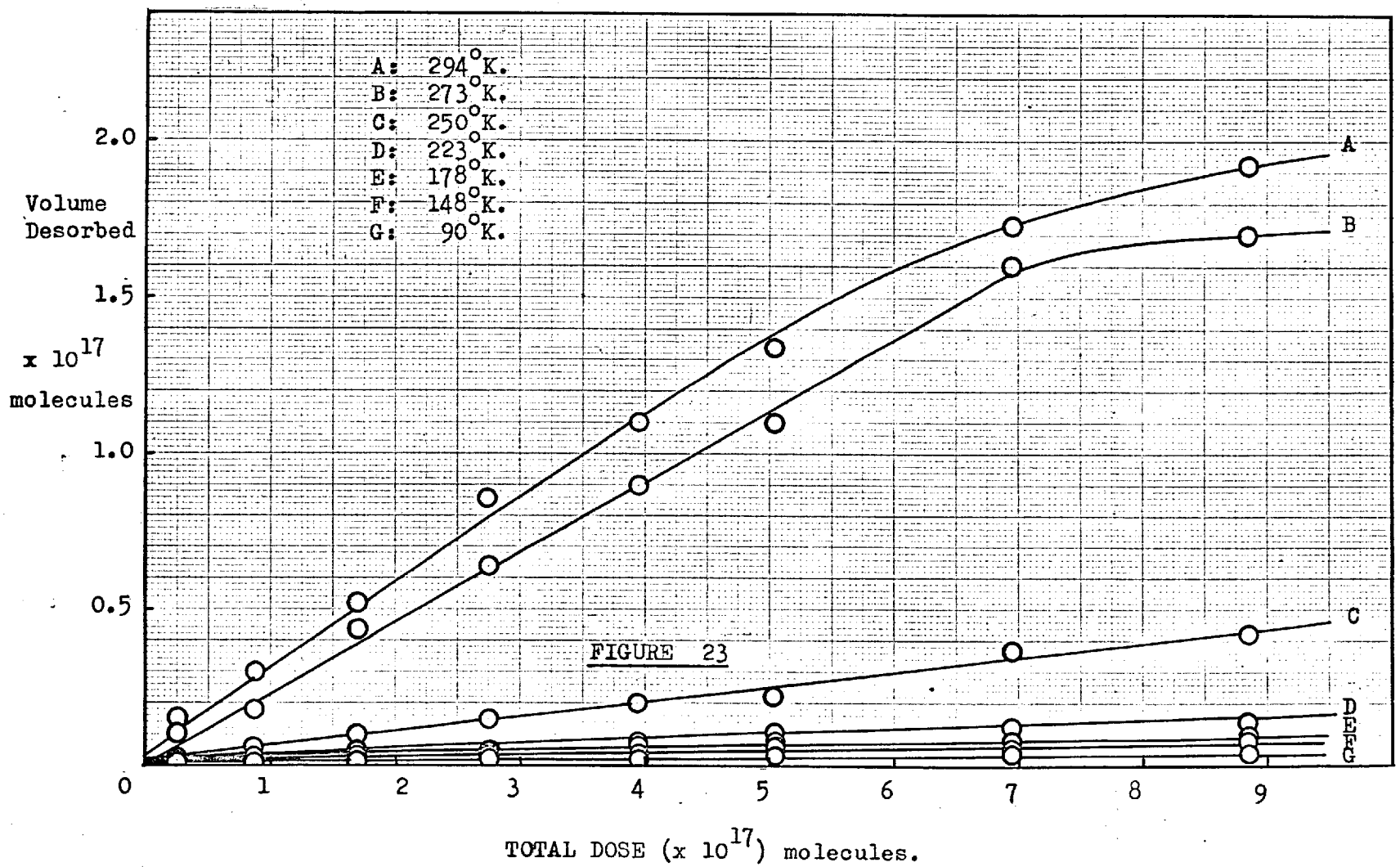
A: 294°K.
B: 273°K.
C: 250°K.
D: 223°K.
E: 178°K.
F: 148°K.
G: 90°K.
Volume Desorbed
x 10^17 molecules
2.0
1.5
1.0
0.5
0
1
2
3
4
5
6
7
8
9
A
B
C
D
E
F
G
TOTAL DOSE (x 10^17) molecules.

FIGURE 23

and the volumes desorbed were then characterised at the higher temperatures (313-413)°K. The volumes desorbed at each temperature are tabulated below in TABLE 12, expressed as a percentage of the volume adsorbed. The resulting rate plots (FIGURE 24) are well fitted by the second order expression (equation 4.05) FIGURE 25.

TABLE 12

TOTAL DOSE ON FILM (x 10^{17} molecules)		8.78 at 78°K.	0.507 at 273°K.	
T°K. ADS	T°K. DES	% Desorbed (corrected to 78°K.)	T°K. ADS & DES	% Desorbed (corrected to 273°K.)
78	78	negligible	273	68
	90	1.8	282.1	73
	148	2.5	293.0	75
	178	5.4	303.2	77
	223	10.3	316.0	79
273	273	72.7		
	313	78.1		
	363	85.1		
	413	93.0		

The normalised rate constants, k, are tabulated below in TABLE 13.

TABLE 13

8.78 x 10^{16} molecules		5.07 x 10^{16} molecules	
T°K	k(x 10^{-16} molecules.$^{-1}$ min.$^{-1}$)	T°K	k(x 10^{-16} molecules.$^{-1}$min.$^{-1}$)
90	0.095	273.0	0.01466
148	0.180	282.1	0.01595
178	0.310	293.1	0.03475
313	0.680	303.2	0.06572
363	1.061	316.0	0.1681
413	3.101		

Unfortunately/...

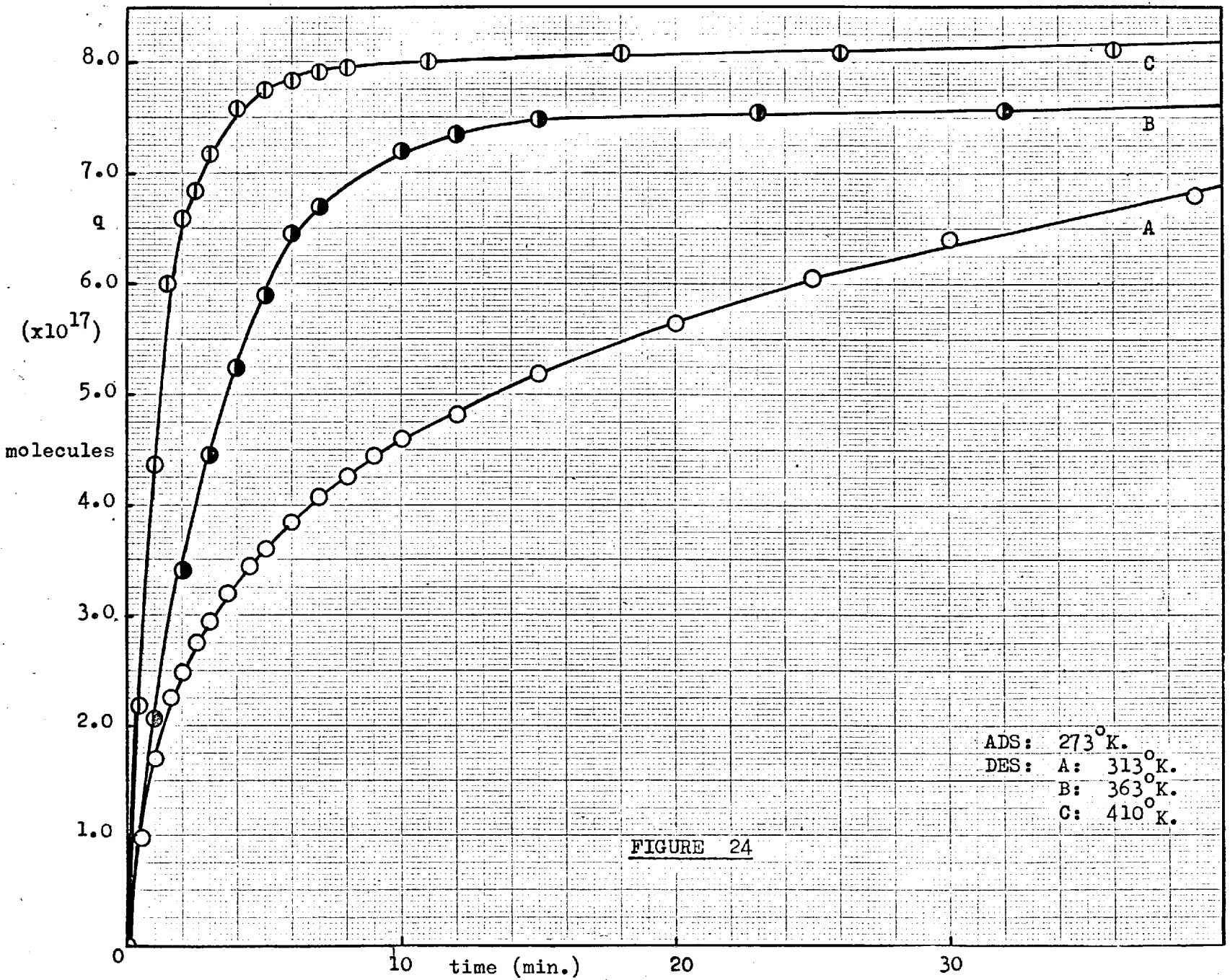
8.0
7.0
q
6.0
(x10^17)
5.0
molecules
4.0
3.0
2.0
1.0
0
10
time (min.)
20
30
C
B
A
ADS: 273°K.
DES: A: 313°K.
B: 363°K.
C: 410°K.

FIGURE 24

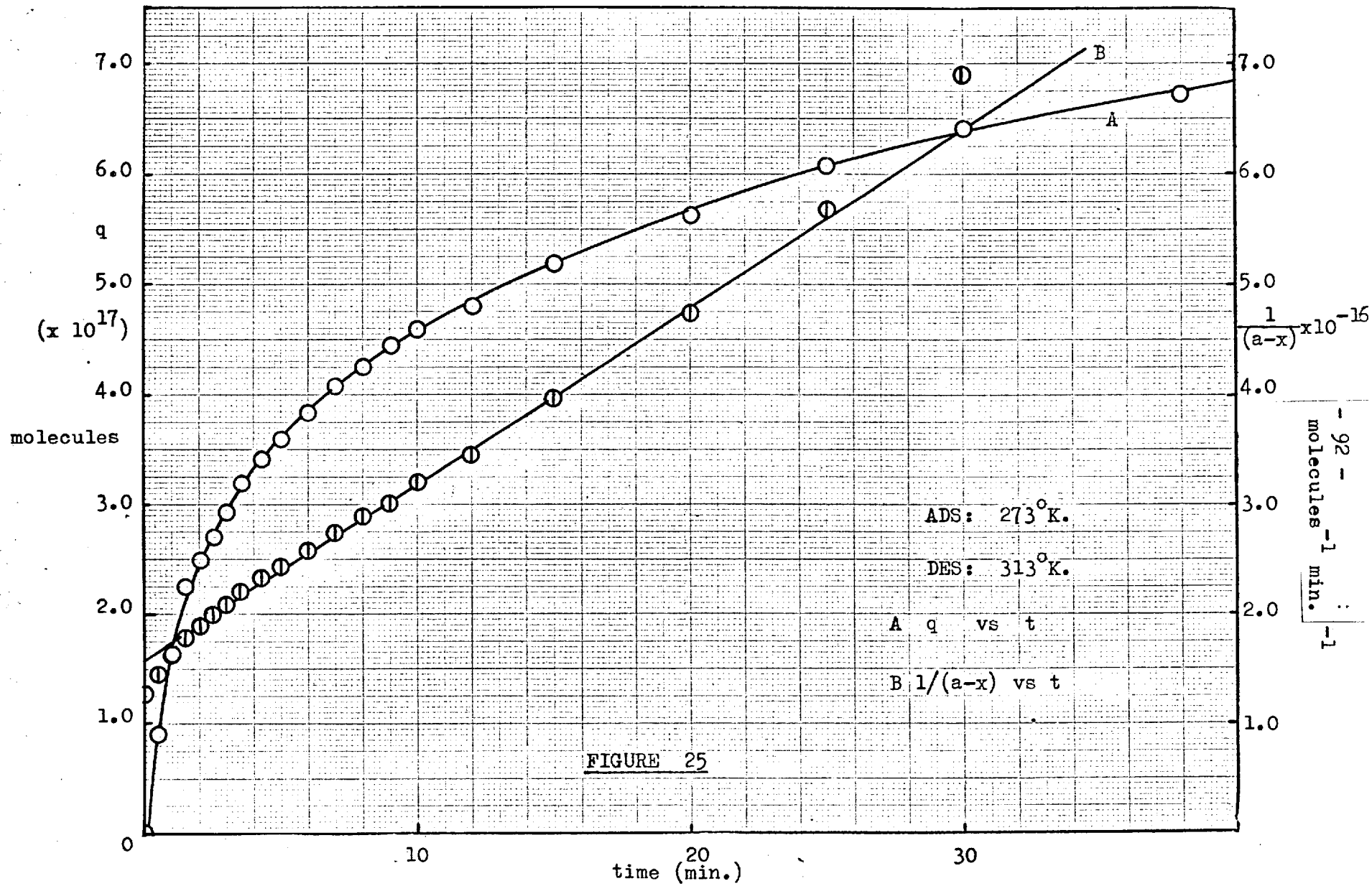
7.0
6.0
5.0
4.0
3.0
2.0
1.0
0
q
(x 10^17)
molecules
10
20
30
time (min.)
B
A
ADS: 273°K.
DES: 313°K.
A q vs t
B 1/(a-x) vs t
1/(a-x) x10^-16
molecules^-1 min.^-1

FIGURE 25

Unfortunately at 413°K. the film lifted from the glass and hence a second film was prepared and dosed as before at 273°K. and the adsorption-desorption process carried out at constant temperature. A dose equivalent in magnitude to a typical dose used by Pritchard was adsorbed. However, unlike Pritchard, the rates were followed until virtually no more gas was evolved and the substrate recooled to 273°K. for a volume comparison to be obtained. In all cases the rate curves were found to obey the second order equation (FIGURE 26) and the resulting normalised rate constants are tabulated in TABLE 13. Unlike Pritchards experiment all the gas was not desorbable until above 100°C. although at the higher temperatures it was observed that sorption of the given dose did take appreciably longer.

The mobility energies associated with the rate constants are calculated using equation (4.08) with $N = 1.47 \times 10^{15}$ sites.cm.$^{-2}$ and the resulting V_D against T°K. plots for two typical dosages are shown in FIGURE 27. As found for nickel, the plots are linear, parallel and a decrease in the apparent activation energy (intercept value of V_D) results on increasing dosage. The resultant straight line is described by

V_D = 56T + 4,500 calories (T°K.) for the smaller dose (0.884×10^{17} molecules) ..... (4.37)

and V_D = 56T + 2,600 calories (T°K.) for the larger dose (8.86×10^{17}) molecules) ..... (4.38)

At temperatures approaching those for the desorption of the second layer on nickel (between 113°K. and 148°K.) the comparable value for V_D for copper is from (9-11) kcal.mole.$^{-1}$; for nickel (7-9) kcal.mole.$^{-1}$ However, for copper the values of V_D range as high as 24 kcal.mole.$^{-1}$ at the higher temperatures. This was not the case for nickel where no

calculation/...

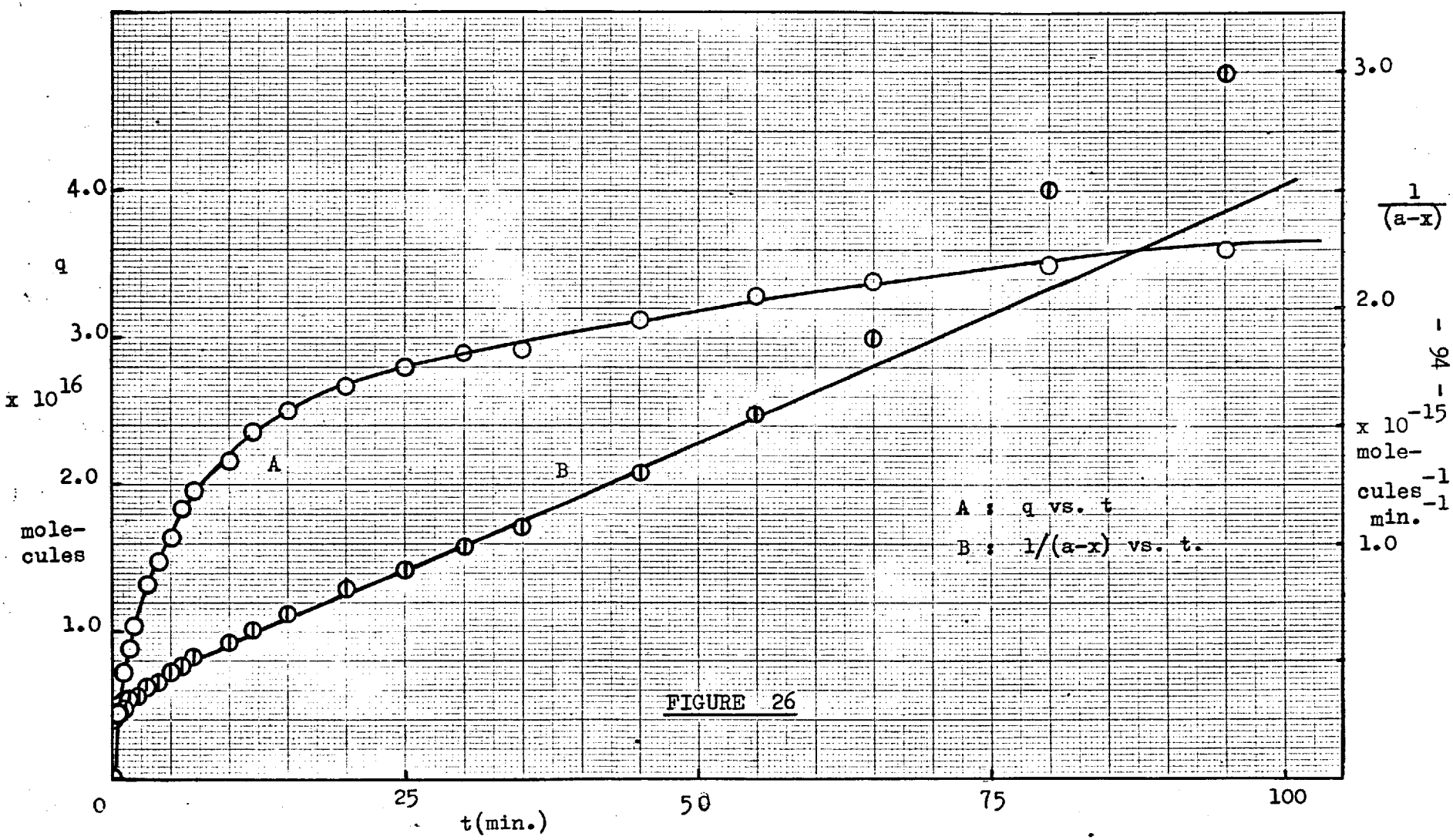
4.0
q
3.0
x 10^16
2.0
molecules
1.0
0
25
50
75
100
t(min.)
A
B
3.0
2.0
1.0
1/(a-x)
x 10^-15
molecules^-1 min.^-1
A : q vs. t
B : 1/(a-x) vs. t.

FIGURE 26

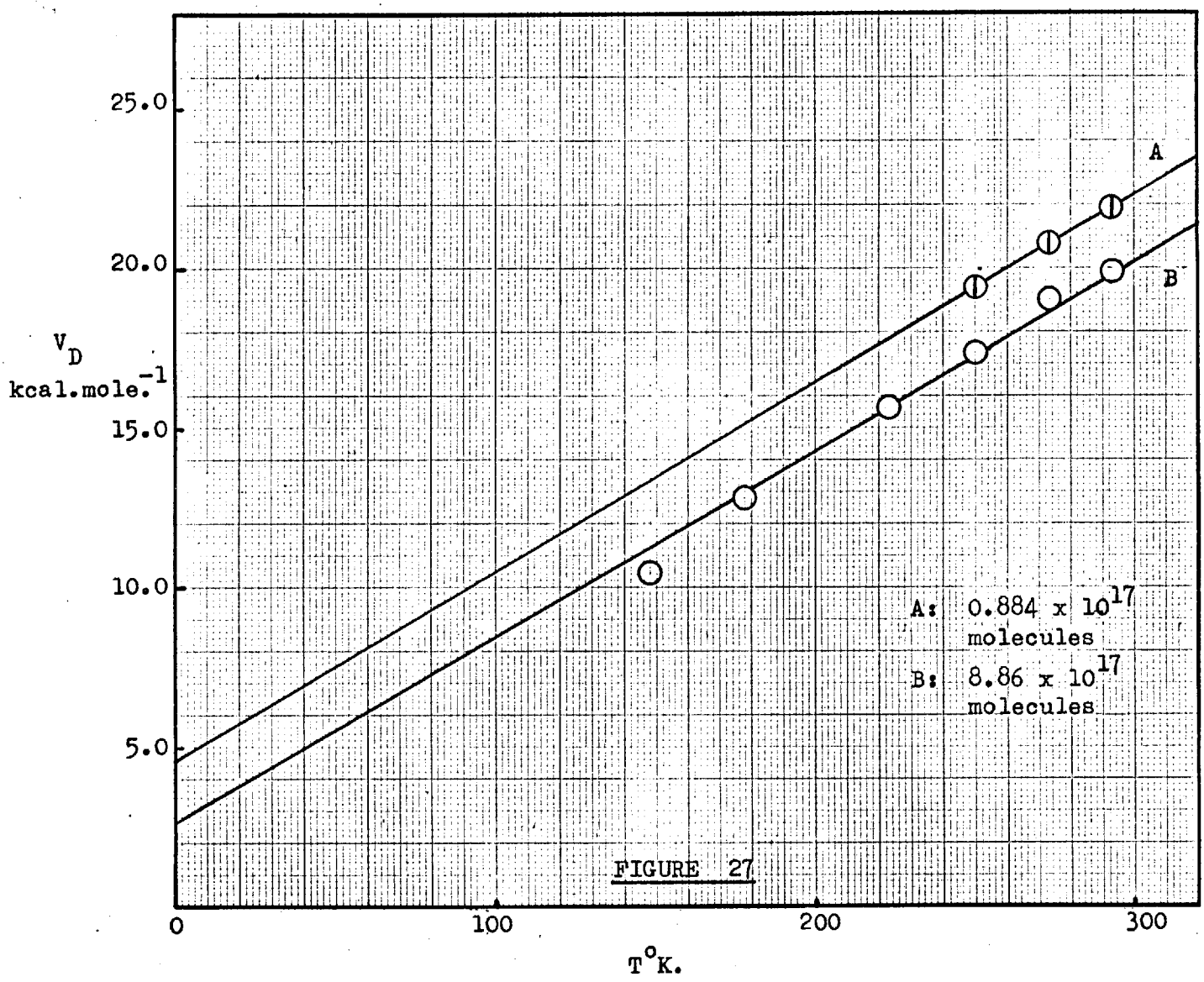
25.0
20.0
15.0
10.0
5.0
V_D
kcal.mole.$^{-1}$
0
100
200
300
T°K.
A
B
A: 0.884 x 10^{17} molecules
B: 8.86 x 10^{17} molecules

FIGURE 27

calculation of V_D could be made above about 190°K. A possible explanation for the high values obtained for copper is in the condition of the substrate. For nickel we were dealing with a second layer constituting about (10-15)% of the available surface. This surface was already covered to a large extent by strongly bonded hydrogen adatoms and hence it would be expected that desorption from a second layer would proceed with a smaller mobility energy than for copper where we are clearly dealing with directly held surface atoms.

The magnitude of the quantity of gas evolved below 220°K. might also support the reported immobility of hydrogen atoms on copper film below 195°K.[76,80]

The distribution function,

$$D_V = (dN/dV) \cdot 1/N_T \quad \ldots\ldots\ldots\ldots\ldots\ldots \quad (4.34)$$

where N = volume desorbed, N_T = the maximum value desorbed and $V = akT + C$, was derived from tangential slopes of the plot of V_{DES} against T°K. (FIGURE 22) and is illustrated in FIGURE 28 for a dose of 8.86×10^{17} molecules. From this plot we note the large number of adatoms with mobility energies in the range 17-18 kcal.mole^{-1}.

It is also of interest to consider the plot of volume desorbed against total dose for various temperatures (FIGURE 23). This plot was found to be linear over nearly the whole coverage range but fell off towards a constant $Vol._{Des.}$ value at higher coverages at the higher temperatures.

If we assume that on deposition the atoms are distributed between the outer surface layer and the bulk solid in such a manner that

$$[H]_{surface}/[H]_{bulk} = \text{constant} \quad \ldots\ldots\ldots\ldots\ldots\ldots \quad (4.39)$$

and that the surface atoms are more readily desorbed than those from the bulk i.e./...

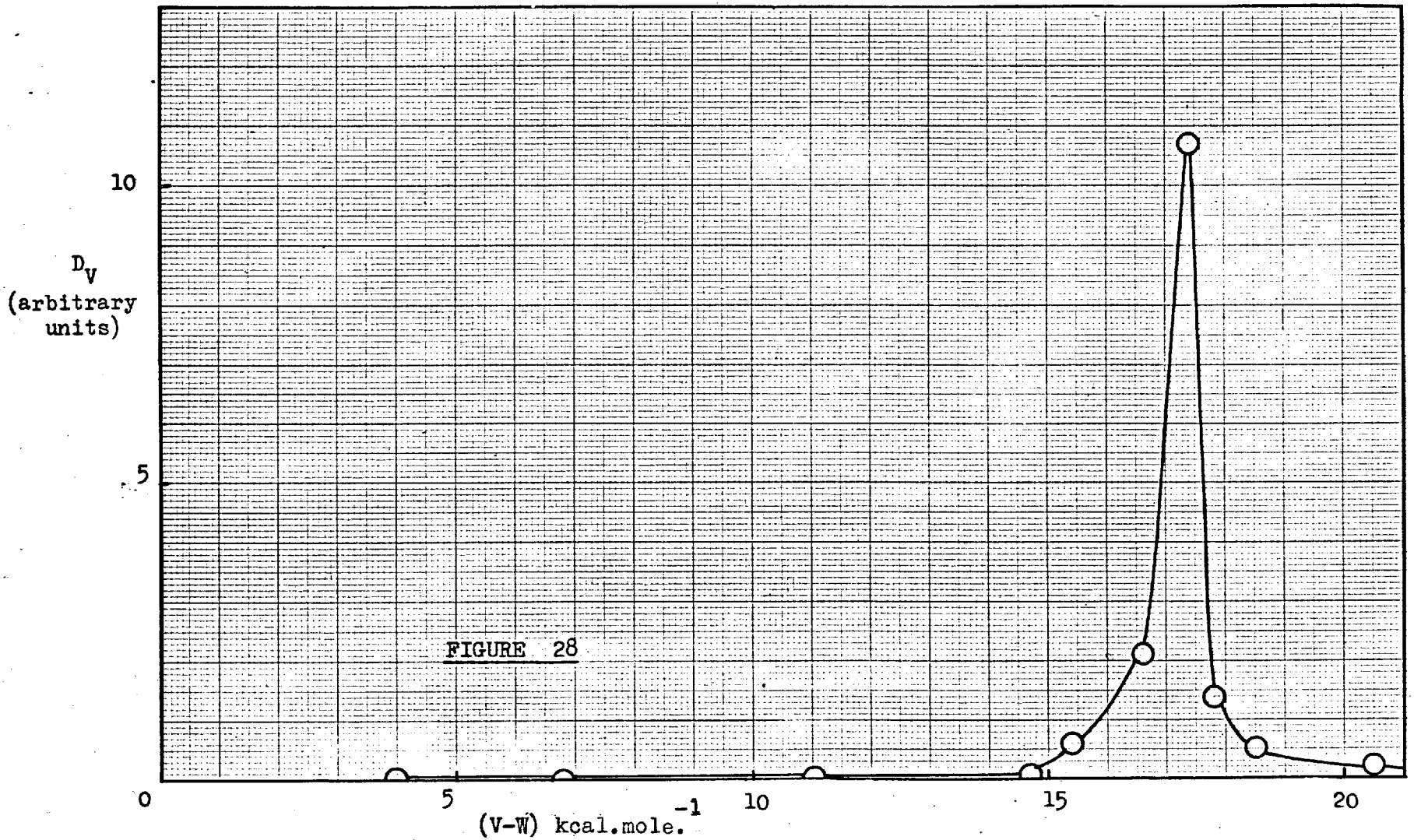

FIGURE 28

bulk i.e. $[H]_{surface} \propto Vol._{Des.}$, while $[H]_{bulk} \propto Vol._{Total}$, ($Vol._{Total} \gg Vol._{Des.}$), then $[H]_{surface}/[H]_{bulk}$ = constant

$$= Vol._{Des.}/Vol._{Total}$$

$$= \frac{K'' \; e^{-E_S/kT}}{K' \; e^{-E_B/kT}} \qquad \ldots\ldots\ldots\ldots\ldots\ldots \quad (4.40)$$

$$= K \; e^{(E_B - E_S)/kT} \qquad \ldots\ldots\ldots\ldots\ldots \quad (4.41)$$

where E_S and E_B are the enthalpies of sorption on the surface and in the bulk of the solid, respectively.

For a given dosage E_S and E_B will remain constant at a given temperature. However, as the dosage increases, E_S will decrease while E_B may remain constant or even increase. Hence, for higher concentrations the $Vol._{Des.}$ will become solely influenced by $[H]$ bulk.

The mobility energies obtained on repeating Pritchards experiment are also of interest (FIGURE 29). Apparently the temperature of adsorption plays little or no part in the desorption phenomena, the mobility energies derived by deposition at 78°K. lie on the same straight line as those derived from deposition on the surface at 273°K. and above. Furthermore, while an apparent activation energy of 5.0 kcal.mole^{-1} arises from the desorption of the moderately small dose (5.07×10^{16} molecules) the mobility energies for the plot lie in the range (18-24) kcal.mole^{-1} between 245°K. and 300°K. That Pritchards activation energy values for low coverage should be of the same value seems purely fortuitous. The separation between the two plots may arise from the difference in dosage and the difference in films used.

4.4 Cadmium /...

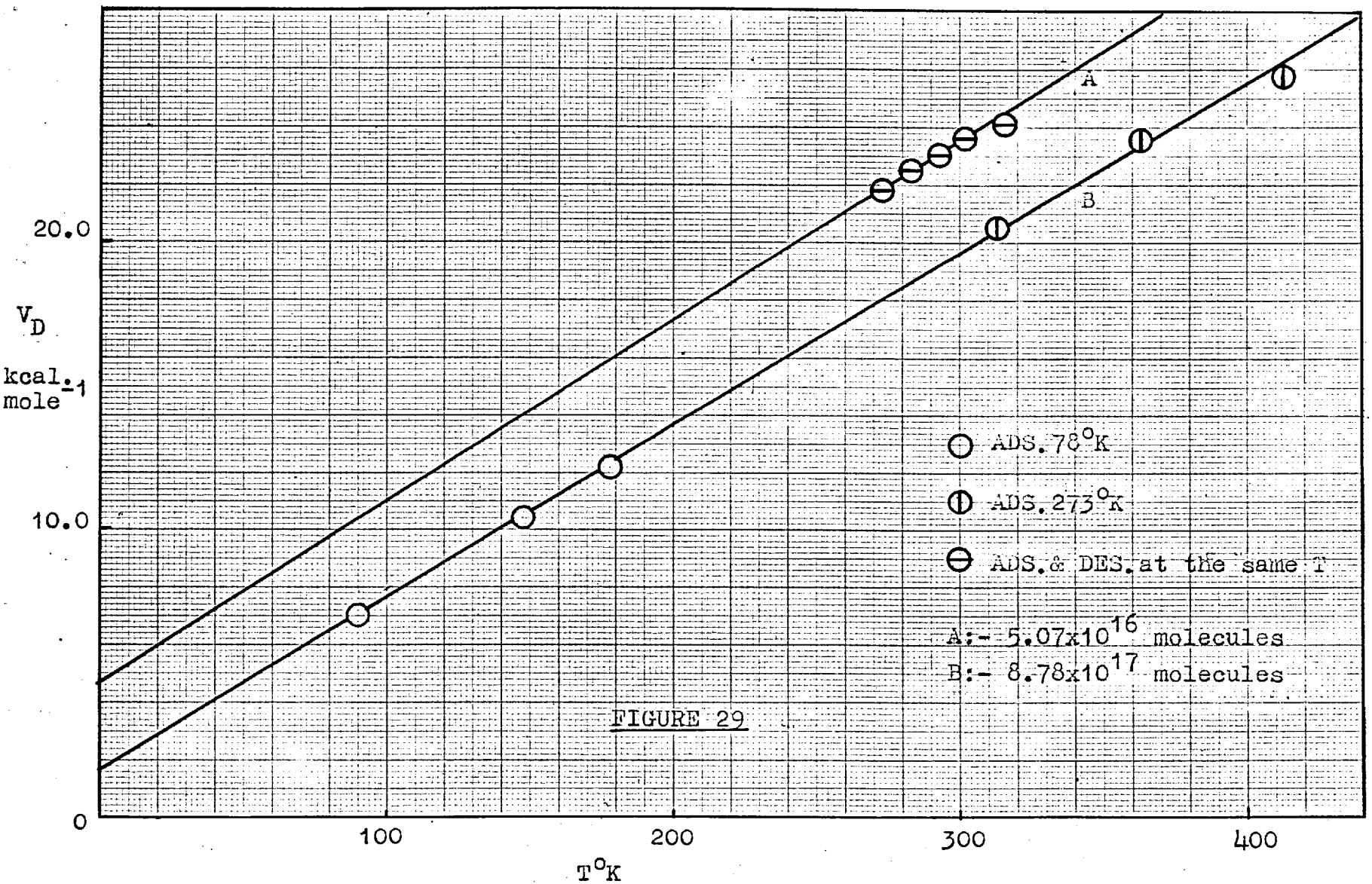
A
B
20.0
10.0
0
V_D
kcal. mole^{-1}
100
200
300
400
T^oK
ADS. 78°K
ADS. 273°K
ADS. & DES. at the same T
A:- 5.07×10^{16} molecules
B:- 8.78×10^{17} molecules

FIGURE 29

4.4 Cadmium

(i) Adsorption

(a) Hydrogen molecules

As found for copper no appreciable adsorption ($\lesssim$ 1%) of molecular hydrogen resulted on exposure of a cadmium film to the gas in the temperature range 78°K. to 273°K.

(b) Hydrogen atoms

The rates of adsorption of equal doses ($\pm 1 \times 10^{17}$ hydrogen molecules) as atoms at 78°K. proceded exactly as found for the previous metals; for the initial dosages the uptake was almost instantaneous (± 2 minutes) while the rate became slower with increasing doses. No coverage greater than 2 θ was used although this by no means represented the complete sorptive capacity of the film.

(ii) Desorption

Upon switching off the filament at 78°K. no detectable desorption was observed. Upon raising the substrate to the required desorption temperature gas was evolved as shown in FIGURE 30. The volume of gas desorbed increased with increasing temperature.

Although varying from film to film reproducibility on any one film was excellent; the rate constants (see later) and the volumes desorbed for three successive doses are tabulated below in TABLE 14. At the highest temperature the substrate was pumped for several minutes before introducing the following dose.

TABLE 14/...

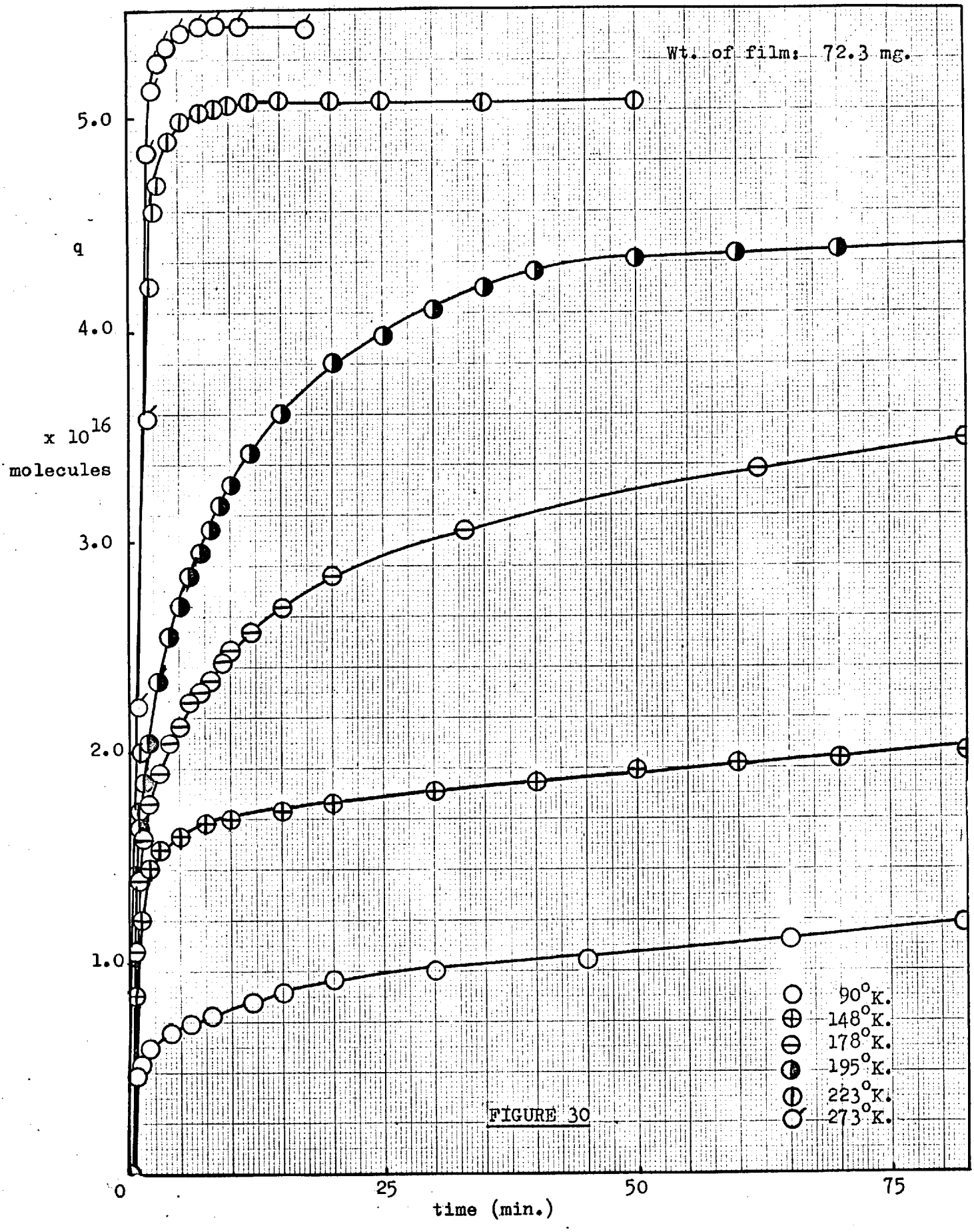
Wt. of film: 72.3 mg.
q
x 10^{16}
molecules
5.0
4.0
3.0
2.0
1.0
0
25
50
75
time (min.)
90°K.
148°K.
178°K.
195°K.
223°K.
273°K.

FIGURE 30

TABLE 14

Dose ($\times 10^{17}$) molecules	Percentage desorbed (corrected to 78°K.) 148°K	178°K	223°K	273°K	$k(\times 10^{-16}$ molecules^{-1} min^{-1} 148°K	178°K	223°K
1.276	34.3	78.5	96.6	98.0	0.0098	0.0144	0.6410
1.139	40.0	83.2	96.9	98.2	0.0104	0.0164	0.6493
3.212	37.1	80.9	97.1	98.6	0.0102	0.0158	0.6333

Another film was subsequently dosed with successively increasing dosages of hydrogen atoms at 78°K. and the rates of desorption and the volume desorbed (corrected to 78°K.) were measured at various temperatures. For the lower temperatures the rates were extrapolated to infinite time.

The results of the volume desorbed against total volume for varying temperatures are tabulated below in TABLE 15 and are illustrated in FIGURE 31.

TABLE 15

Dosage (molecules $\times 10^{17}$)	Volume desorbed (corrected to 78°K.) molecules $\times 10^{17}$ 90°K	148°K	178°K	195°K	223°K	273°K
0.588	0.175	0.226	0.438	0.489	0.539	0.576
1.743	0.216	0.675	0.953	1.131	1.375	1.740
3.423	0.183	0.612	0.899	1.086	1.559	2.000
5.569	0.176	0.432	0.936	1.067	1.698	1.989

FIGURE 32 shows the variation of the volume desorbed with temperature for increasing dosages

(iii) <u>The kinetics of the desorption process</u>

As for the previous metals the rate plots were analysed to determine the order of the reaction and the second order equation (4.05) was found

to be obeyed/...

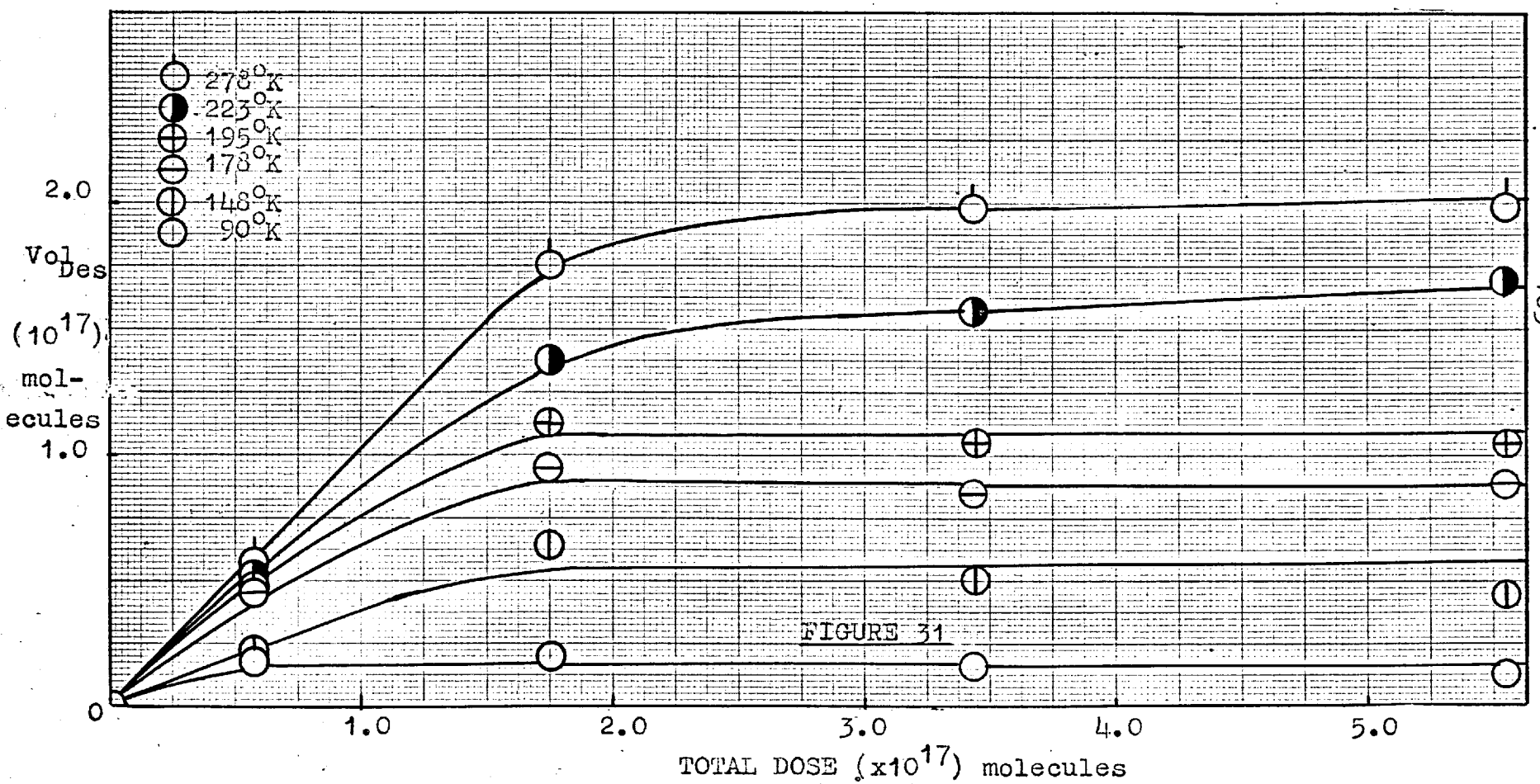
273°K
223°K
195°K
173°K
148°K
90°K
2.0
Vol Des
(10^{17})
mol-
ecules
1.0
0
1.0
2.0
3.0
4.0
5.0
TOTAL DOSE (x10^{17}) molecules

FIGURE 31

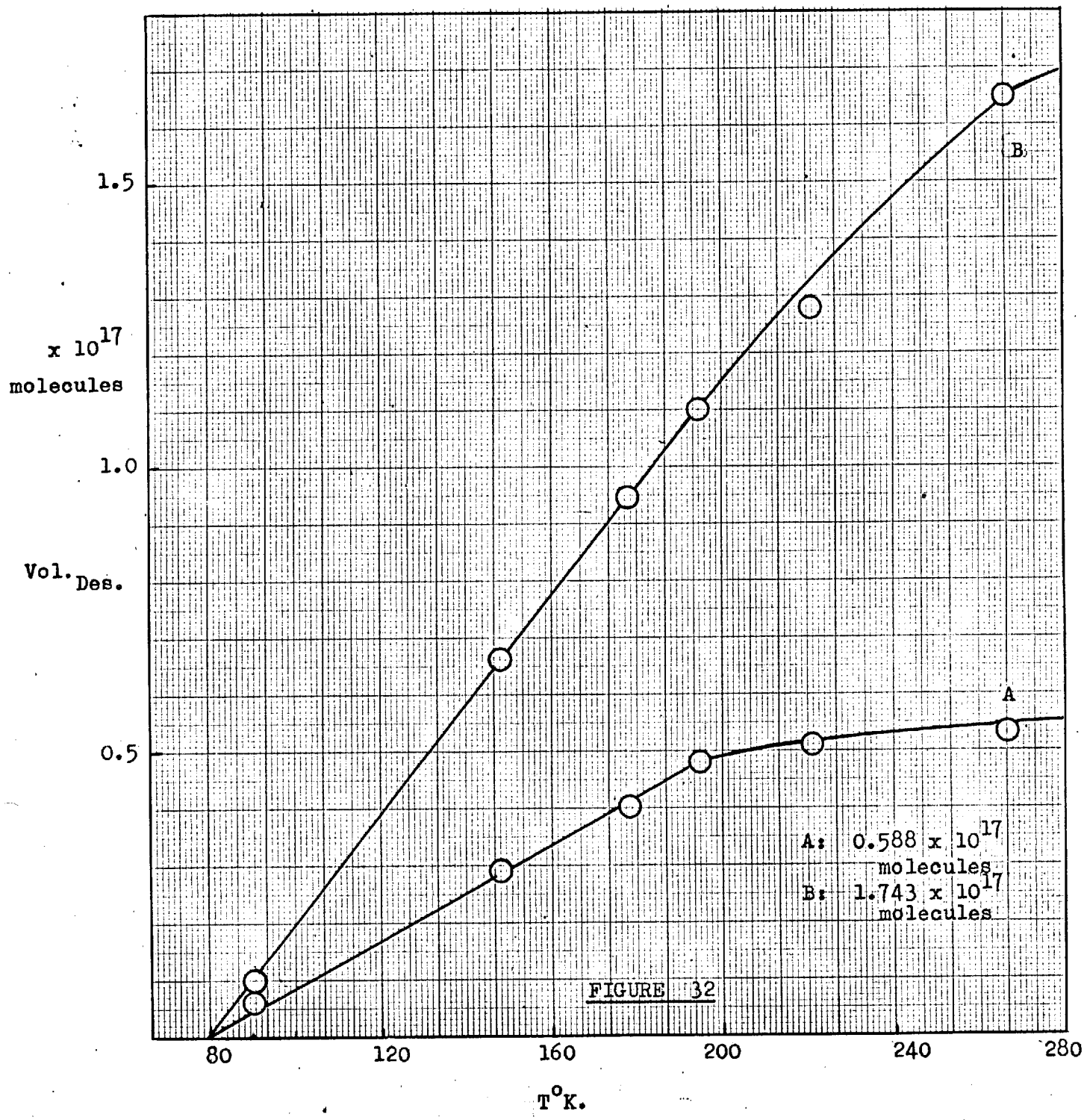
1.5
x 10^17 molecules
1.0
Vol. Des.
0.5
B
A
A: 0.588 x 10^17 molecules
B: 1.743 x 10^17 molecules
80
120
160
200
240
280
T°K.

FIGURE 32

to be obeyed over almost the whole curve and at all temperatures and dosages. A typical plot is shown in FIGURE 33. The resulting rate constants are tabulated below in TABLE 16 for the various dosages.

TABLE 16

Wt. of film: 72.3 mg.

Dosage (molecules x 10^{17})	k(x 10^{-16} molecules.$^{-1}$ min.$^{-1}$)					
	90°K	148°K	178°K	195°K	223°K	273°K
0.588	0.0059	0.0168	0.0193	0.0490	2.040	3.300
1.743	0.0053	0.0068	0.0070	0.0130	0.3200	-

(iv) Surface area determination

After completion of an experiment a film was pumped out at room temperature to remove all the desorbable gas. The surface area of the film was then determined at 78°K. using krypton and the point B method. The resulting surface area was 390 sq.cm. i.e. 3.9 x 1.01 x 10^{17} sites 3.94 x 10^{17} sites.

(v) Discussion

The plot of $Vol._{Des.}$ against $Total_{Volume}$ (FIGURE 31) indicates that up to a critical value ($\pm$1.7 x 10^{17} molecules) at the highest temperature effectively all the gas ($\pm$95%) is desorbed. This was the first metal to show complete desorbability of hydrogen in this temperature range and confirms the assumption that comparatively small amounts of hydrogen are trapped by the glass and other extraneous surfaces present.

Further it has been shown for nickel that exposure to mercury vapour will release all the adsorbed gas on the surface at the higher temperatures. On exposure of a cadmium film to mercury vapour at the highest temperature

no additional gas/...

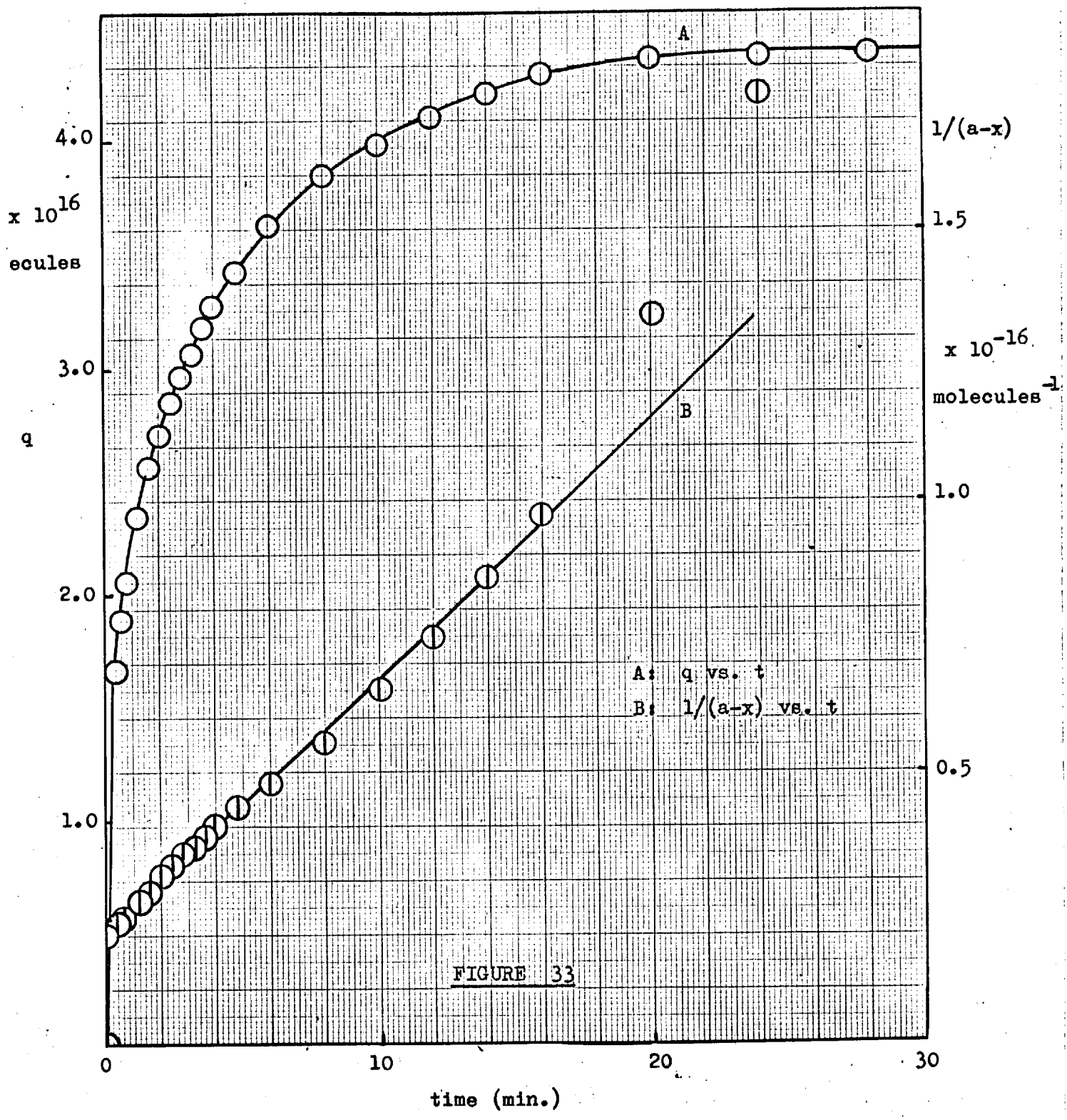
A
B
4.0
3.0
2.0
1.0
x 10^16
ecules
q
1/(a-x)
1.5
1.0
0.5
x 10^-16
molecules^-1
A: q vs. t
B: 1/(a-x) vs. t
0
10
20
30
time (min.)

FIGURE 33

no additional gas was liberated; indicating that the gas which is not desorbed is inaccessible to the mercury vapour. Following our assumption for copper concerning a distribution of atoms between the surface and the bulk it would seem probable that the initial depositions are confined solely to the surface of the metal, but after reaching a point ($\pm 1.7 \times 10^{17}$ molecules: surface area: 3.94×10^{17} sites) no further gas was desorbed. It is thus postulated that after the surface is saturated the atoms are driven into the solid bulk (inaccessible to mercury vapour) and are not removed by the normal desorption process.

Application of the hopping formula (equation 4.08) with $N = 1.01 \times 10^{15}$ yields values of V_D, similar to those found for copper and nickel for various dosages (FIGURE 34). Unfortunately the two doses are not well separated; considerable spattering being observed. The best overall straight line is expressed by the equation

$$V_D = 55T + 2,900 \text{ calories } (T^{\circ}K.) \quad \ldots\ldots\ldots\ldots\ldots \quad (4.4$$

The distribution function, D_V, was derived as for copper from the tangential slopes of the Volume desorbed vs. Temperature plot (FIGURE 32). Variation of D_V with $(V - W)$ are shown in FIGURE 35, from which we note a large plateau of atoms with energies ranging from 4 to 13 kcal.mole.$^{-1}$

4.5 Zinc

(i) Adsorption

Zinc films closely resemble those of cadmium in that no appreciable adsorption of hydrogen molecules occurs in the temperature range $78^{\circ}K.$ to $273^{\circ}K.$ while the uptake of hydrogen atoms at $78^{\circ}K.$ occurs almost instantaneously. Similar behaviour of the adsorption rates for equal doses of hydrogen atoms ($\pm 1 \times 10^{17}$ molecules) was found and no saturation of the film

was attempted./...

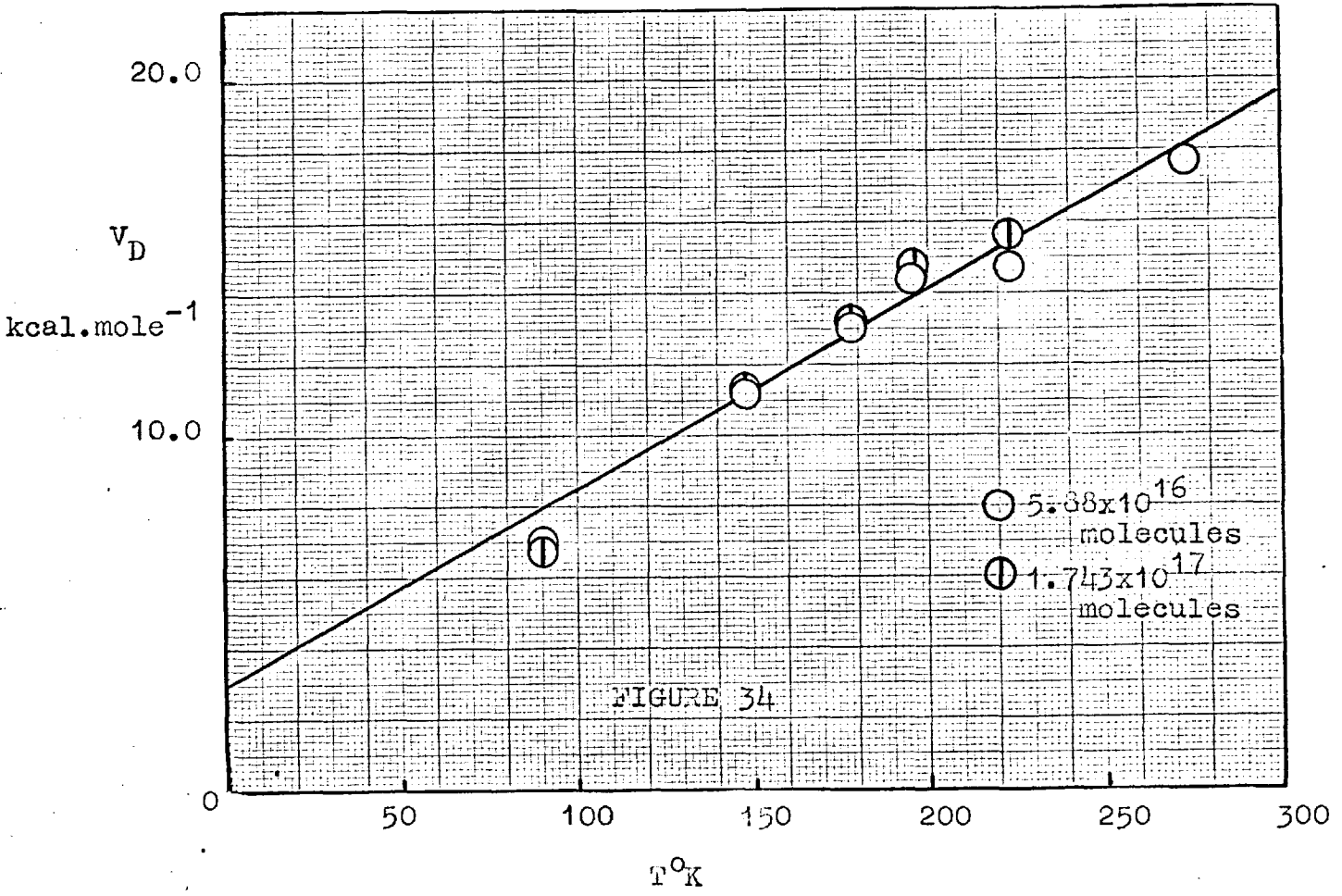
20.0
V_D
kcal.mole^{-1}
10.0
0
50
100
150
200
250
300
T°K
5.88x10^{16} molecules
1.743x10^{17} molecules

FIGURE 34

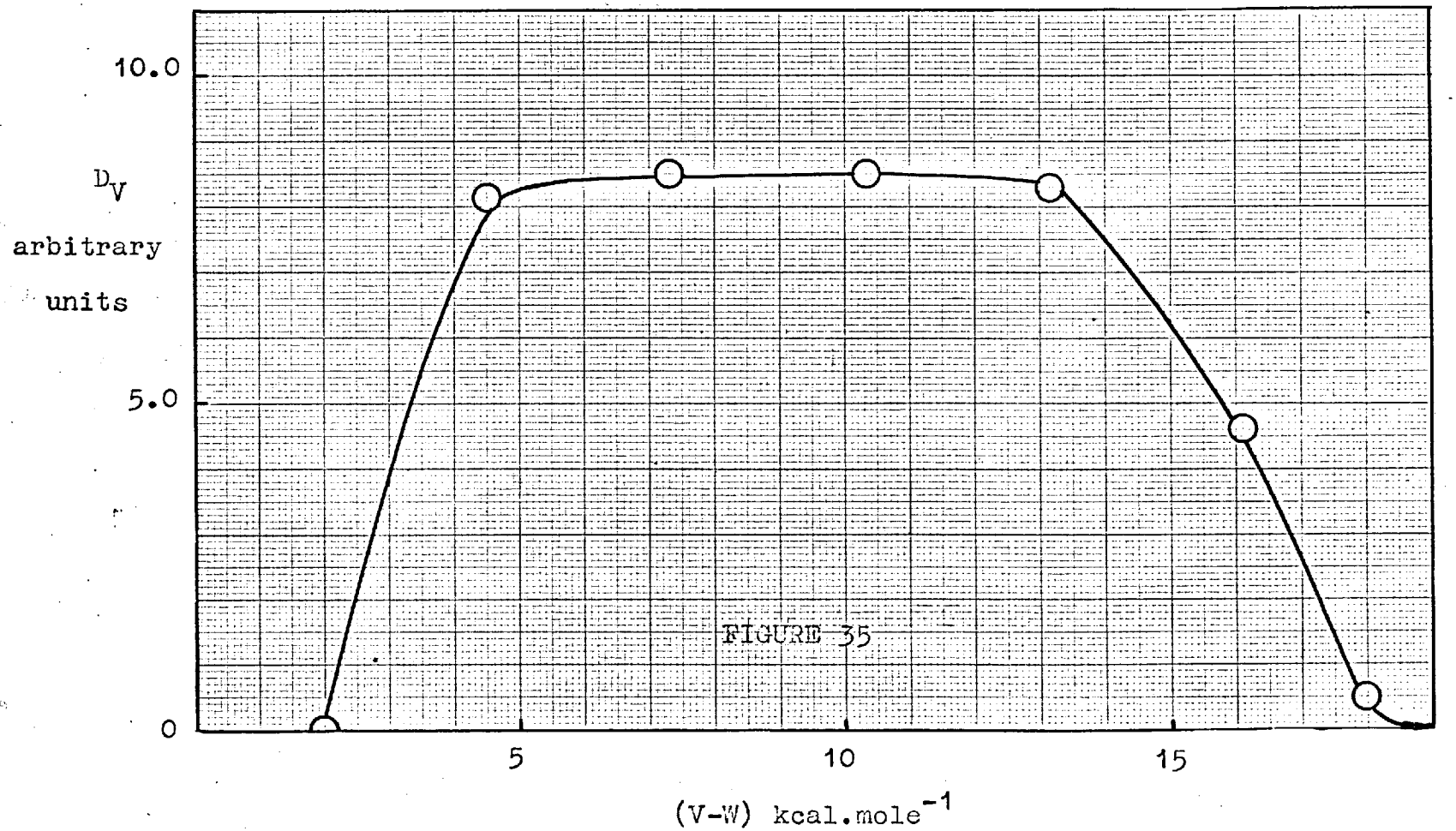

FIGURE 35

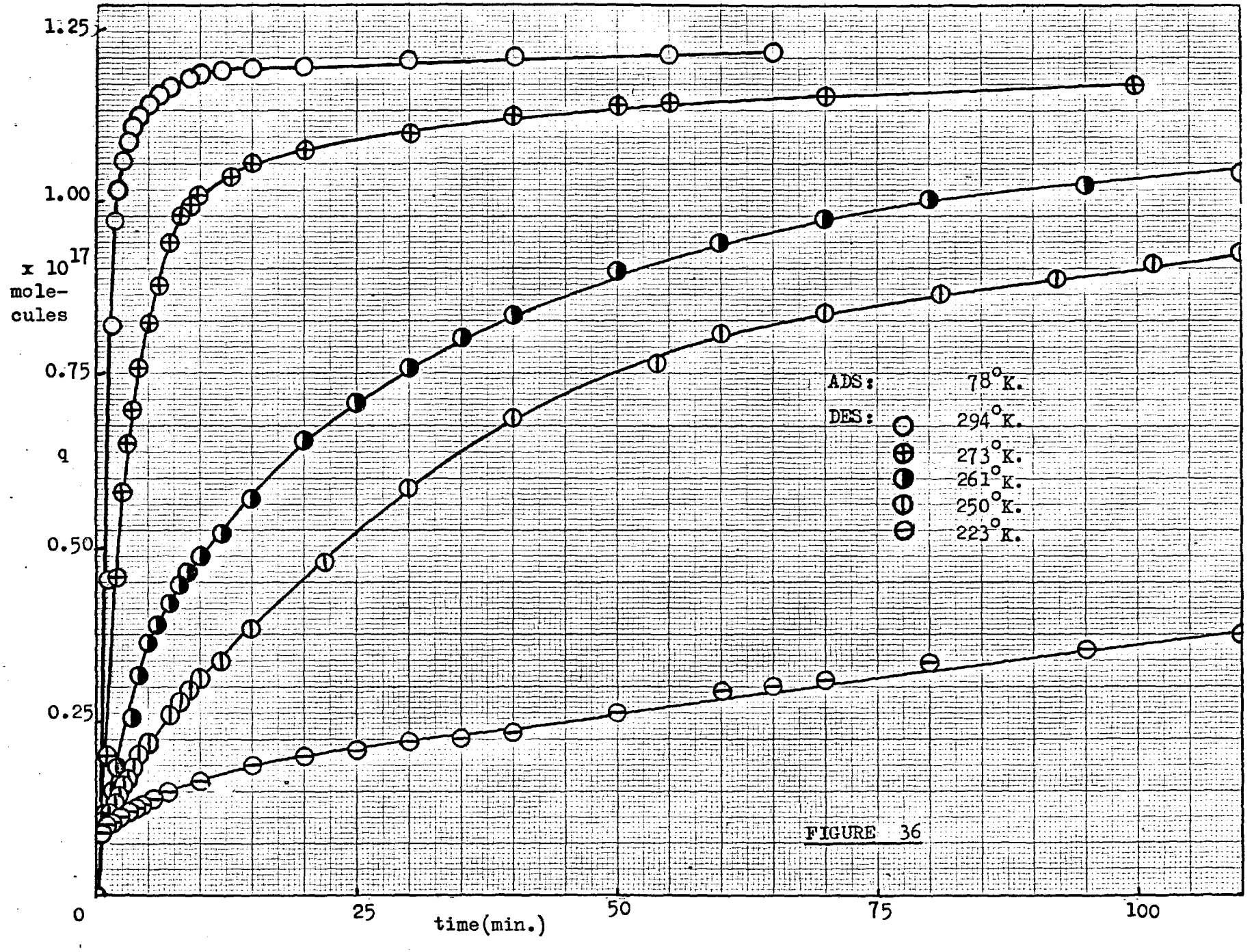
1.25
1.00
x 10^17 molecules
0.75
q
0.50
0.25
0
25
50
75
100
time(min.)
ADS: 78°K.
DES: 294°K.
273°K.
261°K.
250°K.
223°K.

FIGURE 36

was attempted.

(ii) Desorption

A dose of 1.25 x 10^{17} molecules was added to a clean film at 78°K. and rapidly adsorbed. No detectable desorption resulted upon switching off the filament at this temperature. Upon increasing the desorption temperature increasing amounts of gas were desorbed and their rates of desorption noted (FIGURE 36). Before each desorption the amount of gas desorbed was noted with the cell at 78°K. (the temperature of adsorption) and the previously desorbed gas, readsorbed. The volumes desorbed are tabulated below in TABLE 17 and the plot of Volume desorbed against Temperature for this dosage is shown in FIGURE 37. The kinetics of the desorption follow a similar pattern to that found for cadmium; the second order equation is a good fit over almost the whole curve (FIGURE 38).

TABLE 17

Dose added	Volume desorbed (molecules x 10^{17})						
78°K	90°K	178°K	223°K	250°K	261°K	273°K	294°K
1.25 x 10^{17}	negligible	0.125	0.503	0.882	1.000	1.125	1.190

The resulting rate constants are tabulated below in TABLE 18.

TABLE 18

Wt. of film: 80.1 mg.

Dose (molecules x 10^{17})	k x 10^{-16} molecules^{-1} min.$^{-1}$				
	223°K	250°K	261°K	273°K	294°K
1.250	0.0480	0.0624	0.06563	0.4750	2.360

(iii) Discussion/...

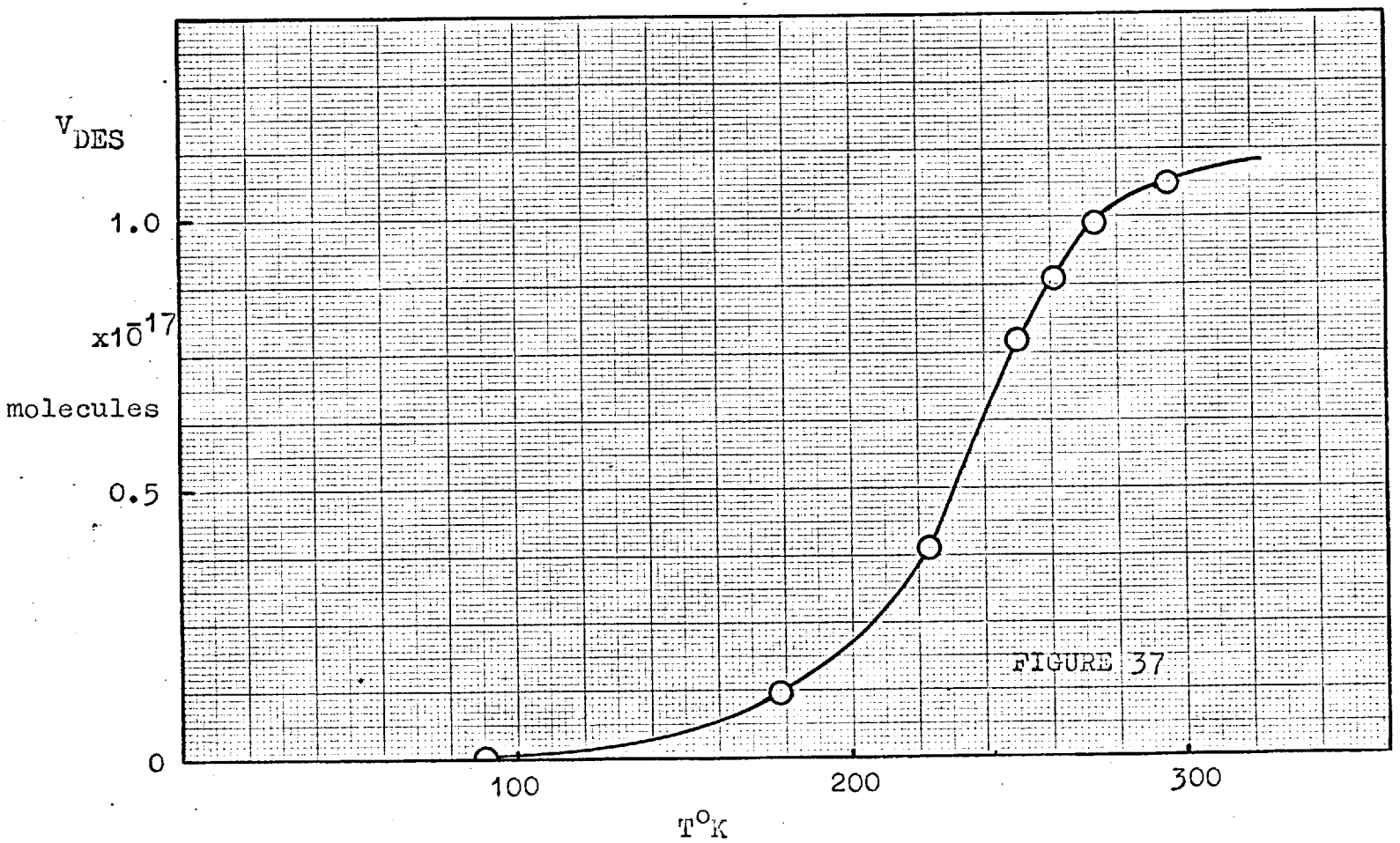

FIGURE 37

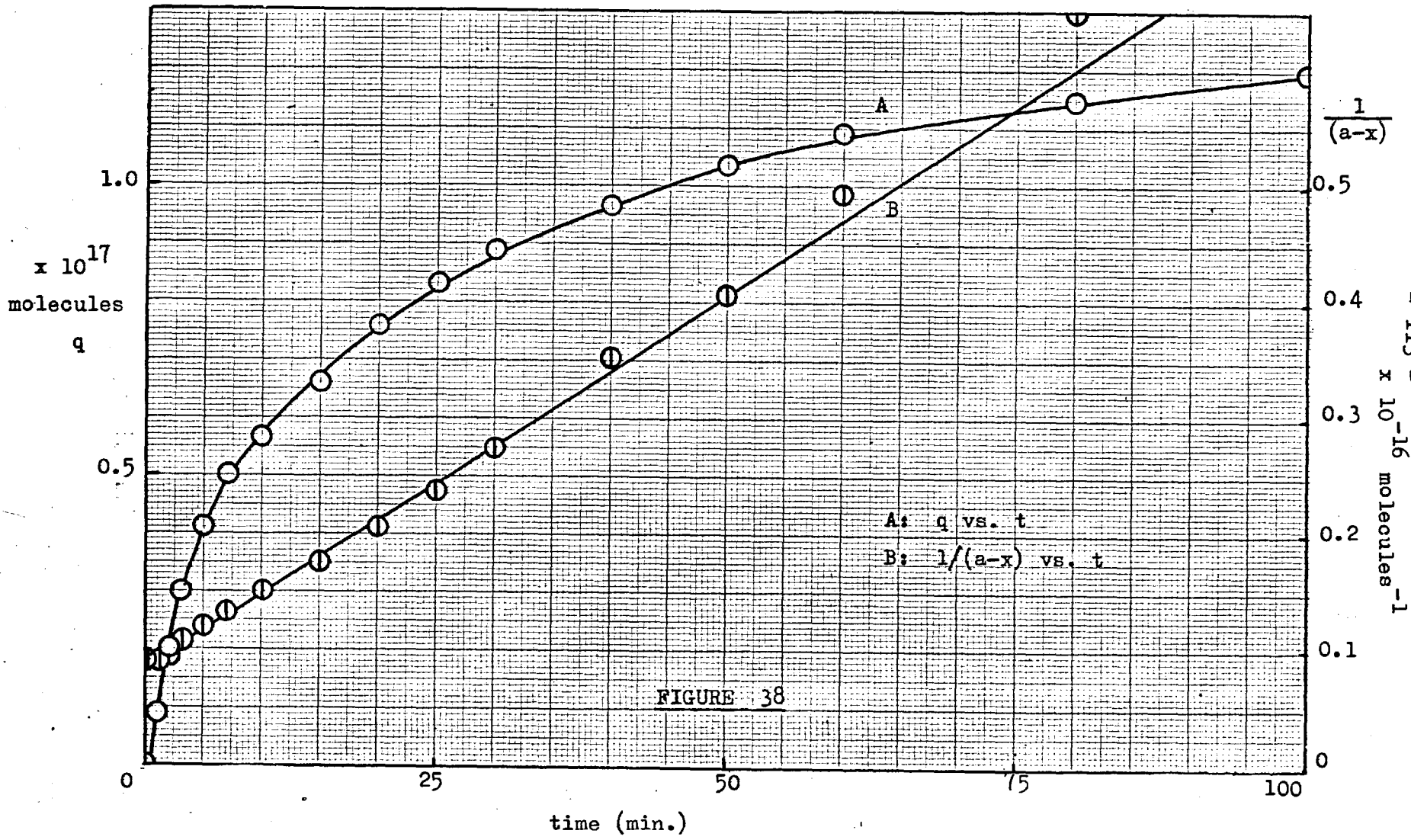
A
B
1.0
0.5
0
x 10^17
molecules
q
0.5
0.4
0.3
0.2
0.1
0
1/(a-x)
x 10^-16 molecules^-1
A: q vs. t
B: 1/(a-x) vs. t
25
50
75
100
time (min.)

FIGURE 38

(iii) Discussion

Zinc films were found to be similar to those of cadmium, copper and nickel in that the desorption kinetics for hydrogen atom removal from the surface is a second order process. Like cadmium effectively all the adsorbed gas can be removed at the highest temperature, 294°K. (FIGURE 36).

Application of the hopping formula, equation 4.08, with N = 1.27×10^{15} sites/sq.cm. yielded values for V_D similar to those found for cadmium (FIGURE 39), and the resultant straight line is best expressed by

$$V_D = 56T + 4,200 \text{ calories } T^{\circ}K. \quad \ldots\ldots\ldots\ldots\ldots\ldots \quad (4.43)$$

The distribution function, D_V, was obtained, as before, from the tangential slopes of the $Vol._{Des.}$ against Temperature plot, (FIGURE 37). The variation of D_V with (V - W) are shown in FIGURE 40. We note that, in the temperature range under investigation, the largest concentration of atoms is found to possess a mobility energy in the region of 13 kcal.mole.$^{-1}$

4.6 Silver

(i) Adsorption

The subsequent experiments confirmed the earlier results reported by Pritchard[80] viz. effectively no molecular hydrogen could be adsorbed on silver films at the temperatures under consideration (78°K. - 273°K.). The magnitude of the hydrogen atom uptakes are similar to those found for the other metals. The rates of uptake of equal doses of the atoms decreased with increasing dosage but at no temperature could equilibrium be attained; a slow sorption persisted at all temperatures. Dosing was discontinued after about 3 θ although again this by no means represented the total sorptive capacity of the film.

(ii) Desorption/...

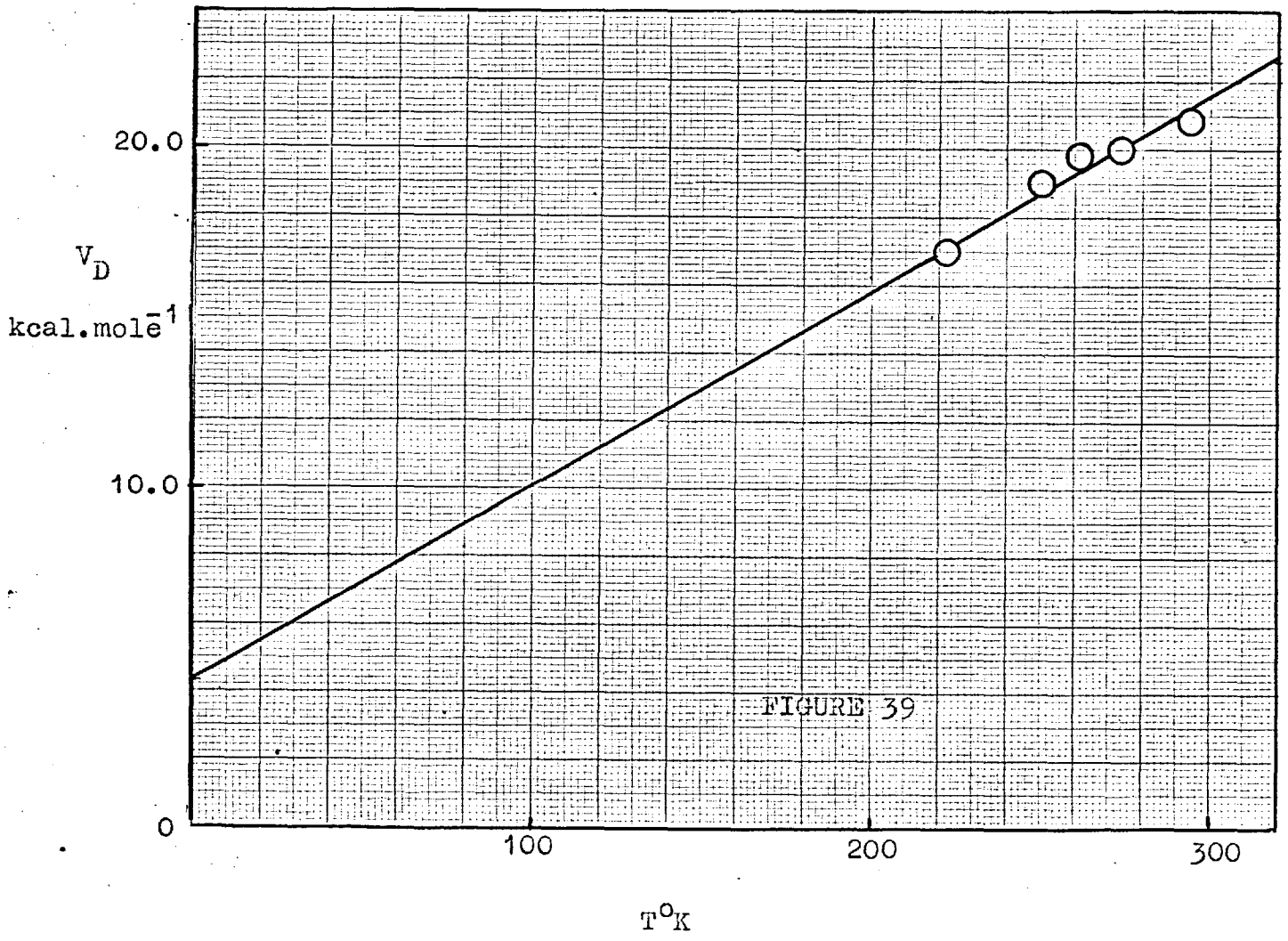

FIGURE 39

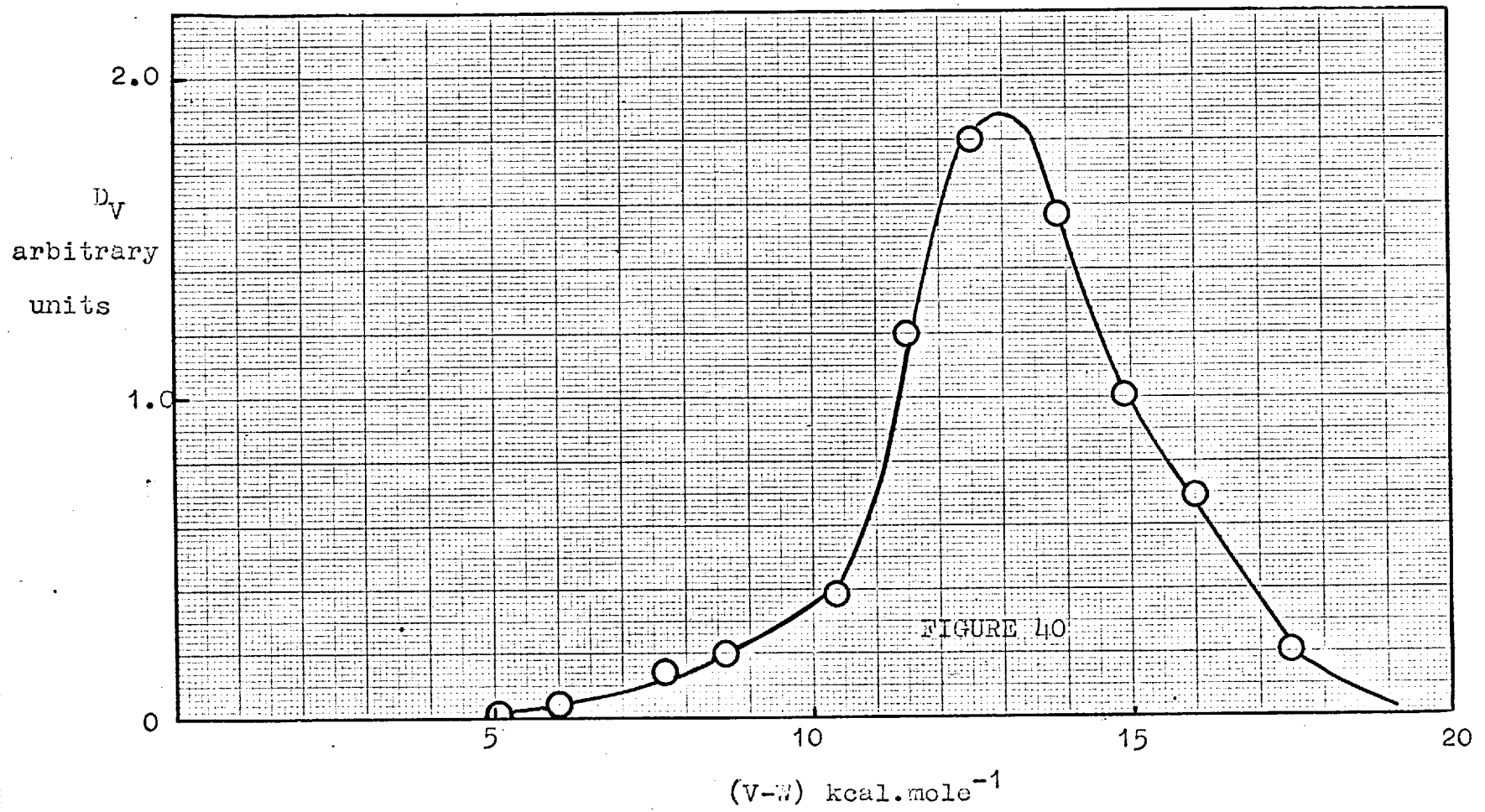

FIGURE 40

(ii) Desorption

As for the previous metals, the films were dosed at 78°K., the filament switched off and the rate of desorption measured upon increasing the temperature of the substrate. An extremely slow desorption rate was detected at 78°K. but no quantitative results could be obtained. Where necessary, the rate plots were extrapolated to infinite time. Readsorption was carried out at 78°K. before each desorption to attain effectively the same surface coverage. The volume desorbed increased with increasing temperature and with increasing dosage, as found for nickel, (FIGURE 41), but even at the highest temperature under consideration not all the gas was desorbed. In this respect silver resembles copper and not cadmium or zinc.

The volumes desorbed (corrected to 78°K.) at various temperatures for several dosages at 78°K. are tabulated in TABLE 19.

TABLE 19

Wt. of film: 68.4 mg.

Total Dose on surface at 78°K. (molecules x 10^{17})	Volume Desorbed at Various T°K. (molecules x 10^{17}) T°K.						
	90	148	178	223	250	273	300
0.223	0.014	0.193	0.196	0.200	0.208	0.202	0.206
0.739	0.012	0.205	0.208	0.207	0.210	0.208	0.212
1.243	0.022	0.206	0.212	0.219	0.219	0.219	0.229
2.201	0.010	0.212	0.230	0.240	0.249	0.242	0.265
3.589	0.031	0.225	0.250	0.265	0.285	0.299	0.314
5.856	0.080	0.251	0.276	0.306	0.353	0.417	0.471
7.954	0.084	0.262	0.301	0.357	0.417	0.488	0.580
9.895	0.158	0.273	0.316	0.384	0.491	0.544	0.678

Reproducibility on any one film was satisfactory; the rate constants, k', (see later) for three successive dosages normalised to the same volume desorbed at the same temperature were found to agree to within 10%.

(iii) The kinetics/...

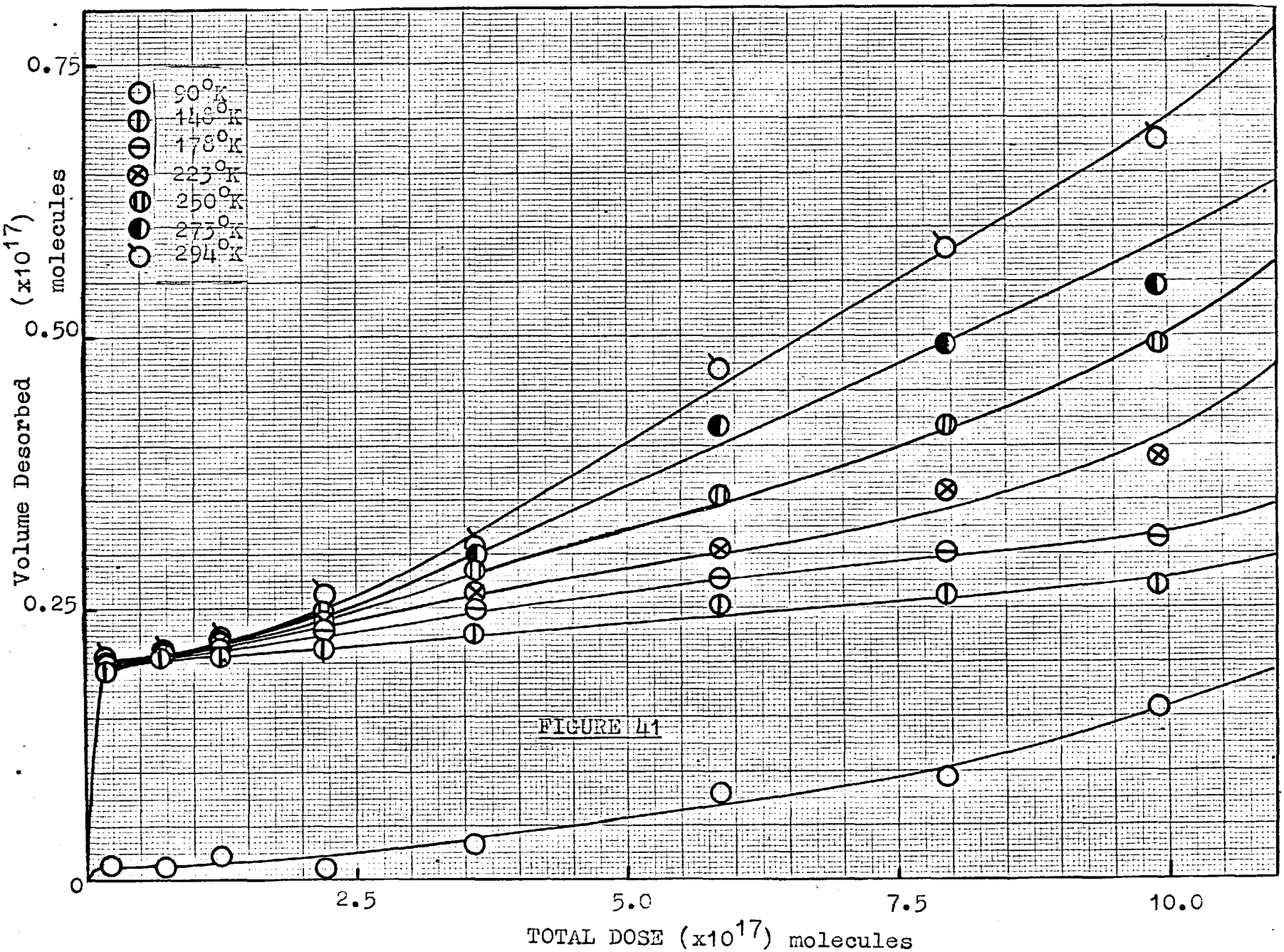
90°K
148°K
178°K
223°K
250°K
273°K
294°K
0.75
0.50
0.25
0
Volume Desorbed (x10^17) molecules
2.5
5.0
7.5
10.0
TOTAL DOSE (x10^17) molecules

FIGURE 41

(iii) The kinetics of the desorption process

A series of rate measurements were carried out on a clean film to determine the order of the reaction and to obtain the rate constants for various dosages. A first order equation,

$$\log(a - x) = k't + c' \quad \ldots\ldots\ldots\ldots\ldots\ldots \quad (4.44)$$

was found to be the best fit over the curves in the temperature range $148^{\circ}K.$ - $223^{\circ}K.$ The applicability of both the second and first order equations is illustrated for a typical plot in FIGURE 42. The resulting rate constants for various dosages are tabulated below in TABLE 20.

TABLE 20

Total Dose on Surface ($\times 10^{17}$ molecules)	k' (min.$^{-1}$)		
	$148^{\circ}K$	$178^{\circ}K$	$223^{\circ}K$
0.739	0.1000	0.5000	0.5400
1.243	0.1320	0.4725	0.6900
2.201	0.09075	0.4125	0.6333
3.589	0.08692	0.3080	0.4825
5.856	0.1517	0.4775	0.6833
7.954	0.08375	0.4738	0.6300
9.895	0.0980	0.4550	0.7450

(iv) Surface area determination

After completion of a typical desorption experiment the film was warmed to room temperature and pumped for about 10 minutes. The system was then isolated from the pumps, the cell recooled to $78^{\circ}K.$ and subsequently reheated to room temperature. No significant desorption of gas was found. The cell was then recooled to $78^{\circ}K.$ and the surface area measured using krypton and the point B method (FIGURE 43). The resulting surface area is ($19.5 \times 10^{-16} \times 2.2 \times 10^{17}$) sq.cm. i.e. 429 sq.cm.

(v) Discussion/...

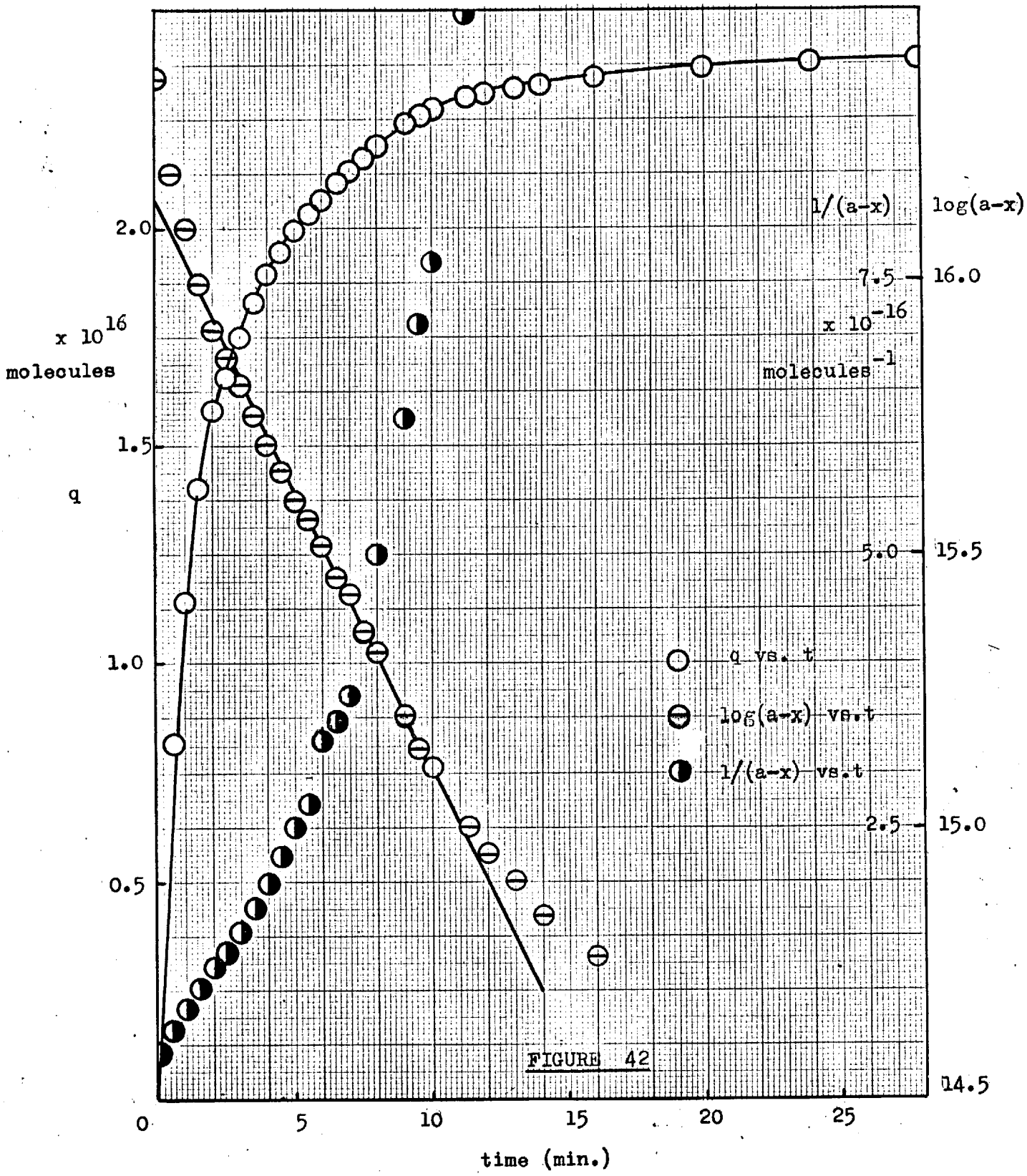
x 10^16 molecules
q
2.0
1.5
1.0
0.5
0
5
10
15
20
25
time (min.)
1/(a-x)
log(a-x)
7.5
16.0
x 10^-16
molecules^-1
5.0
15.5
2.5
15.0
14.5
q vs. t
log(a-x) vs.t
1/(a-x) vs.t

FIGURE 42

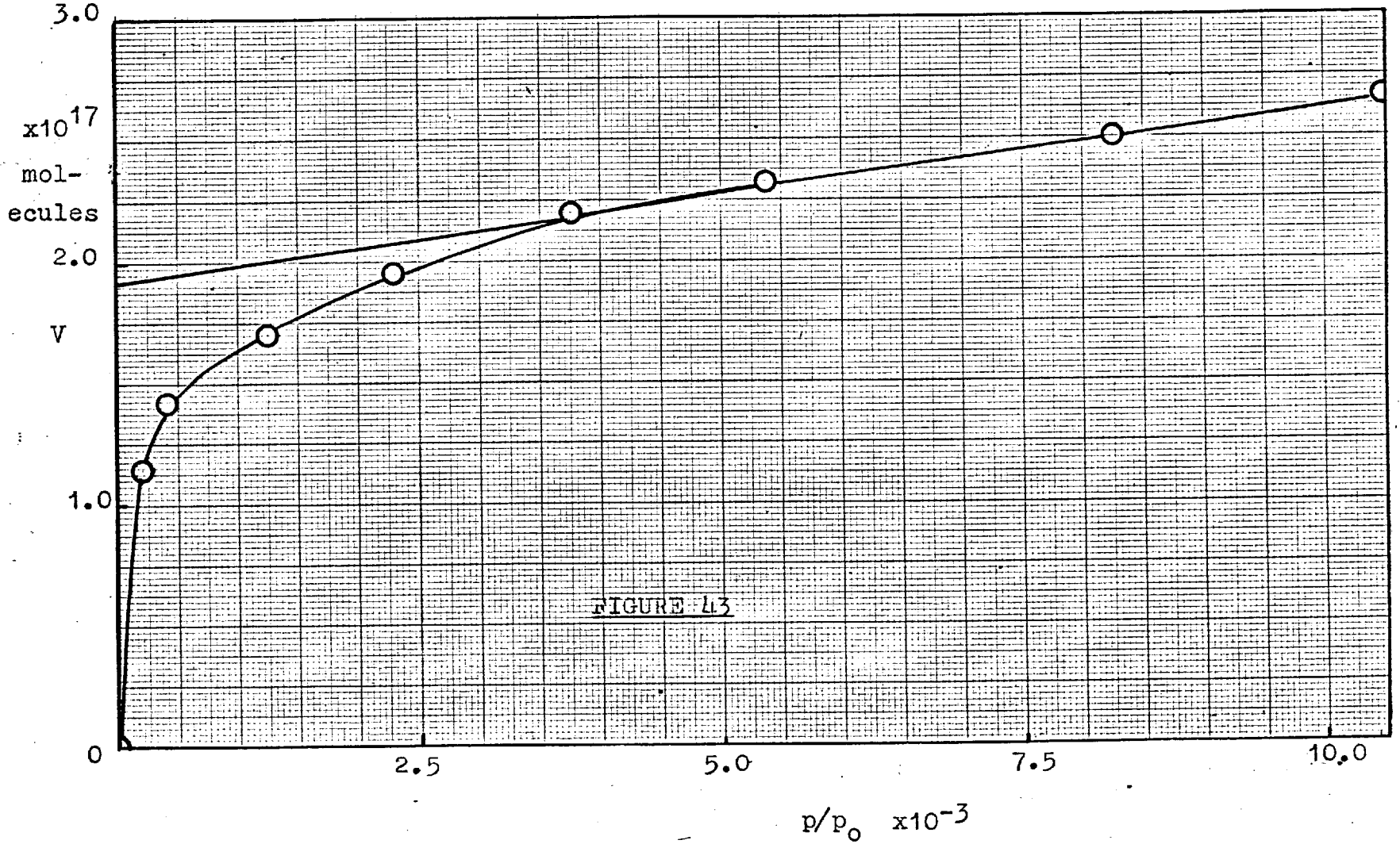

FIGURE 43

(v) Discussion

Pritchard[80] showed that hydrogen atoms adsorbed on silver and gold films at 90°K. could be removed by raising the temperature to 195°K. to the extent of reducing the surface potential from -0.34V to - 0.01V. However, no quantitative measurements of the actual volume of gas desorbed were made. From FIGURE 41 it can be readily seen that a comparatively large quantity of gas is desorbed from 90°K. to 178°K. but that this by no means represents the total quantity of gas adsorbed. It will also be noted that for doses up to $\theta = 1.0$, essentially the same volume is desorbable above 90°K. i.e. about 1/10th volume adsorbed. It thus seems likely that even at the smallest dosage used sorption into the bulk metal as well as chemisorption on the surface takes place. The shape of the plots in FIGURE 41 resemble those found for nickel and it is thus proposed that a similar surface to bulk relationship is obeyed here in the absence of any initial layer (the dissociated hydrogen molecule layer being absent).

The distribution function, derived as before from the tangential slopes of the $\text{Vol.}_{\text{Desorbed}}$ vs. Temperature plots is illustrated in FIGURE 44. It will be noted from this figure that two distinct energy regions of high distribution are evident, the initial occurring at about 5 kcal. is dosage independent while the latter, dependent on the dosage occurs in the higher energy region (>14 kcal.).

First order kinetics have been observed by Hickmott[105] and Tsu and Boudart[104] in their studies of the desorption rate of preadsorbed hydrogen atoms from glass at low temperatures in their flow systems. According to the latter the recombination process is controlled by a set of first order events; the adsorption on, the desorption from, the surface diffusion to

and the reaction/...

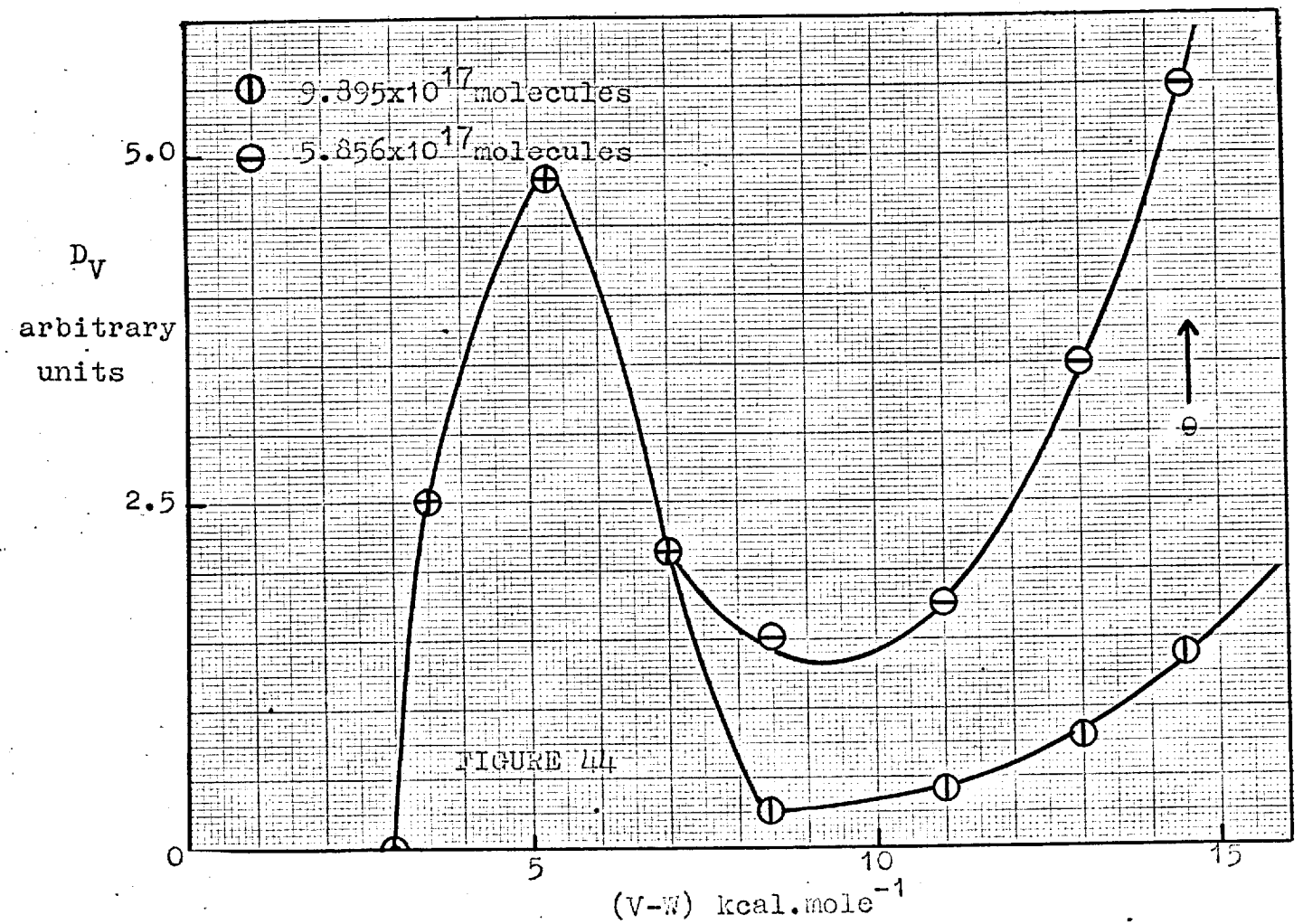
9.895x10^17 molecules
5.856x10^17 molecules
5.0
2.5
0
D_V
arbitrary
units
5
10
15
(V-W) kcal.mole^-1
θ

FIGURE 44

and the reaction at active sites. Hickmott concluded that recombination of the atoms bound to the glass did not occur by surface diffusion followed by reaction since this process would necessarily be second order in the number of adatoms. The slow step appeared to be direct evaporation of the adatoms from the surface. He applied a simple first order relationship at 77°K. and found $-\Delta H_2 \approx 6.6$ kcal.mole.$^{-1}$

In our results, a steric factor similar to that used in the second order expression was also introduced and utilising the expression

$$r = n k_m \nu_m \exp(-V_D/RT) \quad \ldots\ldots\ldots\ldots\ldots\ldots \quad (4.45)$$

where n = the number of atoms desorbed at $t = \infty$,

$k_m = 1/10$

and $\nu_m = 1 \times 10^{13}$,

values of V_D were calculated from the corresponding rates at various temperatures for a given dosage. A typical plot of V_D against T for a given dosage is illustrated in FIGURE 45. The resultant plot is linear and can be expressed by the relationship:-

$$V_D = 52T + 1000 \text{ calories } (T = {}^{\circ}\text{K.}) \quad \ldots\ldots\ldots\ldots \quad (4.46)$$

4.7 Gold

(i) Adsorption

No detectable adsorption of molecular hydrogen on gold films was found to occur over the range of temperature used, confirming the earlier results of surface potential studies on this metal reported by Pritchard[80].

The rates of uptake of equal doses ($\pm 1 \times 10^{17}$ molecules) of hydrogen atoms at 78°K. was similar to that found for the previous metals; the rates decreased with increasing doses and usually the experiment was terminated when the sorption of a dose of $\pm 1 \times 10^{17}$ molecules took longer

than 90 minutes./...

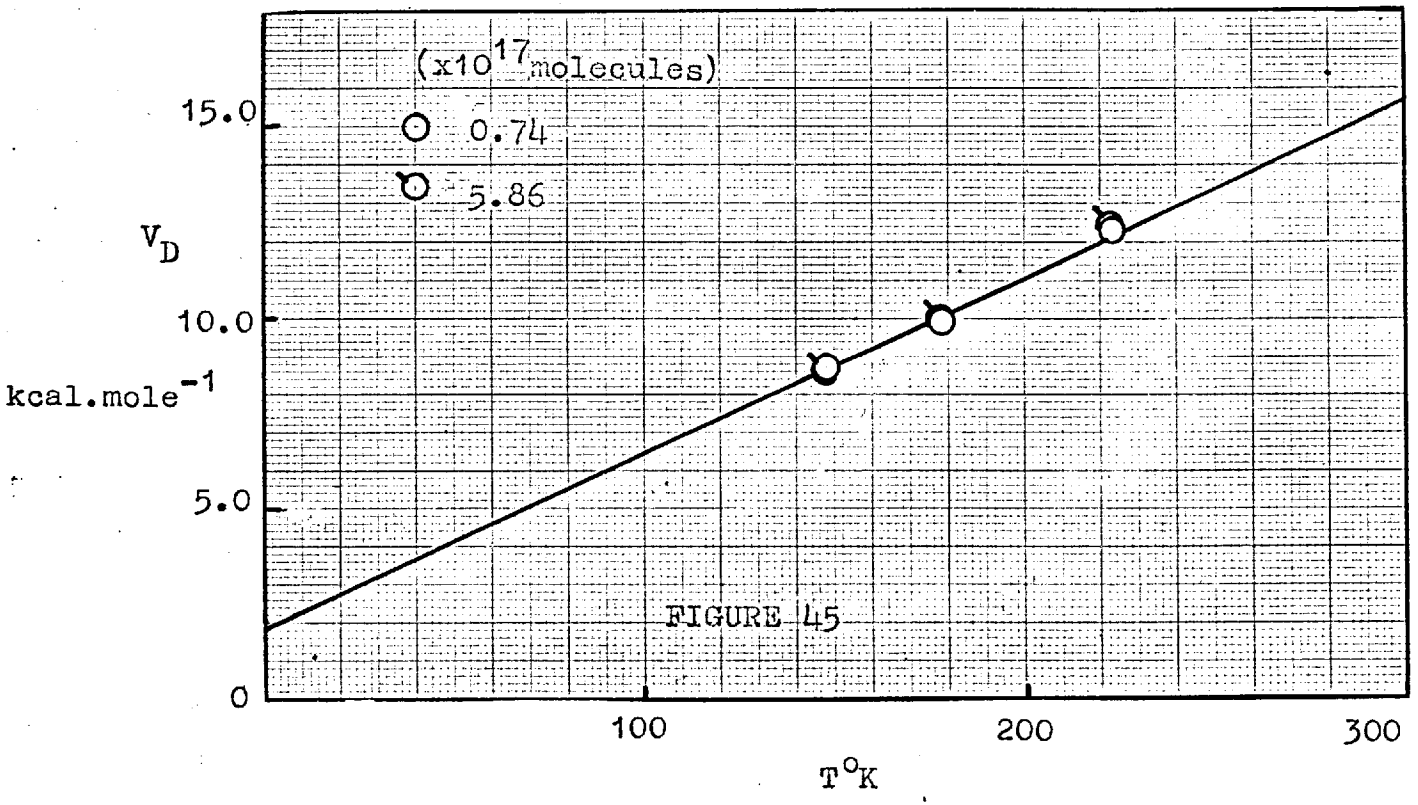
(x10^17 molecules)
0.74
5.86
15.0
10.0
5.0
0
V_D
kcal.mole^-1
100
200
300
T°K

FIGURE 45

than 90 minutes. This corresponds to a total coverage of approximately 3 θ. However the total amount taken up by no means represented the total sorptive capacity of the film, as upon subsequent dosing more gas could be adsorbed.

(ii) Desorption

The clean, annealed films were dosed at 78°K. and, after switching off the filament, the volume desorbed (corrected to 78°K.) and the rates of desorption were noted at various temperatures and for increasing dosages of the hydrogen atoms. As found for silver an extremely slow desorption rate was detected upon switching off the filament after dosing at 78°K. but no quantitative results could be obtained. In the case of gold films there was little, if any, need to extrapolate the rate curves to infinite time; the rate of desorption decreased to an effectively constant value within the time of the run. Readsorption was always carried out at 78°K. before each subsequent desorption. The volume desorbed was found to increase with increasing temperature and with increasing dosage (FIGURE 46) in a similar way to that found for nickel and silver, but even at the highest temperature (294°K.) under consideration only about 10% of the total volume taken up was desorbable. In this respect gold films closely resemble those of silver. The volumes desorbed (corrected to 78°K.) at various temperatures for several dosages at 78°K. are tabulated in TABLE 21 below.

Reproducibility was satisfactory on any one film; the resulting rate constants, k', (see later) for three successive dosages normalised to the same volume desorbed at the same temperature were found to agree to within 10%, while the actual volumes desorbed agreed to within 5%.

TABLE 21/...

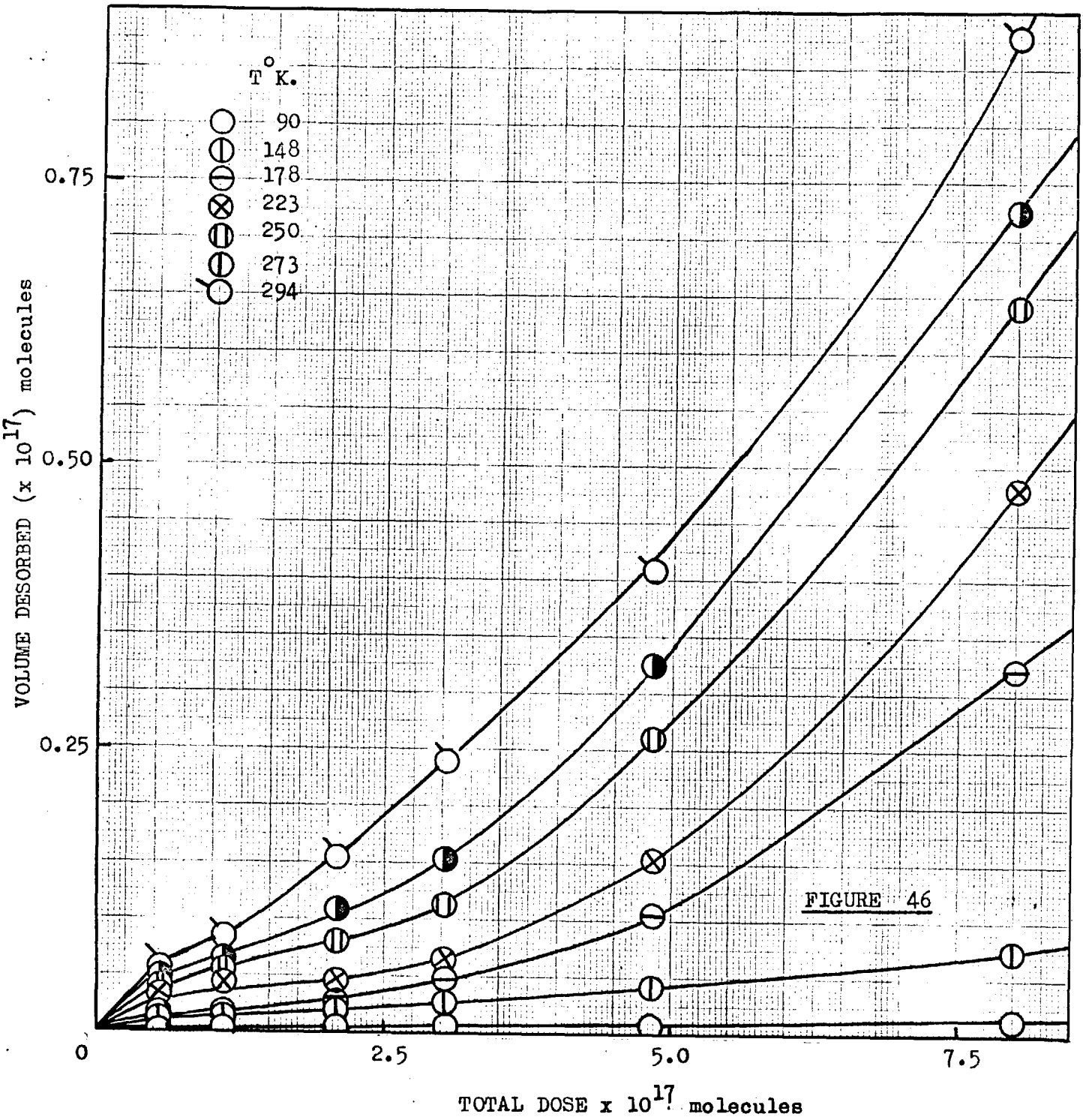
T°K.
90
148
178
223
250
273
294
0.75
0.50
0.25
0
2.5
5.0
7.5
VOLUME DESORBED (x 10^17) molecules
TOTAL DOSE x 10^17 molecules

FIGURE 46

TABLE 21

Wt. of film: 75.5 mg.

Total dose on surface at 78°K. (molecules x 10^{17})	Volume desorbed at various T°K. (molecules x 10^{17}) T°K.						
	90	148	178	223	250	273	294
0.549	0.005	0.012	0.015	0.032	0.040	0.049	0.057
1.080	0.005	0.013	0.017	0.044	0.055	0.065	0.085
2.088	0.006	0.019	0.028	0.045	0.080	0.107	0.153
3.044	0.006	0.026	0.048	0.065	0.113	0.151	0.239
4.814	0.007	0.041	0.105	0.152	0.260	0.325	0.408
8.018	0.015	0.072	0.321	0.480	0.640	0.725	0.877

(iii) The kinetics of the desorption process

Mathematical analyses of the rate plots for various dosages were carried out and a first order equation;

$$\log(a - x) = k't + c' \quad \ldots\ldots\ldots\ldots\ldots\ldots\ldots \quad (4.47)$$

where k', c' = constants,

$a = [H_2]$ at t = infinity,

and $x = [H_2]$ at t = t,

was found to be the best fit over the curves in the temperature range 148°K. - 223°K. Thus gold films resemble those of silver and the applicability of both the second and first order equations is illustrated for a typical plot in FIGURE 47. The resulting rate constants, k', for various dosages are tabulated in TABLE 22.

(iv) Surface area determination

The surface area of gold films using xenon as measured by Pritchard[82] varied from 4 times the area of the bulb when sintered at 90°K. to twice the area of the bulb when deposited and sintered at 333°K. A gold film was pumped at room temperature 298°K. for about ten minutes, the system

TABLE 22/...

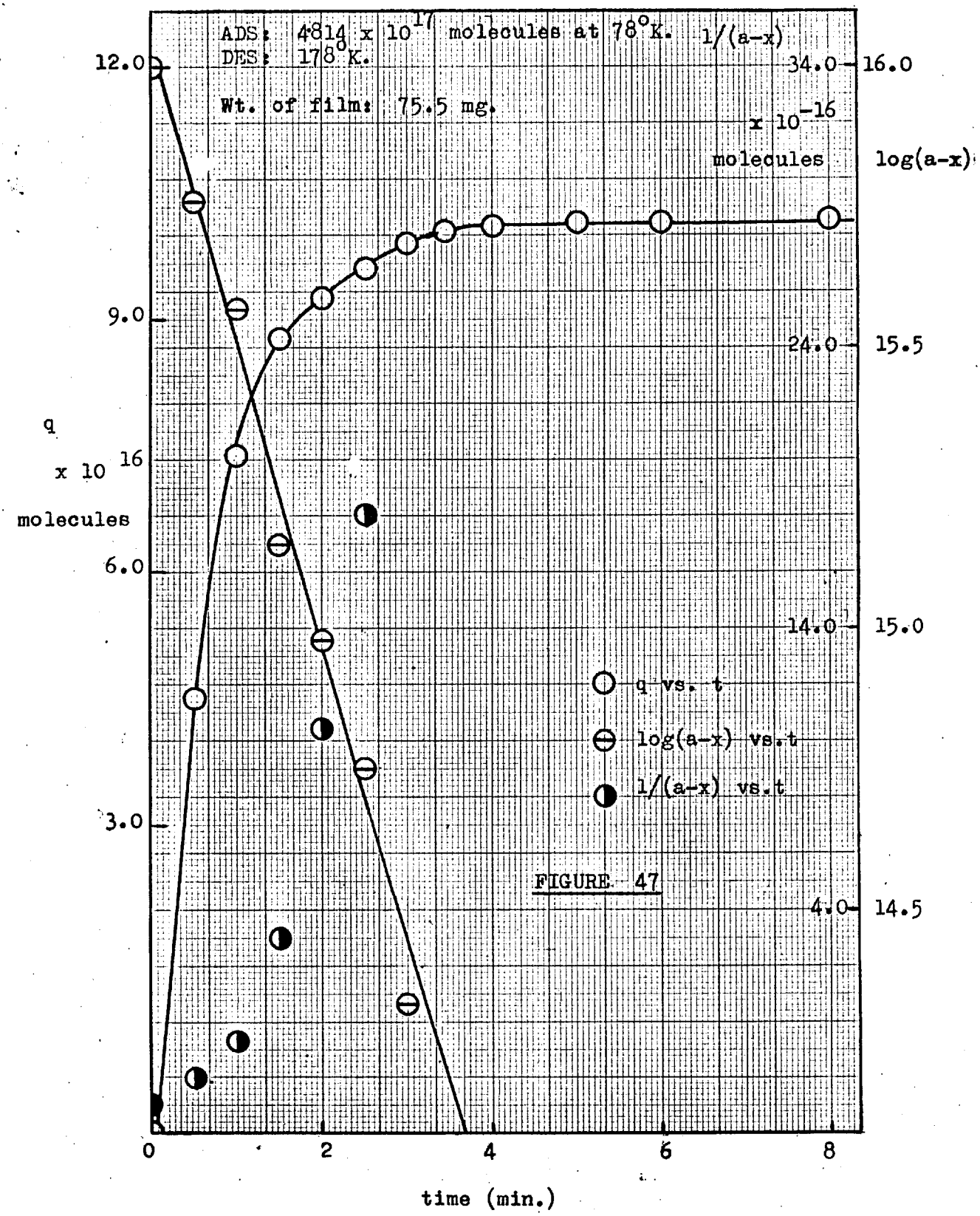
ADS: 4814 x 10^17 molecules at 78°K.
DES: 178°K.
Wt. of film: 75.5 mg.
1/(a-x)
x 10^-16
molecules
log(a-x)
q
x 10^16
molecules
12.0
9.0
6.0
3.0
34.0
24.0
14.0
4.0
16.0
15.5
15.0
14.5
q vs. t
log(a-x) vs.t
1/(a-x) vs.t
0
2
4
6
8
time (min.)

FIGURE 47

TABLE 22

Total Dose on film ($\times 10^{17}$ molecules)	k' ($min.^{-1}$)		
	148°K.	178°K.	223°K.
0.549	0.4300	0.4760	0.5000
1.080	0.4414	0.4818	0.5200
2.088	0.4614	0.4914	0.5389
3.044	0.4492	0.4800	0.5163
4.814	0.4816	0.5106	0.5374
8.018	0.4918	0.5163	0.5422

isolated from the pumps, the cell cooled to 78°K. and the surface area measured using krypton and the point B method. The resulting surface area was 401 sq.cm. (Geometric area $\pm$200 sq.cm.).

(v) Discussion

Pritchard[82] has reported that the adsorption of hydrogen atoms on a gold film at 90°K. gave rise to a very slight desorption when the filament was switched off and that complete desorption from the surface (as indicated by a return to an effectively zero surface potential) takes place at 195°K.; no quantitative measurements of the desorbed volumes were carried out. Our findings confirm the slight desorption at 90°K. but the volume desorbed at 195°K. is only about 5% of the total volume adsorbed at 78°K. (FIGURE 46).

The relationship between the volume desorbed and the total volume on the surface is similar to that found for silver and nickel. As only 5% of the dose is removable, even at the highest temperature, 294°K., it is assumed that distribution between the surface and the bulk occurs even for the smallest dose and because of the variation of the ratio of the heats

of adsorption/...

of adsorption on the surface and the heat of "solution" in the bulk with dosage an increasing volume of gas is desorbed with increasing dosage. The volume desorbed at any given dosage was also found to increase with increasing temperature; the resulting distribution function, derived from tangential slopes at a fixed temperature on the plot of Volume desorbed vs. Temperature is shown for a typical dosage, 8.02×10^{17} molecules, in FIGURE 48. It will be noted that, like cadmium films there appears to be a plateau of sites with energies slightly greater than 5 kcal. up to 15 kcal.

The first order relationship was similar to that found for silver and will be discussed in greater detail in the final section. Using the same rate equation as that derived for silver i.e.

$$r = k_m n \nu_m \exp(-V_D/kT) \quad \ldots\ldots\ldots\ldots\ldots\ldots \quad (4.48)$$

values of V_D were calculated from the rates at the corresponding temperatures for a given dosage. A typical plot of V_D against T for a dosage of 3.04×10^{17} molecules is illustrated in FIGURE 48. The resultant plot is linear and can be expressed by the relationship:-

$$V_D = 50T + 1000 \text{ calories } (T = {}^{\circ}K.) \quad \ldots\ldots\ldots\ldots \quad (4.49)$$